Piotr Maloszewski

Mathematical Modelling of Tracer Experiments in Fissured Aquifers

Freiburger Schriften zur Hydrologie

Herausgegeben von / Edited by:

Prof. Dr. Ch. Leibundgut
Professur für Hydrologie, Universität Freiburg i.Br.

Schriftleitung / Editorial office:

Dr. habil. Siegfried Demuth
Ingeborg Vonderstraß

Verlag und Vertrieb / Published and saled by:

Professur für Hydrologie
Universität Freiburg i. Br.
im Selbstverlag
Anschrift: Werderring 4, D-79098 Freiburg

ISSN 0945-1609

FREIBURGER SCHRIFTEN ZUR HYDROLOGIE

Band 2

Piotr Maloszewski

Mathematical Modelling of Tracer Experiments in Fissured Aquifers

48 Figures, 15 Tables

1994

Professur für Hydrologie an der Universität Freiburg i. Br.

Unterstützt durch / Supported by:

Förderverein Hydrologie an der Albert-Ludwigs-Universität
Freiburg i. Br.

Preface

For an editor to establish a new scientific series has always a pioneering touch. With the second volume of the 'Freiburger Schriften zur Hydrologie' an edition in English will be presented.

The second issue is again a 'Habilitation' finished at the Faculty of Geosciences at the University of Freiburg in 1993. It is a result of a long lasting, fruitful collaboration between the author and the editor in the research field of tracer hydrology. The thinking and methodological approach of the physicist Dr. Maloszewski is of particular significance for the progress in hydrological sciences.

The present study is one of the special topics Dr. Maloszewski has worked on the last few years. Without any doubt the authors research will significantly contribute to the progress in the field of mathematical modelling of tracer experiments in fissured aquifers with special emphasize on the analytical approaches.

I would like to thank the author for his constructive collaboration during the preparation of the volume and the 'Förderverein Hydrologie' for the financial support respectively. I hope this volume will help to facilitate and support the intensive international expert activities of the author worldwide.

Christian Leibundgut

Editor

List of contents

Mathematische Modellierung von Tracerversuchen in klüftigen Grundwasserleitern

Zusammenfassung

Es wird gezeigt, daß das Parallelkluft-Dispersionsmodell (PFDM) und seine Vereinfachungen (SFDM und DM) zur quantitativen Interpretation von Tracer- und Umweltisotopendaten in Kluftgrundwasserleitern geeignet sind. Das Einkluft-Dispersionsmodell (SFDM) dient zur Auswertung von Versuchen mit kurzen Fließzeiten, das Dispersionsmodell (DM) für Versuche mit langen Fließzeiten. Die Sensitivität von bestimmten Modellparametern wurde durch die Lösung des Direktproblems für die angenommenen Parameterwerte überprüft und in graphischer Form dargestellt.

Die Lösung des Inversproblems, d.h. die Bestimmung von hydraulischen Parametern durch Kalibrierung (Anpassung) des Modells an gemessene Tracerdurchgangskurven, wurde für zahlreiche Versuche durchgeführt. Es konnte nachgewiesen werden, daß eine gute Anpassung des Modells an die experimentellen Daten nicht automatisch die Anwendbarkeit des Modells bedeutet. Die Validierung oder zumindest die partielle Validierung des Modells sollte immer erreicht werden.

Die Voraussetzungen für die Anwendbarkeit der vereinfachten Modelle (SFDM und DM) wurde ermittelt und deren Gültigkeit bei verschiedenen Tracerversuchen demonstriert. Für alle Untersuchungsgebiete, die in der Arbeit analysiert wurden, konnte nachgewiesen werden, daß die Matrixdiffusion des Tracers (Diffusiver Austausch des Tracers zwischen dem mobilen Wasser in den Klüften und dem stagnierenden Wasser in der porösen Matrix) eine entscheidende Rolle spielt.

Es wurde gezeigt, daß die Interpretation der Verweilzeiten des mobilen Wassers aus den ^{14}C- und Tritiumaltern ohne Berücksichtigung der Retardierung des Tracers, verursacht durch die Matrixdiffusion, zur Überschätzung des mobilen Wasservolumens im unterirdischen Speicher führt. Beispielhaft wurde gezeigt, daß Versuche mit künstlichen Tracern zur Bestimmung von Retardationsfaktoren als Folge von Matrixdiffusion und Austauschreaktionen zur Interpretation von Radioisotopenaltern notwendig sind. Erst wenn die Retardationsfaktoren bekannt sind, können die mobilen Wasservolumina oder Wassergeschwindigkeiten aus ^{14}C- und Tritiumalter abgeleitet werden. Es wurde jedoch auch gezeigt, daß das Retardationskonzept nicht immer die Relation zwischen dem Alter des radioaktiven Tracers und den hydraulischen Parametern richtig beschreibt. Für konkrete Fälle muß immer die Anwendbarkeit des Retardationskonzepts überprüft werden.

Des weiteren konnte gezeigt werden, daß die Parameter des Dispersionsmodells (DM) nicht durch Kalibrierung des Dispersionsmodells an Ergebnissen von Versuchen mit kurzer Fließzeit gewonnen werden können. Die benötigten Parameter können aber durch Anwendung des SFDM-Modells ermittelt werden, um sie dann mit Hilfe des Dispersionsmodells für langfristige Prognosen des Stofftransportes in Kluftaquifern zu nutzen.

Mathematical modelling of tracer experiments in fissured aquifers

Abstract

Models of solute transport in fissured rocks applicable for the interpretation of tracer experiments are discussed in detail. All the models derive from the Parallel Fissure Dispersion Model (PFDM), which couples the transport equation in fissures with the diffusion equation in matrix. In short-term tracer experiments its approximation, i.e. the Single Fissure Dispersion Model (SFDM), or the Single Fissure Piston Flow Model (SFPFM), are shown to be applicable. For long-term tracer experiments and for the interpretation of environmental tracer data, the common Dispersion Model (DM) with parameters governed by matrix diffusion is shown to be adequate. Other models applicable to the dating of old waters are obtained from steady and transient states solutions to the basic model, i.e. the PFDM. The influence of parameters on the tracer curves yielded by particular models is investigated theoretically and demonstrated graphically by making use of direct solutions.

Case studies show how the inverse problem can be solved, i.e. how some parameters of an investigated system can be found by calibration (fitting) of the model to the experimental data. It is shown, that a good fit is a necessary but not sufficient condition for the applicability of a model. Validation, or a partial validation at least, should be obtained wherever possible.

Conditions for the applicability of the approximate models have been derived and their usefulness demonstrated. In all field case studies interpreted so far by the author, the matrix diffusion was shown to play a dominant or important role.

The mean transit time of water obtained from the ^{14}C or tritium ages, interpreted without taking into account the retardation factor resulting from the matrix diffusion, is shown to lead to greatly overestimated volumes of mobile water in fissured systems. Artificial tracer experiments, designed for finding the retardation factor caused by matrix diffusion and possible reactions, are shown to be potentially useful for the interpretation of environmental tracer data. Once the retardation factor is known, it can be used to interpret the mobile water content and/or other hydrogeological parameters from the environmental tracer ages. However, the concept of the retardation factor, which is well defined for conservative tracers, is not generally applicable for relating the environmental radiotracer ages with hydrogeological parameters. Its applicability has to be examinated for each case study.

It has also been demonstrated, that the parameters of the common dispersion model (DM) cannot be obtained from short-term tracer experiments, even if a good fit of that model is obtained. However, the SFDM applied to short-term experiments can be used to determine the physical parameters of the system, which can in turn serve for obtaining the parameters of the DM, applicable at large scales, and then for the prediction of pollutant movement.

1 Introduction

The aim of this work is to describe and summarize the Parallel Fissure Dispersion Model (PFDM) and its approximations: the Single Fissure Dispersion Model (SFDM) for short-term tracer experiments and the common Dispersion Model (DM) for long-term tracer experiments. The applicability of these models to the interpretation of artificial tracer experiments is discussed in detail and some examples of the interpretation of environmental tracer data are also given.

An analytical solution to the differential equations of the PFDM was developed by SUDICKY & FRIND (1982), who described the behaviour of contaminants injected to fractured rocks in the form of a step function. They came to a conclusion, that the solute transport is strongly influenced by diffusion between mobile water in the fractures and stagnant water in the micropores of rock matrix. NERETNIEKS (1981) obtained a solution for a radioactive tracer in a steady state and came to a conclusion, that in fractured rocks the ^{14}C ages can also be strongly influenced by that phenomena. A numerical solution to the transport equations for the parallel fracture model for a step input function was earlier obtained by GRISAK & PICKENS (1980), who also verified experimentally the importance of matrix diffusion. The present author obtained solutions for both, the PFDM and SFDM, in the case of an instantaneous injection, and further developed both models for reactive solutes, which follow partly an instantaneous equilibrium and partly the first order kinetic exchange reactions in the matrix. Conditions, required for the applicability of the SFDM in short-term tracer experiments and of the ordinary dispersion model (DM) in long-term experiments, were also found. Together with coworkers, the author applied these solutions for the interpretation of artificial tracer experiments performed under natural, radial-convergent and injection-withdrawal flow conditions (MALOSZEWSKI & ZUBER 1984, 1985, 1990a, 1993a; HIMMELSBACH & MALOSZEWSKI 1992; SEILER et al. 1989), and to interpret quantitatively a number of studies on environmental tracer data (MALOSZEWSKI & ZUBER 1985, 1991, 1992b; MALOSZEWSKI et al. 1990, 1992; HERRMANN et al. 1986, 1989; RANK et al. 1992). It is worth mentioning, that the SFDM derived for a transient state has also appeared to be successful for the interpretation of environmental tracer data in extended thin porous aquifers, in which the diffusion of dissolved species into the aquiclude may play an important role (NOLTE et al. 1991).

Theoretically, the PFDM and its approximations seem to be little justified, because the fractures and fissures are seldom parallel and of equal aperture and spacing (e.g., SNOW 1969, 1970). However, many examples of successful interpretations obtained with the aid of the SFDM and PFDM justify the applicability of these models. Successful interpretations are understood here as those, which yield both a good fit of the model to the experimental data (calibration) and the values of parameters, which are in agreement with those obtained by independent methods (validation or partial validation, as defined by MALOSZEWSKI & ZUBER 1992). The applicability of the SFDM and PFDM results from the dominant role of the matrix diffusion in the solute transport in flow through fractured media and from the ease in mathematical handling of that process without a prohibitive increase in the number of adjusted (fitted) parameters. A low number of fitting parameters is especially important for solving the inverse problems. With an increased number of parameters one often obtains a better fit, but in turn, the possibility for obtaing a unique inverse solution decreases. An example of the dominance of matrix diffusion over the fracture network parameters was shown by MALOSZEWSKI & ZUBER (1990a), who interpreted a multitracer experiment of GARNIER et al. (1985). Different tracers yielded different tracer curves which were shown to be depend on the coefficients of molecular diffusion

and exchange reaction constants of particular substances in the matrix. If the fracture network characteristics were the governing parameters, all the curves should be the same.

A number of solutions to the PFDM and SFDM and different applications of these models were given in a number of papers (HERRMANN et al. 1986, 1989; HIMMELSBACH & MALOSZEWSKI 1992; MALOSZEWSKI et al. 1990, 1992; MALOSZEWSKI & ZUBER 1984, 1985, 1989, 1990a, 1990b, 1991, 1993a; RANK et al. 1992). Therefore it seems, that a paper summarizing the state of the art is needed. In the present work all the important solutions are given, and an attempt is made to define the ranges of their applicability. The principles of interpretation are presented for several chosen field studies.

Nonreactive solutes are usually employed as tracers. However, some commonly applied tracers are not ideal, and, on the other hand, in some cases reactive tracers can also be of interest, especially when behaviour of nonconservative pollutants is to be predicted. Due to these reasons, the transport equation and its solutions are presented within the present work in a general form applicable to reactive solutes. The reactions are taken into account by a combined model of solute-rock interaction.

Due to space limitations a detailed discussion of other models is not possible. However, a short review of other approaches follows. All the approaches can practically be divided into two groups. The first approach is related to the subject of present work and regards the diffusion into porous matrix as a main dominant process, the second considers only the fissure network arrangement and neglects the influence of diffusion. The first approach was initiated by FOSTER (1975), who suggested, that the diffusion to the porous matrix can explain anomalously low tritium concentrations observed in the English Chalk. GRISACK & PICKENS (1980) formulated the transport equation combined with diffusion equation and found a numerical solution by applying the Galerkin Finite Element Method for the system of parallel indentical fissures equally distributed in porous matrix. GRISACK et al. (1980) used this solution to interpret a laboratory experiment performed in a fractured glacial till for a continuously injected tracer. GRISACK & PICKENS (1981) developed an analytical solution for a single fissure with a piston flow in the fissure and diffusion to the matrix for a constant input and fitted it to the experimental data of GRISACK et. al (1980). A similar solution, but with an instantaneous equilibrium reaction in the matrix, was developed by NERETNIEKS (1980) to show the importance of matrix diffusion for the radioactive pollutant movement in rocks. TANG et al. (1981) further developed that model and obtained an analytical solution for continuous injection of a radioactive tracer into a single fissure, taking into account the dispersive transport in the fissure and instantaneous equilibrium reactions in both, the fissure and the matrix. SUDICKY & FRIND (1981) found a steady state solution ($t \approx \infty$) for that model and adopted it for the interpretation of ^{14}C data in the case of a confined aquifer with molecular diffusion into the aquiclude. SUDICKY & FRIND (1984) extended the single fissure approximation given by TANG et al. (1981) to the case of a two-member decay chain. MORENO & RASMUSON (1986) gave a solution for a constant flux concentration at the inlet to the fracture and compared it with the solution of TANG et al. (1981) to demonstrate the influence of tracer injection mode on the interpretation. LOWELL (1989) obtained a solution for a periodic inlet concentration as a function of time. CHEN (1985, 1986) found a solution for the single fissure in the radial coordinates and adopted it to describe the diffusion from the porous aquifer into the adjacent strata. For the interpretation of laboratory experiments on diffusion in a fractured crystalline rock, LEVER et al. (1985) introduced mathematical model which took into account the effect of additional diffusion into dead-end pores as a part of microporous matrix. JOHNS & ROBERS (1991) offered a new version of the single fracture approach, in which the fracture is divided into two parts with different constant apertures. BIBBY (1981) successfully applied a numerical

solution to the equations of the parallel fissure model for the prediction of the behaviour of a conservative pollutant in the English Chalk. However, the numerical values of the parameters obtained by BIBBY (1981) can be questioned. SUDICKY & FRIND (1982) found an analytical solution for parallel fractures of equal aperture and spacing in the case of continuously injected tracer, which follows dispersive or piston flow in fractures, diffusion into the matrix, and instantaneous exchange reactions in fissures and in matrix. They used that model only for solving the direct problems. For the same assumptions, MALOSZEWSKI & ZUBER (1984) found a solution for an instantaneous injection of tracer (PFDM) and showed, that for long-term tracer transport the ordinary dispersion model (DM) with apparent parameters can also be successfully used. They gave the relation between mean transit time of tracer and the PFDM parameters, whereas for the dispersion parameter the relation was found later (MALOSZEWSKI & ZUBER 1992). An approximate condition for the applicability of the DM instead of the PFDM is given in this study. Assuming the same conceptual model, HODGKINSON et al. (1984) used numerical inversion of Laplace transforms to solve a more general problem of variable input concentration and the first order kinetic reaction on the fracture wall. By solving the direct problem they found, that the matrix diffusion is the most dominant process in radioactive pollutant (^{237}Np) movement in a fractured granitic rock of the eastern Central Sweden. MALOSZEWSKI & ZUBER (1985) found an analytical solution for an instantaneous injection in a single fissure (SFDM) and showed, that for short-term tracer experiments the tracer output concentration curves calculated with the aid of the PFDM and SFDM are the same. Further, MALOSZEWSKI & ZUBER (1990a) extended the SFDM for the reactive solutes, which follow the first order kinetic exchange reaction in the porous matrix and an instantaneous reaction in the fissures and matrix. The same model of exchange reactions was used by MALOSZEWSKI & ZUBER (1991) to find the solution for the steady state ($t \approx \infty$) and the piston flow in the system of parallel fissures.

Interesting numerical approach, based on Finite Element Methods, was proposed by HUYAKORN et al. (1983a, 1983b). The idea of the model is similar to that introduced by TANG et al. (1981) and SUDICKY & FRIND (1982, 1984). The three dimensional fissured system is divided into the prismatic or spherical blocks having the same dimensions. The blocks simulate porous matrix, whereas the slits between the blocks simulate fissures. RASMUSON (1984) followed this idea and obtained the solution for a system of sheres, applying the Laplace transform method and inversion in the complex plane. In comparison to the solution given by SUDICKY & FRIND (1982), this one is simpler in structure, since it consists of one infinite integration only. The weak point of the sphere approximation is the assumption of a constant water velocity between the spheres, whereas flow cross-sections between spheres vary. NERETNIEKS & RASMUSON (1984) found a numerical solution, based on the integrated finite difference method for variable water velocity between the blocks and for all other assumptions the same as those used by SUDICKY & FRIND (1982). Similarly, GERMAIN & FRIND (1989) developed a two-dimensional numerical model for the porous matrix approximated by rectangular blocks and for variable flow in the fissures.

NERETNIEKS (1981, 1983) introduced a new approach based on channeling coupled with diffusion, i.e. the piston flow through the system of fissures having a log-normal distribution of apertures, coupled with diffusion from each fissure into the matrix. The influence of adjacent fissures was neglected, i.e. infinitely large matrix was assumed for each fissure. It was shown that channeling may have a great impact on the dispersion of a pollutant whereas the diffusion process on its retardation. From the discussed paper it is evident that the channeling may be dominant at the short distances whereas the diffusion at large distances. The channeling effect can especially be important for the prediction of pollutant movement in sparsely fissured rocks because in the case of dominance of channeling, the dispersivity increases linearly with a flow

distance. That model was used for the interpretation of a long-term (two year duration) tracer experiment performed under natural flow conditions at the distance of about 50 m in the fractured granite of the Stripa test site (ABELIN et al. 1991a, 1991b). On the other hand, MALOSZEWSKI & ZUBER (1990b) showed theoretically that for densely fissured rock with a matrix of high porosity the dominance of diffusion is so strong that practically it does not matter if one assumes a constant or distance dependent dispersivity. BARKER (1985) introduced the block-geometry functions to describe the transport in densely fissured media. That author applied numerical Laplace transfer inversion to obtain the solution for the direct problem.

As mentioned, the second approach concentrates on an adequate presentation of the fracture network whereas the matrix diffusion is usually neglected. SCHWARTZ et al. (1983) modelled the distribution of fractures as a stochastic process and calculated the tracer passage with the aid of the particle-tracking method without taking into account the diffusion into the matrix. They concluded that classical dispersion theory cannot be used to analysing the mass transport in a network of discrete fractures. RASMUSON (1985) also neglected the diffusion into the matrix and analyzed channeling using the method of moments. That author found an equivalent dispersion coefficient from the time variance of tracer concentration curve, which can be used to predict intrinsic dispersion parameter from the fracture aperture distribution of nonconnected parallel fractures. MORENO et al. (1985) compared the model of TANG et al.(1981) with a modified version of channeling model. The channels were attributed to a single fracture which consisted of different flow paths as a result of variable fissure cross-section. In each flow path the piston flow was assumed with diffusion into the porous matrix. The most interesting finding was that the single fissure dispersion model and new channeling model yield nearly the same concentration curves. The dispersion parameter (or Peclet number), resulting from calibration of model, agreed well with the predicted one from the variance of the fissure apperture distribution. Following the concept of channeling, TSANG & TSANG (1987) developed a model of flow through the system of channels having variable aperture. It was practically either two- or three-dimensional flow model consisting of a number of separate channels. The channels are characterized by an apperture density distribution and a spatial correlation lenght. Apperture profiles are statistically generated and the tracer transport is considered as a result of piston flow through each channel (without diffusion). The transit time through a single channel is calculated from the water volume in the channel divided by the volumetric flow rate which was found from the cubic law of flow in the fracture. In a later paper MORENO et al. (1988) applied the same model to the single fracture flow. The fracture plane was discretized into a square mesh to which variable apertures were assigned. Spatially varying apertures of a single fracture were generated using geostatistical methods, based on an assumed aperture probability density distribution and a specified spacial correlation lenght. The tracer transport was generated using particle tracking method, without dispersion and diffusion into porous matrix. A simple model of instantaneous reactions on the fracture walls was included. TSANG et al. (1988) analyzed the sensibility of the model results to channel volume, the mean transit time and the channel volumetric flow rate, for the model of TSANG & TSANG (1987). They found the relation of the intrinsic dispersion coefficient to the statistical distribution of fissures. It is possible, by inverse modelling, to find the parameters of the aperture distribution from such parameters as the apparent dispersion and the mean transit time of tracer. SHAPIRO & NICHOLAS (1989) applied the channeling concept with lognormal and a truncated gamma distribution of a fissure aperture to interpret tracer experiments in radial flow through a single fracture of a constant aperture. The diffusion into rock matrix was neglected. These experiments were also interpreted by MALOSZEWSKI & ZUBER (1992, 1993a) who obtained much better fits with the three-parameter SFDM than those of SHAPIRO & NICHOLAS (1989) with the four parameter models, and showed that matrix diffusion probably should be taken into account even in a such short-term experiment with the duration of tracer curve up to 3 hrs. However, the mean flow times obtained by the latter authors

were nearly the same as those obtained by SHAPIRO & NICHOLAS (1989). In a recent paper CACAS et al. (1990b) used a three-dimensional stochastic model of a dense network of fractures consisting of discs combined with particle-tracking technique to simulate tracer experiments in fractured granite of uranium mine. The diffusion into the matrix was neglected. Due to a low number of tests the common fitting of model to the experimental data was not considered.

However, though the stochastic models better describe the inhomogenity of fractured medium by taking into account the distributions of fissure spacing and aperture, it seems that they are of little practical applicability to the inverse modelling of short-term tracer experiments in the cases of nonnegligible matrix diffusion. In fact, the matrix diffusion has already been well documented to play a dominant role in densely fissured rocks with a high matrix porosity. All the experiments discussed within this study are shown to be strongly influenced by matrix diffusion, which may lead to a conclusion that matrix diffusion is negligible only under extremely favourable conditions.

2 Mathematical models of tracer transport in fissured aquifers

2.1 Parallel fissure models

2.1.1 Parallel Fissure Dispersion Model (PFDM)

The conceptual model of tracer transport of SUDICKY & FRIND (1982) is followed. The dual-porosity medium is approximated by a semi-infinite system of identical parallel fissures (having the same aperture) equally spaced in a porous matrix (Fig. 1). A radioactive tracer enters the fissures with water and is transported along them by groundwater flow. The flow in the microporous matrix is neglected. The tracer transport in the porous matrix is governed only by molecular diffusion and reversible reaction with a linear adsorption isotherm. A similar reaction model is also assumed for the fissures. Under these assumptions the transport equations for solutes fissures and in the matrix are as follows:

$$R_{af}\frac{\partial C_f}{\partial t} + v\frac{\partial C_f}{\partial x} - D\frac{\partial^2 C_f}{\partial x^2} - \frac{n_p D_p}{b}\frac{\partial C_p}{\partial y}\Bigg|_{y=b} + \lambda R_{af} C_f = 0 \qquad \text{for } 0 \le y \le b \qquad (1)$$

$$\frac{\partial C_p}{\partial t} - \frac{D_p}{R_{ap}}\frac{\partial^2 C_p}{\partial y^2} + \lambda C_p = 0 \qquad \text{for } b \le y \le L/2 \qquad (2)$$

where C_f and C_p are the tracer concentrations in water per unit volume of water in the fissures and in the matrix, respectively, v is the mean water velocity in the fissures, x is the spatial coordinate taken in the direction of flow, y is the spatial coordinate perpendicular to the fissure extension, D is the dispersion coefficient in the fissures, 2b is the fissure aperture, t is the time variable, n_p is the matrix porosity, D_p is the molecular diffusion coefficient in the porous matrix, L is the fissure spacing, λ is the radioactive decay constant, R_{af} is the retardation factor due to an instantaneous equilibrium adsorption on the fissure wall, whereas R_{ap} is the retardation factor due to a reversible adsorption in the matrix, equal to

$$R_{ap} = 1 + (1 - n_p)\rho k_3 / n_p \qquad (3)$$

where k_3 is the distribution coefficient for the linear adsorption isotherm and instantaneous equilibrium expressed in units of volume per unit weight of the solid material and ρ is the density of the matrix material.

Equation (1) describes the dispersive-convective tracer transport in fissures, whereas eq. (2) describes the diffusive transport in the matrix in the direction perpendicular to the fissures. In the case of an instantaneous injection of tracer the following initial and boundary conditions apply (MALOSZEWSKI & ZUBER 1984):

$$C_f(x,0) = 0 \tag{4.1}$$

$$C_f(0,t) = M/Q\ \delta(t) \tag{4.2}$$

$$C_f(\infty,t) = 0 \tag{4.3}$$

$$C_p(y,x,0) = 0 \tag{4.4}$$

$$C_p(b,x,t) = C_f(x,t) \tag{4.5}$$

$$\left.\frac{\partial C_p}{\partial y}\right|_{y=L/2} = 0 \tag{4.6}$$

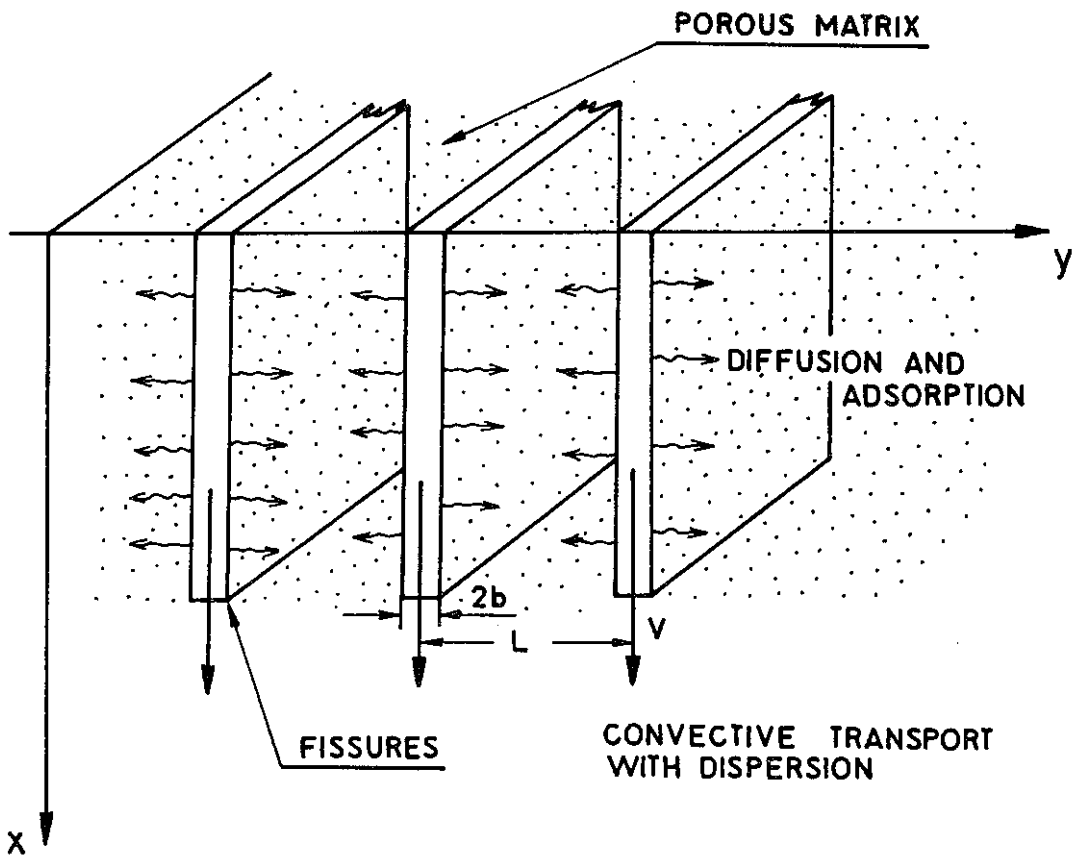

Fig. 1 Conceptual model of the tracer transport through fissured aquifer

where M is the mass of tracer instantaneously injected, $\delta(t)$ is the Dirac delta function in time domain, and Q is the volumetric flow rate through the system, which for natural flow conditions is equal to

$$Q = n_f v S \tag{5}$$

where S is the cross-section area perpendicular to the flow, and n_f is the fissure porosity ($n_f = 2b/L$).

The solution to eqs (1) and (2) for constant D and v with boundary conditions (4) was derived by the author using the method of Laplace transforms similarly to the derivation shown in MALOSZEWSKI & ZUBER (1984) for $R_{af} = 1$ and $k_3 = 0$. For a fixed distance, $x = X$, it has the following form:

$$C_f(t) = \frac{2M}{Q\pi^{3/2}} \exp(-\lambda t) \exp(Pe/2) \int_w^\infty \exp\left[-\frac{(4u^2)^2 - (Pe)^2}{(4u)^2}\right] \cdot$$

$$\int_0^\infty \epsilon \exp[-\epsilon_1(\epsilon,u)] \cos[\epsilon_2(\epsilon,u)]\, d\epsilon\, du \tag{6}$$

where

$$w = 0.5\,(Pe\, t_o'/t)^{1/2} \tag{7}$$

$$\epsilon_1(\epsilon,u) = \frac{Pe\, t_o' a\, \epsilon}{4u^2} \frac{\sinh(p\epsilon) + \sin(p\epsilon)}{\cosh(p\epsilon) + \cos(p\epsilon)} \tag{8.1}$$

and

$$\epsilon_2(\epsilon,u) = \frac{\epsilon^2}{2}\left(t - \frac{Pe\, t_o'}{4u^2}\right) - \frac{Pe\, t_o' a\, \epsilon}{4u^2} \frac{\sinh(p\epsilon) - \sin(p\epsilon)}{\cosh(p\epsilon) + \cos(p\epsilon)} \tag{8.2}$$

where u and ϵ are the integration variables.

The solution (6), called by MALOSZEWSKI & ZUBER (1985) the Parallel Fissure Dispersion Model (PFDM), describes the tracer concentration as a function of time in the outflow from the fissures.

2.1.2 Parameters of the Parallel Fissure Dispersion Model (PFDM)

The PFDM has six physical parameters v, D, 2b, L, n_p, D_p, and two combined reaction parameters R_{af} and R_{ap}, which are further combined into four nondisposable (fitting) parameters:

$$Pe = vX/D \tag{9.1}$$

is the Peclet number, or the reciprocal of the dispersion parameter ($P_D = D/(vX) = 1/Pe$), assumed to be constant for a given X.

$$t_o' = t_o R_{af} \tag{9.2}$$

$$a = n_p (R_{ap} D_p)^{1/2} / (2bR_{af}) \tag{9.3}$$

and

$$p = (L/2 - b)(R_{ap}/D_p)^{1/2} \tag{9.4}$$

These four nondisposable parameters are futher called the model parameters.

If reactions in the fissures are neglected the parameter t_o' simplifies to

$$t_o = X/v = V_f/Q \tag{10.1}$$

which is the mean transit time of water (V_f is the volume of the fissures i.e. volume of mobile water in the system). The a-parameter (9.3) is reduced to:

$$a = n_p (R_{ap} D_p)^{1/2} / (2b) \tag{10.2}$$

For a nonreactive tracer the fitting parameters are Pe (eq. 9.1), t_o (eq. 10.1) applied instead of t_o' in eq. (6), whereas the parameters a (eq. 9.3) and p (eq. 9.4) are equal to:

$$a = n_p D_p^{1/2} / (2b) \tag{11.1}$$

and

$$p = (L/2 - b)/D_p^{1/2} \tag{11.2}$$

which for $n_f << 1$ simplifies to

$$p = n_p/(2an_f) \tag{11.3}$$

The parameters a and p in the case of an ideal tracer can be regarded as the diffusion parameters for a given network system of parallel fissures.

In the case of a reactive tracer the adsorption retardation factors R_{af} and R_{ap} appear in the equations of the fitting parameters. The R_{af} factor is expressed as (e.g., FREEZE & CHERRY 1979)

$$R_{af} = 1 + Z_f k_a / n_f \qquad (12.1)$$

For parallel fissures it simplifies to (FREEZE & CHERRY 1979; or MALOSZEWSKI & ZUBER 1985)

$$R_{af} = 1 + 2k_a/(2b) \qquad (12.2)$$

where Z_f is the fissure wall surface per unit volume of rock and k_a is defined as the distribution coefficient in the fissure expressed as

$$k_a = (q_s/C_f)_{equilibrium} \qquad (13)$$

where q_s is the concentration in the solid phase expressed as a mass of tracer adsorbed per unit rock surface.

According to (12.2), for a large fissure aperture, the R_{af} factor is close to 1, but for a strongly adsorbed tracer and a very small fissure aperture, it may differ from 1. The estimation of R_{af} requires the measurements of k_a and 2b.

If the microporous matrix is assumed to consist of a set of parallel and equal diameter (d_c) capillaries, the R_{ap} factor can be expressed as (MALOSZEWSKI & ZUBER 1985)

$$R_{ap} = 1 + 4k_a/d_c \qquad (14)$$

The distribution coefficient defined for a hard rock, or more generally for any geometrical form of material, can be related to the distribution coefficient (k_3 in eq. 3) measured on a fine ground material consisting of spheres by (MALOSZEWSKI & ZUBER 1985):

$$k_a = \rho k_3 / [3 \sum_{i=1}^{j} (v_i/r_i)] \qquad (15)$$

where the grain size curve of the ground material is divided into j groups of weight fractions, v_i, and the radii of r_i.

It is evident that whereas some estimates of k_a are possible, an independent determination of the R_{ap} factor requires also the microscope observation on the micropore dimensions and shape. In the case of the simple model given by eq. (14) it is sufficient to know the diameter of the micropores.

The Parallel Fissure Dispersion Model is considered here as a general model of tracer transport in fissured aquifers. MALOSZEWSKI & ZUBER (1984, 1985, 1990b) applied this model for solving the direct problems. However, its application is difficult in the case of the inverse problem. The analysis of the influence of the parameters on the shape of tracer curves showed that in short-term tracer experiments the single fissure approximation is applicable (MALOSZEWSKI & ZUBER 1985; - see Chapter 2.2), whereas in the case of long-term experiments the ordinary dispersion model with apparent parameters can be used (MALOSZEWSKI & ZUBER 1984, 1985; - see Chapter 2.3).

2.1.3 Parallel Fissure Piston Flow Model (PFPFM)

In some cases the piston flow in the fissures can be assumed. Then, the system of equations (1)-(2) is solved for D=0, which yields for $R_{af} \geq 1$ (MALOSZEWSKI & ZUBER 1984):

$$C_f(t) = \frac{M}{Q\pi} \exp(-\lambda t) \int_0^\infty \epsilon \exp[-\epsilon_3(\epsilon)] \cos[\epsilon_4(\epsilon)] \, d\epsilon \qquad \text{for } t > t_o' \qquad (16.1)$$

and

$$C_f(t) = 0 \qquad \text{for } t \leq t_o', \qquad (16.2)$$

where

$$\epsilon_3(\epsilon) = t_o' a \epsilon \frac{\sinh(p\epsilon) + \sin(p\epsilon)}{\cosh(p\epsilon) + \cos(p\epsilon)} \qquad (17.1)$$

and

$$\epsilon_4(\epsilon) = \frac{\epsilon^2}{2} (t - t_o') - t_o' a \epsilon \frac{\sinh(p\epsilon) - \sin(p\epsilon)}{\cosh(p\epsilon) + \cos(p\epsilon)} \qquad (17.2)$$

This model is called the Parallel Fissure Piston Flow Model (PFPFM) and consists of three fitting parameters t_o', a and p which are defined by eqs (9.2), (9.3) and (9.4), respectively. For the nonreactive tracers, the parameters a and p are defined by eqs (11.1) and (11.2), and t_o' is replaced by t_o (eq. 10.1).

2.2 Single fissure models

2.2.1 Single Fissure Dispersion Model (SFDM)

It has been shown by MALOSZEWSKI & ZUBER (1985) that in short-term tracer experiments the tracer flow through the system of parallel fissures can be approximated with a sufficient accuracy by the transport through a single fissure in an infinite matrix (mathematically it means: $L \approx \infty$). This implies that, if the mean transit time of water is sufficiently short, the tracer has no time to diffuse into the matrix deep enough to be affected by adjacent fissures. The problem can be solved either by a comparison of directly calculated concentration curves for different assumed combinations of parameters, or by comparison of the Laplace transforms of both models. In the latter case one can estimate the time, t_k, up to which the Laplace transforms of the PFDM and SFDM are the same with an accuracy of, say, 4 percent. Taking the Laplace transforms given in MALOSZEWSKI & ZUBER (1984, 1991) and by making use of the properties of the tanges hiperbolic function [$\tanh(\Theta)=1$ for $\Theta \geq 2$], one obtains after simple

rearrangements for an ideal tracer (or in the case of instantaneous equilibrium reaction in the matrix):

$$t_k < p^2/4 \tag{18.1}$$

After introducing eq. (9.4) for the p-parameter and knowing that $n_f << 1$, it gives:

$$t_k < R_{ap}(2b)^2/(16D_p n_f^2) \tag{18.2}$$

A simple model of instantaneous equilibrium reactions in the porous matrix and in the fissures was used in Chapter 2.1.1 for reactive tracers. However, MALOSZEWSKI & ZUBER (1990a), who interpreted a multitracer experiment in a densely fissured aquifer found this simple model of exchange reaction inapplicable for the reactive solutes used in that experiment. Therefore, it was necessary to introduce a more complicated reaction model. An instantaneous equilibrium model with the linear sorption isotherm was assumed for the fissures, whereas for the microporous matrix a combined liquid-solid reaction model was applied. That model was proposal by CAMERON & KLUTE (1977) for granular media, and successfully applied by KLOTZ et al. (1988, 1992) for modelling the ^{85}Sr transport in sands. The idea of that model is schematically shown in Fig. 2. The following governing equations are used:

$$R_{af}\frac{\partial C_f}{\partial t} + v\frac{\partial C_f}{\partial x} - D\frac{\partial^2 C_f}{\partial x^2} - \frac{n_p D_p}{b}\left.\frac{\partial C_p}{\partial y}\right|_{y=b} + \lambda R_{af} C_f = 0 \tag{19}$$

for solute transport in the fissures, and

$$n_p\frac{\partial C_p}{\partial t} - n_p D_p\frac{\partial^2 C_p}{\partial y^2} + (1-n_p)\rho(\Phi_1 + \Phi_2) + \lambda n_p C_p = 0 \tag{20}$$

for solute transport in the microporous matrix.

The solute distribution between the water and solid phase in the matrix is described by the following equations:

$$\Phi_1 = \frac{\partial q_1}{\partial t} + \lambda q_1 = k_3\frac{\partial C_p}{\partial t} + \lambda k_3 C_p \tag{21.1}$$

$$\Phi_2 = \frac{\partial q_2}{\partial t} + \lambda q_2 = k_1\frac{n_p}{(1-n_p)\rho} C_p - k_2 q_2 = 0 \tag{21.2}$$

where Φ_1 is the mass transfer of solute between the liquid and solid phase in the matrix governed by a linear adsorption isotherm and an instantaneous equilibrium, Φ_2 is the mass transfer of solute between the liquid and solid phase in the matrix governed by the first-order nonequilibrium kinetic reaction, q_1 and q_2 are the partial solute concentrations in the solid phase of the porous matrix expressed per unit weight of the solid material, k_1 and k_2 are the forward

and the backward rate constants for nonequilibrium kinetic reaction, respectively. The remainig parameters and variables were described in Chapter 2.1.2.

If eq. (19) is applied to a system of more than one fissure, 2b is the effective fissure aperture, and D is the effective dispersion coefficient resulting from the spectrum of velocities in fissures. If the fissures are not interconnected, the dispersion coefficient will be proportional to both the velocity and the distance, i.e. the dispersivity, D/v, will be proportional to the distance (NERETNIEKS 1983), which imposes some limitations on the applicability of the dispersion model. If the fissures are interconnected and the space scale is large enough, the dispersivity will probably reach an asymptotic value, and the model should be less restricted.

The boundary and initial conditions for the Single Fissure Dispersion Model have been given by MALOSZEWSKI & ZUBER (1990a). They are similar to that discussed in Chapter 2.1.1, only instead of eq. (4.6) one should put

$$C_p(\infty,x,t) = 0 \tag{22.1}$$

and

$$q_1(x,0) = 0 \tag{22.2}$$

$$q_2(x,0) = 0 \tag{22.3}$$

The solution to eqs (19)-(21) with the boundary and initial conditions (4.1)-(4.5) and (22.1)-(22.3) was derived by the author for a nonradioactive tracer ($\lambda=0$) in MALOSZEWSKI & ZUBER (1990a). For a radioactive tracer the final solution is multiplied by $\exp(-\lambda t)$, so it reads:

$$C_f(t) = \frac{aM}{2\pi Q}(Pet_o')^{1/2}\left\{\int_0^t \exp\left[-\frac{Pe(t_o'-u)^2}{4ut_o'} - \frac{a^2u^2}{t-u} - k_1'(t-u)\right]\frac{du}{[u(t-u)^3]^{1/2}} + \right.$$

$$(k_1'k_2)^{1/2}\int_0^t \exp\left[-\frac{Pe(t_o'-u)^2}{4ut_o'} - \frac{a^2u^2}{t-u} - k_1'(t-u)\right]\cdot$$

$$u^{-1/2}\int_u^t \exp\left[-\frac{a^2u^2}{\tau-u} - (k_1'-k_2)(\tau-u)\right]\cdot I_1\left\{[4k_1'k_2(\tau-u)(t-\tau)]^{1/2}\right\}\cdot$$

$$\left.\frac{d\tau\,du}{(\tau-u)(t-\tau)^{1/2}}\right\}\exp(-\lambda t) \tag{23}$$

where

$$k_1' = k_1/R_{ap} \tag{24}$$

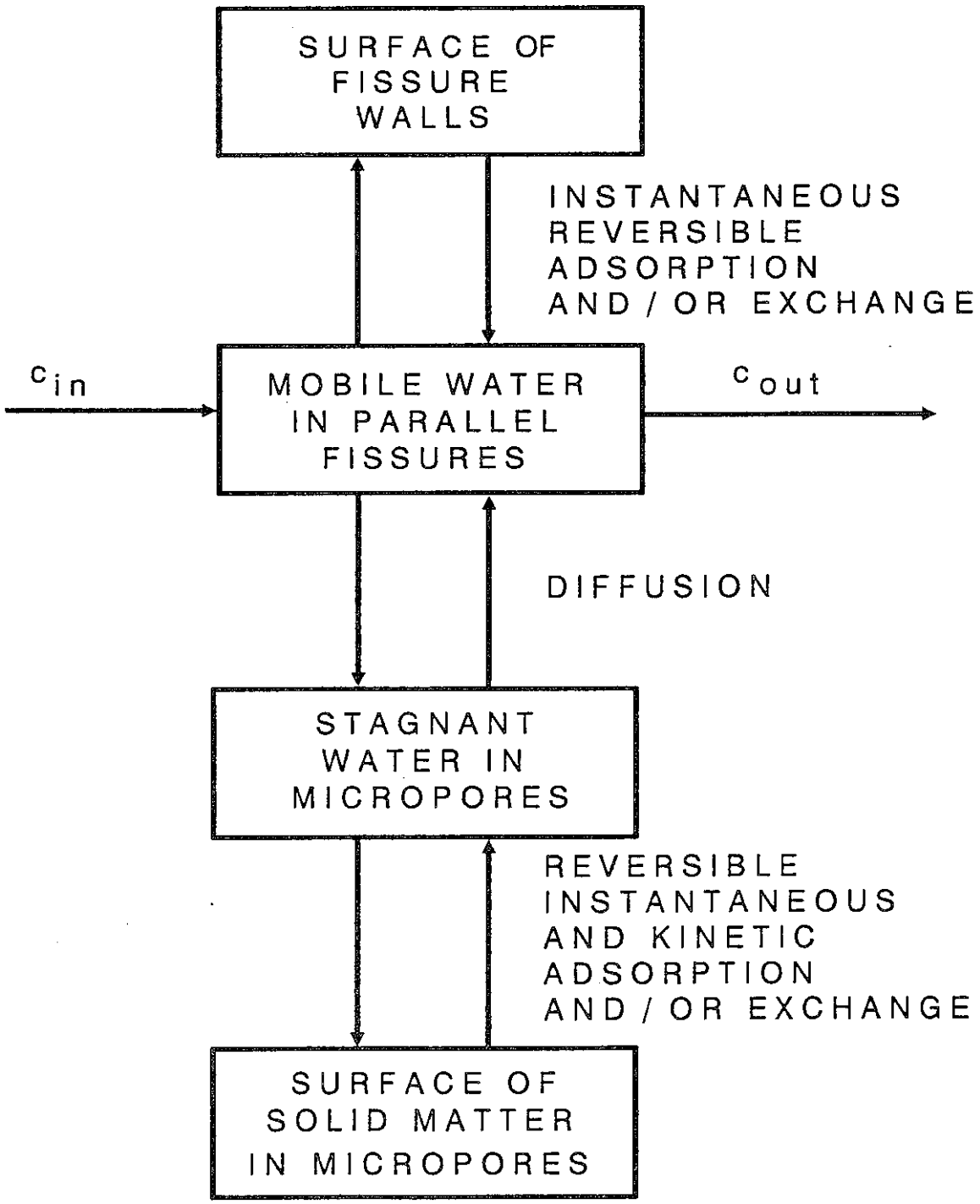

Fig. 2 **Multibox presentation of transport and exchange reaction models used**

Equation (23) describes the tracer concentration in the outflow from either a single fissure or a system of fissures in short-term tracer experiments. This model has five fitting parameters: Pe (eq. 9.1), t_o' (eq. 9.2), a (eq. 9.3), k_1' (eq. 24) and k_2, whereas the departure parameters are: t_o or v, Pe or D/v, 2b, n_p, D_p, k_1, k_2, R_{ap} and R_{af}. Note that the reaction constants are bulk parameters defined by the model and do not supply details on the physical and chemical processes of the involved reactions.

From eq. (23) one can easily obtain other solutions, for nonreactive (ideal) tracers or for reactive tracers which follow simpler exchange reactions. For a nonradioactive and nonreactive (ideal) tracer, the reaction parameters are equal to zero, $k_1=k_2=k_3=0$ ($R_{af}=R_{ap}=1$), and the solution (23) simplifies to

$$C_f(t) = \frac{aM}{2\pi Q}(Pet_o)^{1/2}\int_0^t \exp\left[-\frac{Pe(t_o-u)^2}{4ut_o} - \frac{a^2u^2}{t-u}\right]\frac{du}{[u(t-u)^3]^{1/2}} \qquad (25)$$

which describes the concentration of an ideal tracer in the outflow from the fissures. The fitting parameters of the model (eq. 25) are t_o, Pe and a, however, the a-parameter is now expressed by eq. (11.1).

Other solutions for simple reaction models are directly result from eq. (25). When the tracer follows only an instantaneous equilibrium with a linear adsorption in the matrix ($R_{af}=1$, $R_{ap}>1$), eq. (25) remains the same, but the a-parameter is expressed by eq. (10.2). It means that the number of fitting parameters remains the same as for an ideal tracer. When additionally to the instantaneous reaction in the matrix, it is necessary to take into account an instantaneous equilibrium reaction in fissures ($R_{af}>1$, $R_{ap}>1$), one should replace t_o by t_o'. The a-parameter is then expressed by eq. (9.3). The number of fitting parameters still remains the same but their meaning differs from that of an ideal tracer, because they combine additional physical parameters.

The SFDM model developed by the author is applicable in the tracer hydrology for the interpretion of experiments performed in fissured aquifers at the short distances. The fitting parameters of the model yield the physical parameters of the groundwater system can as shown in the next Chapter.

2.2.2 Determing the parameters of the Single Fissure Dispersion Model

2.2.2.1 Nonreactive tracers

The transport model of an ideal tracer (eq. 25) has three nondisposable fitting parameters which can be found by solving the inverse problem, i.e. by fitting eq. (25) to the tracer concentration curve measured. In the natural flow field, the cross-section area (S) is undefined, and, therefore the volumetric flow rate (Q) through the system of fissures has to be eliminated from eq. (25). To achieve that, both the tracer concentration curve measured and the theoretical output concentration, $C_f(t)$, are normalized to their maximum concentrations C_{max} obtained at time $t=t_{max}$. Then, instead of eq. (25), the following function is fitted to the normalized experimmental data:

$$C_n(t) = \frac{C_f(t)}{C_{max}} = \frac{C_f(t)}{C_f(t=t_{max})} \tag{26}$$

For flow distance (X) and the mean transit time of water (t_o), the mean water velocity is $v=X/t_o$. The Peclet number (Pe) yields the longitudinal dispersivity, $\alpha_L=D/v=X/Pe$. From the a-parameter, the fissure aperture ($2b=n_p\sqrt{D_p}/a$) can be obtained, if the matrix porosity (n_p) and the diffusion coefficient (D_p) are either known from laboratory experiments or can be assumed as known quantities.

Though eq. (25) was obtained for unidimensional flow, there are physical reasons to expect the unidimensional model to work satisfactorily for the radial flow (see Fig. 3), if tracer is injected in a well situated within the radial symmetry of the depresion cone and its concentration is measured in the pumping well. These physical reasons are related to the convergence of flow lines in the pumping well, which diminishes the effects caused by transverse dispersion. Examples of a good fit of the unidimensional model and reasonable values of the parameters obtained, reported in number of papers, seem to confirm such an approximation (e.g., LENDA & ZUBER 1970; ZUBER 1974; NOVAKOWSKI et al. 1985; MALOSZEWSKI & ZUBER 1985, 1990a, 1992, 1993a; RAVEN et al. 1988; SHAPIRO & NICHOLAS 1989).

If the volume of depression cone is negligible in the comparison with the volume of water in the investigated part of the system, i.e. in the cylinder of radius X and height m (thickness of the aquifer), the fissure porosity (n_f) can be calculated as follows (e.g., ZUBER 1974):

$$n_f = Q\, t_o/(\pi m X^2) \tag{27}$$

where Q is the volumetric pumping rate, m is the thickness of the aquifer, and X is the distance between wells.

The fissure porosity, in turn, may serve for estimation of the fissure width for a given model of the fissure network. For instance, for a model of a network of tortuous fissures of the same aperture, isotropically oriented in space, the following formula was obtained (MALOSZEWSKI & ZUBER 1993a; ZUBER 1974):

$$K = n_f(2b)^2/(12\tau_f^2) \tag{28}$$

where K is the permeability coefficient and τ_f is the tortuosity factor for fissures. Equation (28) is very close to equations derived for a network of isotropically oriented capillaries (SAFFMAN 1959) and for a network of tortous capillaries (PIRSON 1963). As the hydraulic conductivity (k) is known from the pumping test, the fissure aperture may be estimated from eq. (28) as follows:

$$2b = 4.29 \cdot 10^{-6}\, \tau_f(k/n_f)^{1/2} \tag{29}$$

where 2b is expressed in meters, k in meters per day for 10°C, and τ_f is the tortousity factor for fissures ($\tau_f \approx 1.5$).

Finally, if the molecular diffusion coefficient in the free water (D_m), is known and the constrictivity factor (δ) is also known or equal to unity, the matrix porosity (n_p) can be found by combining eq. (11.2) with $D_p=\delta D_m/\tau_p$ (NERETNIEKS 1980):

$$n_p = [(2ba)^2 \tau_p/(\delta D_m)]^{1/2} \qquad (30)$$

where τ_p is the tortuosity factor for the matrix ($\tau_p \approx 1.5$) and the a-parameter is found from a nonreactive tracer experiment. Equation (30) seems to be well satisfied for some carbonate rocks where the constrictivity factor is probably equal to one for the majority of typical tracers (see MALOSZEWSKI & ZUBER 1990a; where eq. (30) was however given with an error). For magmatic rocks of low matrix porosity the constrictivity factor is usually much smaller than 1 (SKAGIUS & NERETNIEKS 1986) and then eq. (30) is not applicable.

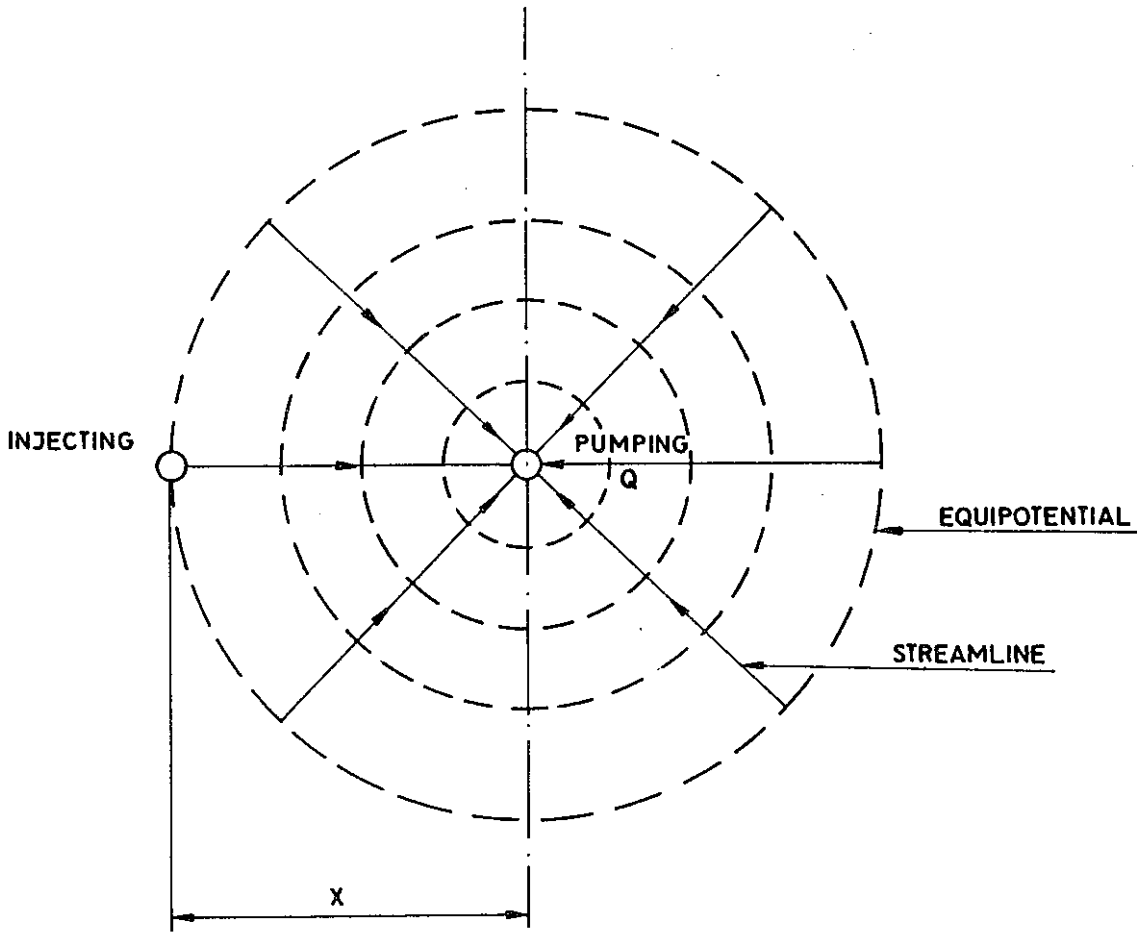

Fig. 3 **Schematic presentation of the hydrodynamic field in radial convergent flow (monopole test)**

Some authors (e.g., NOVAKOWSKI et al. 1985; or RAVEN et al. 1988) apply injection-withdrawal tracer tests (dipole tests). A steady state groundwater flow field is forced by a pumping and recharging well pair. If (1) the volumetric flow rates in pumping and recharging wells are the same, (2) natural gradient between wells is negligible, and (3) the groundwater system is homogeneous and isotropic, the hydrodynamic field has the form of a symmetrical dipole (see Fig. 4). The tracer is injected into the recharging well and its concentration is observed in the pumping well. The water from the pumping well is not reinjected into the recharging well (so called "open dipole test") to avoid the recirculation of the tracer. Assuming that the wells are parallel to each other, the transport of tracer can be considered on each streamline (stream tube) separately as unidimensional. However, the water velocities vary along streamlines, and therefore, the unidimen-sional transport model described by eq. (25) approximates the variable flow conditions with the average constant velocity for each stream tube. The output concentration $C_f(t)$ observed in the pumping well is the weighted sum of the stream tube flows:

$$C_f(t) = \sum_{i=1}^{2I} [q_i \, C_{fi}(t)] / Q \tag{31.1}$$

where Q is the pumping rate, q_i and $C_{fi}(t)$ are the partial volumetric flow rate and the output concentration from the i-th stream tube, respectively, and 2I is the number of the stream tubes. One may assume, that the partial volumetric flow rates (q_i) are the same, i.e. $q_i = Q/(2I)$. Taking additionaly into account the symmetry of the hydrodynamic field the weighted output concentration of tracer is then

$$C_f(t) = \sum_{i=1}^{2I} C_{fi}(t) / (2I) = \sum_{i=1}^{I} C_{fi}(t) / I \tag{31.2}$$

Assuming, according to ZUBER (1974), that the mass of tracer transported in each stream tube M_i is proportional to the partial volumetric flow rate ($M_i/q_i = M/Q$) and that the dispersivity (α_L) is constant and the same for all the stream tubes, the output concentration from the i-th stream tube, $C_{fi}(t)$, is equal to:

$$C_{fi}(t) = C_f(t_o = t_{oi}, Pe = Pe_i) \tag{32}$$

where t_{oi} and Pe_i are the mean transit time of water and Peclet number for the i-th stream tube, respectively. According to GROVE & BEETEM (1971) t_{oi} and Pe_i are given by:

$$t_{oi} = \frac{\pi \beta X^2}{Q} \, \frac{1 - \Theta_i \cot\Theta_i}{\sin^2\Theta_i} \tag{33.1}$$

and

$$Pe_i = \frac{X}{\alpha_L} \, \frac{\Theta_i}{\sin\Theta_i} \tag{33.2}$$

where Θ_i varies positively from 0 to π [$\Theta_i = \pi(i-1)/I$ with $i = 2,I$].

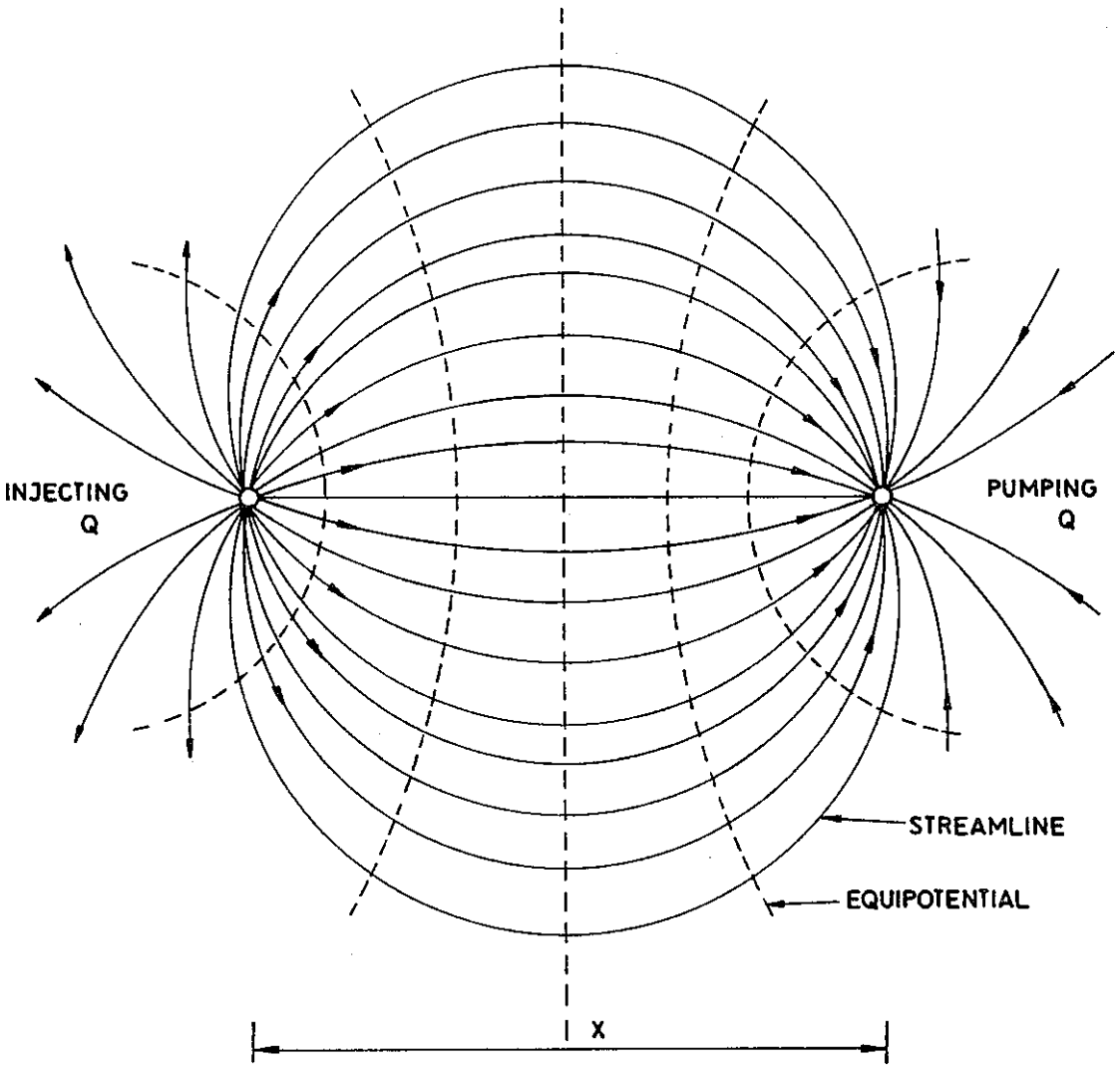

Fig. 4 **Schematic presentation of the hydrodynamic field by injection-withdrawal (dipole) test**

The stream tube connecting both wells rectilinearly in the shortest way (for $i=1$, $\Theta_1=0$) has the mean transit time and the Peclet number equal to:

$$t_{o1} = \frac{\pi \beta X^2}{3Q} \tag{34.1}$$

$$Pe_1 = X/\alpha_L \tag{34.2}$$

where ß is equal to the fissure aperture for a tracer experiment performed in a single fracture, (ß=2b), whereas for a densely fissured system ß=mn_f.

The calibration of the model, eq. (32) with (31.2), is possible only numerically for an assumed number of stream tubes. NOVAKOWSKI et al. (1985) have shown that acceptable results of calculation can be obtained using only 48 stream tubes. In the present work 120 stream tubes (I=60) were used (see Chapter 4.1.3). The fitting parameters of the model for dipole tracer test are t_{o1} (eq. 34.1), Pe_1 (eq. 34.2) and the a-parameter (eq. 11.1). From the parameter t_{o1} one can easily find ß by making use of eq. (34.1) for the known distance (X) and pumping rate (Q). Consequently, for a single fracture, the ß factor is directly equal to the fissure aperture (2b) whereas for a densely fissured system the fissure porosity (n_f) can be obtained when the thickness of the aquifer is known. In the latter case the mean fissure aperture 2b and the matrix porosity n_p may be calculated identically as it was described for the monopole tracer test.

The monopole or dipole radial flows are especially suitable for tracer experiments because they allow to include the concept of the tracer mass recovery (ZUBER 1974). Then, the normalization of the concentration scale is not needed, and, consequently, additional information is available from the from the test. The mass recovery curve or the relative mass recovery curve as a function of time was included by the author (KLOTZ et al. 1988; MALOSZEWSKI & ZUBER 1990a, 1993a) in the fitting procedure, which improves the model calibration. The mass recovery curve, R(t), is defined by eq. (35.1), whereas the relative tracer recovery, RR(t), is defined by eq. (35.2).

$$R(t) = Q \int_0^t C_f(t)\, dt \tag{35.1}$$

$$RR(t) = R(t)/M \tag{35.2}$$

The experimental values of the R(t) and RR(t) can be calculated from the experimental tracer curve by making use of eqs (35.1) and (35.2) whereas the theoretical values are obtained by putting into these equations $C_f(t)$ from eq. (25) for the monopole test or eq. (32) for the dipole test. The fitting procedure consists of trial-and-error procedure applied in turn to the concentration tracer curve and the mass recovery curve until a given set of parameters gives the best fit of the both theoretical curves to the experimental data. The fitting procedure is stopped when the sum of the squared differences between the theoretical and experimental values is at minimum.

Note that combined eqs (35.2) and (25) yield the solution for a continuous injection given by TANG et al. (1981).

2.2.2.2 Reactive tracers

For reactive tracers the number of fitting parameters is too large to obtain an unambiguous interpretation without a prior determination of t_o, a and Pe from an ideal tracer concentration curve. Therefore, a simultaneous injection of both ideal and reactive tracers has to be performed. Under natural flow conditions, the calibration of model [eq. 26 with tracer concentration curves $C_f(t)$ and C_{max} expressed by eq. 23] is easy but not unique, because then the concept of mass recovery cannot be applied.

For a tracer experiment performed in radial-convergent flow, eq. (23) is directly applicable, whereas in injection-withdrawal tracer test that equation is used in eq. (32). For the Peclet number known from ideal tracer experiment, the number of fitting parameters in eq. (23) is reduced to four: a, t_o', k_1' and k_2. However, the calibration of the model is still not unique. Theoretically, when a good fit is obtained for a reactive tracer curve, the R_{af} factor can be found by comparison of t_o' with t_o, and next R_{ap} can be found by comparison of the values of the a-parameters obtained for nonreactive (eq. 11.1) and reactive tracers (eq. 9.3). The diffusion coefficients (D_p) for both tracers have to be independetly known. The rate constants k_1' and k_2 are determined directly as a fitting parameters. For the known R_{ap}, the reaction rate constant k_1 can be calculated be making use of eq. (24).

If the reaction in fissures can be neglected ($R_{af}=1$), the number of fitting parameters in eq. (23) is reduced to three: a, k_1' and k_2 and the calibration is more reliable. However, for any additional evaluation of the parameters like R_{ap} and k_1, the values of D_p for each of two tracers must be known.

It remains unknown if the field values of the reaction parameters can be predicted with a satisfactory accuracy from laboratory batch or column experiments. However, it is interesting to point out that the reaction parameters, k_1, k_2 and k_3, are related to the common distribution coefficient (k_d) by the following formula (MALOSZEWSKI & ZUBER 1990a)

$$k_d = k_3 + \frac{n_p}{(1-n_p)\rho} k_1/k_2 \qquad (36)$$

The larger the k_1/k_2 ratio, the larger the k_d value, whereas an increase in both k_1 and k_2 leads to a faster equilibrium. It has to be remembered that eq. (36) is valid only for a given system. For a transfer of the reaction parameters obtained in laboratory experiments on ground materials to hard rocks in the field a model relating the surface available for sorption with other parameters of the system is required (cf. eq. 14).

The SFDM model described by eq. (23) was derived for unidimensional flow, whereas, as mentioned, the model is also used to interpret the data in convergent-radial flow (monopole test), and in symmetrical dipole flow. The advantages of the dipole-test over the monopole-test lie in a much shorter measuring time and larger aquifer volume tested for the same pumping rate and distance between the wells (ZUBER 1974). The disadvantage of the dipole-test lies in different travel times of flow lines. This causes additional flattening effects which in consequence may overshadow the differentiation caused by matrix diffusion. A second disadvantage of the dipole-test lies in the escape of some tracer with the flow lines which go away from the test area (see Fig. 4), and, in consequence the relative mass recovery is always below unity. A third disadvantage lies in a possible higher influence of the transverse dispersion in comparison with the monopole-test. As mentioned, the transverse dispersion is neglected in the both methods discussed.

2.2.3 Single Fissure Piston Flow Model (SFPFM)

In some practical cases, for a quick and approximate determination of parameters, the solution for the piston flow in the fissure ($D=0$) can be used, which reads for a nonradioactive tracer (MALOSZEWSKI & ZUBER 1985):

$$C_f(t) = \frac{aM}{Q(\pi t_o)^{1/2}} \exp\left[-\frac{a^2 t_o}{(t/t_o - 1)}\right] \frac{1}{(t/t_o-1)^{3/2}} \qquad \text{for } t > t_o, \qquad (37)$$

and

$$C_f(t) = 0 \qquad \text{for } t \leq t_o.$$

The above solution is called the Single Fissure Piston Flow Model (SFPFM) and has two fitting parameters: a and t_o. The a-parameter is expressed by eq. (11.1) for an ideal tracer, or by eq. (10.2) for an instantaneous equilibrium reaction in the porous matrix. From eq. (37) it is easy to find the time (t_{max}) at which the maximal concentration (C_{max}) should appear:

$$t_{max} = t_o + [2(at_o)^2]/3 \qquad (38)$$

2.3 Ordinary Dispersion Model (DM)

2.3.1 Ordinary Dispersion Model for an instantaneous tracer injection

It was theoretically shown by MALOSZEWSKI & ZUBER (1984) that in long-term tracer experiments the tracer may have enough time for a full penetration of the microporous matrix between fissures. In such a situation the ordinary dispersion model (DM) has parameters related by simple formulas to parameters of the PFDM. It means that, the tracer concentration curve obtained in the outflow from the fissures can be described both by the DM and the PFDM. Considering the diffusion equation (2) for a nonradioactive tracer, with boundary condition (4.6) and continuous injection of tracer into the fissures, the tracer will be equally distributed in the matrix between $x=0$ and $x=X$ after the time t_{min} given by:

$$t_{min} \geq 16p^2 / (1+2ap) \qquad (39.1)$$

For $n_f << 1$ eq. (39.1) can be rearranged to

$$t_{min} \geq 4(2b)^2 / [D_p n_f (n_f+n_p)] \qquad (39.2)$$

The above equations can be considered as rough approximations of the time after which the matrix will already be fully penetrated by an ideal tracer ($R_{ap}=1$ and $R_{af}=1$) up to the flow distance $x=X$.

The unidimensional solutions for the common dispersion equation were obtained by many authors. Here, the solution derived for granular media by LENDA & ZUBER (1970), whose physical meaning was explained by KREFT & ZUBER (1978) is followed. In a normalized form it reads:

$$C(t) = \frac{M}{Qt_o[4\pi P_D(t/t_o)^3]^{1/2}} \exp\left[-\frac{(1-t/t_o)^2}{4P_D t/t_o}\right] \quad (40)$$

where Q is the volumetric flow rate through the system and $Qt_o = V$ is the volume of water in porous system, and P_D is the dispersion parameter equal to D/(vx) or 1/Pe.

This model has two fitting parameters: the mean transit time of water, t_o, and the dispersion parameter, P_D. It is clear that by calibration of the DM to the tracer concentration curve measured in double-porosity fissured aquifers one cannot obtain the values of t_o and P_D, but only apparent parameters denoted as t_t and $(P_D)^*$. In such a case eq. (40) should be written in the following form (MALOSZEWSKI & ZUBER 1985, 1989):

$$C(t) = \frac{M}{Qt_t[4\pi(P_D)^*(t/t_t)^3]^{1/2}} \exp\left[-\frac{(1-t/t_t)^2}{4(P_D)^* t/t_t}\right] \quad (41)$$

The relation between the apparent and physical parameters can be found by applying the method of moments (see e.g., KREFT & ZUBER 1978; or RASMUSON 1985). Generaly from any tracer concentration curve one may find the mean transit time of tracer t_t and the time variance of the curve $(\sigma_t)^2$ as the first moment and the second central moment, respectively. This method can also be applied directly to the known theoretical tracer concentration at the outlet from the fissures (eq. 6 or 16). In this way one obtains the relation between t_t and $(\sigma_t)^2$ and the physical parameters of the PFDM. The ratio $(\sigma_t)^2/[2(t_t)^2] = (P_D)^*$ is further called in this paper the apparent dispersion parameter.

Following the above mentioned principle, the mean transit time of tracer is defined as:

$$t_t = \int_0^\infty t\,C(t)\,dt \;/\; \int_0^\infty C(t)\,dt \quad (42)$$

where C(t) is the tracer output concentration resulting from an instantaneous injection.

By inserting $C(t) = C_f(t)$ (eq. 6 or 16) into eq. (42) and by making use of the Laplace transform and its properties one gets for a nonradioactive tracer ($\lambda = 0$) (MALOSZEWSKI & ZUBER 1984):

$$t_t = (1 + 2ap)\,R_{af} t_o = Rt_o, \quad \text{or} \quad v_t = v/R \quad (43)$$

where v_t is the mean tracer velocity, and R is the total retardation factor. For a reactive tracer which follows an instantaneous equilibrium reaction with a linear adsorption isotherm in both matrix and fissures, the R-factor is:

$$R = R_{af}\left[1 + (n_p/n_f - n_p)R_{ap}/R_{af}\right] \approx R_{af}\left[1 + n_p R_{ap}/(n_f R_{af})\right] \quad (44)$$

For a nonreactive tracer ($R_{af} = R_{ap} = 1$), eq. (44) simplifies to:

$$R = R_p = 1 + (n_p/n_f) - n_p \approx 1 + n_p/n_f \quad (45)$$

with R_p defined as the retardation factor due to matrix diffusion without any reaction.

Equations (44) and (45) do not depend on the geometry of the fissure network, therefore one may guess that they are valid for any double-porosity medium. This finding can be confirmed by the results of GOLZ & ROBERTS (1986), who investigated theoretically granular media of double porosity. From their results one can easily obtain eq. (45) with the microporosity of grains replaced by n_p, and the macroporosity of the granular medium replaced by n_f. Note that from eq. (43) the retardation factor is equal to the mean relative transit time of tracer.

As mentioned, the time variance of the tracer is defined by the second central moment, i.e. by:

$$(\sigma_t)^2 = \int_0^\infty (t - t_t)^2 \, C(t) \, dt \; / \; \int_0^\infty C(t) \, dt \tag{46}$$

which for the PFDM (eq. 6), and a nonradioactive and nonreactive tracer was given in MALOSZEWSKI & ZUBER (1992a). A more general form, i.e., for $R_{af} > 1$ and $R_{ap} > 1$, it reads:

$$(\sigma_t)^2 = 2(t_t)^2 \left[P_D + \frac{5ap^3}{6t_o(R)^2}\right] \tag{47.1}$$

For the PFPFM the variance is:

$$(\sigma_t)^2 = 2(t_t)^2 \, \frac{5ap^3}{6t_o(R)^2} \tag{47.2}$$

For eq. (41) with apparent parameters, eq. (46) yields

$$(\sigma_t)^2 = 2(t_t)^2 \, (P_D)^* \tag{48}$$

By combining eqs (47.1)-(47.2) with (48) one obtains finally that for the theoretical tracer concentration curve the apparent dispersion parameter is:

$$(P_D)^* = P_D + 5ap^3/[6t_o(R)^2] \qquad \text{for PFDM,} \tag{49.1}$$

or

$$(P_D)^* = 5ap^3/[6t_o(R)^2] \qquad \text{for PFPFM.} \tag{49.2}$$

The above equations relate the mean transit time (t_t) and the apparent dispersion parameter $(P_D)^*$ to the physical parameters of the models discussed. To solve the inverse problem it is necessary to define the conditions under which the ordinary dispersion model can be calibrated and when its apparent parameters obtained by calibration are related to fracture rock parameters by eqs (43) and (49.1) or (49.2). As the first approximation, based on eq. (39.1), one can

assume that if the mean transit time $t_o \geq t_{min}$, the DM can be applied. However, when interpreting a field experiment one never knows if the condition (39.1) is satisfied. In other words one may often fit the DM but the obtained values of t_t and $(P_D)^*$ are doubtful unless the parameters are checked posteriori. An example of such a procedure is given in Chapter 4.2.1.

When the ordinary dispersion model is applicable and its parameters known (t_t and P_D^*), it is possible to solve some types of direct problems (e.g., to predict pollutant transport) without using the PFDM. In general, in such a case, a detailed knowledge on the fissure network is not needed. These problems are further discussed in Chapter 4.

For the single fissure approximations, the parameter $p \approx \infty$ and the mean transit time $t_t \approx \infty$, the method of moments is then theoretically inapplicable and attempts to its practical applications will lead to serious errors.

2.3.2 Ordinary Dispersion Model for a variable input concentration

The ordinary dispersion model is particularly useful for the interpretation of some environmental tracer data. However, the final interpretation should be based on conditions drawn from the PFDM as shown below. The well known convolution integral is used to relate a variable input concentration, $C_{in}(t)$, to the output concentration, C(t),

$$C(t) = \int_0^\infty C_{in}(t-\tau)\exp(-\lambda\tau)\, g(\tau)\, d\tau \qquad (50)$$

where $g(\tau)$ is the normalized response of the system to an instantaneous injection of an ideal tracer at $\tau=0$. For the known $g(\tau)$ function, eq. (50) yields the output tracer concentration for any $C_{in}(t)$ function. The system response function can be found from the following formula:

$$g(\tau) = C_f(t=\tau,\lambda=0)\, Q/M \qquad (51)$$

In the lumped-parameter approach the $g(\tau)$ function usually represents the distribution of the transit times related to different flow paths, but not to the hydrodynamic dispersion in the system. For instance, Pe in eq. (6) is related to the dispersion coefficient in fissures, whereas in the case the DM employed in eq. (50), Pe is an apparent quantity related to the ratio of recharge area length to the total lenght of the system measured along the flow lines (MALOSZEWSKI & ZUBER 1982; ZUBER 1986). In other words, the exit age distribution function and its parameters are used in a macroscopic meaning, whereas eq. (6) describes the behaviour of tracer in a microscopic meaning. Thus, the solution (6) cannot be applied directly in (50) for interpreting the environmental tracer data at a large scale.

In the previous Chapter it was shown that, the ordinary dispersion model (eq. 41) calibrated to experimental data yields t_t. Equation (41) normalized in order to obtain the $g(\tau)$ function reads

$$g(\tau) = \frac{1}{\tau[4\pi(P_D)^*(\tau/t_t)]^{1/2}} \exp\left[-\frac{(1-\tau/t_t)^2}{4(P_D)^*\tau/t_t}\right] \qquad (52)$$

By anology to artificial tracer experiments in fissures one may expect, that the equation

$$t_t = R_p t_o = t_o[1 + (n_p/n_f) - n_p] \approx t_o(n_f + n_p)/n_f \tag{53}$$

will also be applicable, if the tracer remains long enough in a system to occupy the whole microporous matrix. Equation (10.1) put into eq. (53) yields

$$t_t = t_o(V_f + V_p)/V_f = (V_f + V_p)/Q = V/Q \tag{54}$$

where Q is the volumetric flow rate of water through the system, measured in the outflow (discharge of a spring or stream), V_f and V_p are the volumes of water in the fissures (mobile) and in the porous matrix (stagnant), respectively, and V is the total volume of water in the system (mobile + stagnant).

The above considerations show that the interpretation of environmental tracers (e.g., tritium) by making use of the ordinary dispersion model (eq. 52) yields the mean transit time of tracer, which for an ideal tracer is related to the fissure system by (eq. 54). If the discharge (Q) is known, the total volume of water in the groundwater system is $V=t_tQ$. The volume of the mobile water in the system remains unknown unless the retardation factor (R_p) is known.

2.4 Models for steady and transient states in the case of a constant input concentration

2.4.1 Parallel Fissure Piston Flow Model in a steady state

The Parallel Fissure Piston Flow Model (PFPFM) in a steady state developed by the author (MALOSZEWSKI & ZUBER 1991), which is an extended form of the model introduced by NERETNIEKS (1981), accounts for possible reactions. The model is particularly useful for the ^{14}C tracer. The radiocarbon has entered groundwater systems since thousands of years with a constant input concentration, and at present, in the time domain, it already exists in a steady state. It means that the solution of the transport equation for $C_f(0,t)=C_o$, $t=\infty$, and $D=0$ is sought. For the reaction model discussed in Chapter 2.2.1 the transport equation reads:

$$\frac{\partial C_f}{\partial t} + \frac{v}{R_{af}}\frac{\partial C_f}{\partial x} - \frac{n_p D_p}{R_{af} b}\frac{\partial C_p}{\partial y}\bigg|_{y=b} + \lambda C_f = 0 \tag{56}$$

$$R_{ap}\frac{\partial C_p}{\partial t} - D_p\frac{\partial^2 C_p}{\partial y^2} + \frac{(1-n_p)\rho}{n_p}\left[\frac{\partial q_2}{\partial t} + \lambda q_2\right] + \lambda R_{ap} C_p = 0 \tag{57}$$

$$\frac{\partial q_2}{\partial t} = k_1\frac{n_p C_p}{(1-n_p)\rho} - k_2 q_2 - \lambda q_2 = 0 \tag{58}$$

The solution of eqs (56)-(58) with boundary conditions (4.1), (4.3)-(4.6), (22.2)-(22.3) and $C_f(0,t)=C_o$, where C_o is the constant input concentration, was derived for $t \approx \infty$ by the author in MALOSZEWSKI & ZUBER (1991) and has the following form

$$C_f(x,\infty)/C_o = \exp\left\{ -\lambda R_{af} t_o [1 + 2aB\lambda^{-1/2}\tanh(Z)] \right\} \tag{59}$$

where a is expressed here by eq. (9.3) and

$$Z = R_{ap}\lambda^{1/2}(1-n_f)n_p B/(2an_f R_{af}) \tag{60.1}$$

$$B = \left[(k_2+\lambda+k_1/R_{ap})/(k_2+\lambda) \right]^{1/2} \tag{60.2}$$

Equation (59) describes the distribution of a radioactive and reactive tracer along the system of parallel fissures, after infinitively long time since the begining of injection with a constant concentration. This solution can be simplified by making use of the following known relations:

$$\tanh(\Theta) = \Theta \qquad \text{for } \Theta \le 0.25 \tag{61.1}$$

$$\tanh(\Theta) = 1 \qquad \text{for } \Theta \ge 2 \tag{61.2}$$

If $R_{ap}(1-n_f)n_p B\lambda^{1/2} / (2an_f R_{af}) \le 0.25$, eq.(59) has the form

$$C_f(x,\infty)/C_o = \exp\left\{ -\lambda R_{af} t_o [1 + R_{ap}(1-n_f)n_p B^2/(R_{af} n_f)] \right\} \tag{62.1}$$

whereas if $R_{ap}(1-n_f)n_p B\lambda^{1/2} / (2an_f R_{af}) \ge 2$, eq. (59) simplifies to

$$C_f(x,\infty)/C_o = \exp\left[-\lambda R_{af} t_o (1 + 2aB\lambda^{-1/2}) \right] \tag{62.2}$$

For $n_f << 1$ and $k_2 >> \lambda$, which is probably the most common case in practice, eq. (59) simplifies to:

$$C_f(x,\infty)/C_o = \exp\left(-\lambda R_{af} t_o \left\{ 1 + 2a\lambda^{-1/2}[1+k_1/(k_2 R_{ap})] \tanh(E) \right\} \right) \tag{63}$$

where

$$E = b\,[\lambda(R_{ap}+k_1/k_2)]^{1/2} / (n_f D_p^{1/2}) \tag{64}$$

From eqs (61.1) and (61.2) some additional simplifications of eq. (63) can easily be found.

If $b\,[\lambda(R_{ap}+k_1/k_2)]^{1/2} / (n_f D_p^{1/2}) \le 0.25$

$$C_f(x,\infty)/C_o = \exp\left\{ -\lambda t_o [R_{af} + (R_{ap}+R_{ak})n_p/n_f] \right\} \tag{65.1}$$

whereas if $b\,[\lambda(R_{ap}+k_1/k_2)]^{1/2} / (n_f D_p^{1/2}) \geq 2$

$$C_f(x,\infty)/C_o = \exp\left(-\lambda R_{af} t_o \left\{ 1 + 2a[(R_{ap}+R_{ak})/(\lambda R_{af})]^{1/2} \right\} \right) \tag{65.2}$$

where

$$R_{ak} = k_1/k_2 \tag{66}$$

is the contribution to the retardation factor, caused by the kinetic reaction in the matrix.

If there is no kinetic reaction between the solute and the matrix, i.e. $k_1 = R_{ak} = 0$, the main solution (59) simplifies to

$$C_f(x,\infty)/C_o = \exp\left\{ -\lambda R_{af} t_o [1 + 2a\lambda^{-1/2}\tanh(F)] \right\} \tag{67}$$

where

$$F = R_{ap}(1-n_f)n_p\lambda^{1/2} / (2an_f R_{af}) \tag{68}$$

For $R_{ap}(1-n_f)n_p\lambda^{1/2} / (2an_f R_{af}) \leq 0.25$, eq. (67) simplifies to

$$C_f(x,\infty)/C_o = \exp\left\{ -\lambda R_{af} t_o [1 + R_{ap}(1-n_f)n_p/(R_{af} n_f)] \right\} \tag{69.1}$$

whereas for $R_{ap}(1-n_f)n_p\lambda^{1/2} / (2an_f R_{af}) \geq 2$ to

$$C_f(x,\infty)/C_o = \exp\left[-\lambda R_{af} t_o (1 + 2a\lambda^{-1/2}) \right] \tag{69.2}$$

Finally for a nonreactive tracer ($R_{af} = R_{ap} = 1$, $R_{ak} = 0$), the solution (59) simplifies to

$$C_f(x,\infty)/C_o = \exp\left(-\lambda t_o \left\{ 1 + 2a\lambda^{-1/2}\tanh[\lambda^{1/2}(1-n_f)n_p/(2an_f)] \right\} \right) \tag{70}$$

where the a-parameter is now expressed by eq. (11.1).

Equation (70) can further be simplified.

If $(1-n_f)n_p\lambda^{1/2} / (2an_f) \leq 0.25$

$$C_f(x,\infty)/C_o = \exp\left\{ -\lambda t_o [1 + (1-n_f)n_p/n_f] \right\} \tag{71.1}$$

whereas, if $(1-n_f)n_p\lambda^{1/2} / (2an_f) \geq 2$

$$C_f(x,\infty)/C_o = \exp\left[-\lambda t_o (1 + 2a\lambda^{-1/2}) \right] \tag{71.2}$$

The main model (eq. 59) and its simplifications are applicable for the interpretation of the environmental radioactive tracer data (e.g., ^{14}C) in fissured aquifers. To decide which simplification can be used, an independent information on the system and reaction parameters is required. Due to a large number of parameters the model cannot be used to solve the inverse problem. However, by solving the direct problem, the differences between the water velocity obtained from the ^{14}C age and from hydrologic methods can be explained (see also Chapter 4.2.3).

The radioisotope age (t_a) in the piston flow approximation is defined by the well known formula

$$C_f(x,\infty)/C_o = \exp(-\lambda t_a) \tag{72}$$

For a reactive tracer (e.g., radiocarbon) which follows the exchange reactions described above, one obtains the relation between the mean transit time of water (t_o) and radioisotope age (t_a) by combing eqs (72) and (59):

$$t_a/t_o = R_{af} + R_{af}\Big\{2a\lambda^{-1/2}[(k_2+\lambda+k_1/R_{ap})/(k_2+\lambda)]^{1/2} \cdot \tanh\big(R_{ap}\lambda^{1/2}(1-n_f)n_p/(2an_fR_{af})[(k_2+\lambda+k_1/R_{ap})/(k_2+\lambda)]^{1/2}\big)\Big\} \tag{73}$$

with the a-parameter expressed by eq. (9.3).

For nonsorbable radioisotope, eqs (72) and (70) yield

$$t_a/t_o = 1 + 2a\lambda^{-1/2}\tanh[\lambda^{1/2}(1-n_f)n_p/(2an_f)] \tag{74}$$

Practical simplification of eqs (73) and (74) can easily be obtained by applying the solutions discussed above within this Chapter.

From eqs (73) and (74) it is self-evident that in a fissured aquifer, even in the case of the piston flow, the radioisotope age differs from the mean transit time of water, and is not related by the simple concept of the diffusion retardation factor given by eq. (43).

2.4.2 Single Fissure Piston Flow Model (SFPFM) in steady and transient states

In some cases one may assume that the tracer flows only through a single fissure. Then the system of eqs (56)-(58) is solved by applying the boundary condition (22.1), instead of (4.6). After simple recalculation of the Laplace transforms given in MALOSZEWSKI & ZUBER (1991) one obtains

$$C_f(x,\infty)/C_o = \exp\Big(-\lambda t_o R_{af}\big\{1 + 2a\lambda^{-1/2}[(k_1/R_{ap}+k_2+\lambda)/(k_2+\lambda)]^{1/2}\big\}\Big) \tag{75}$$

where a is expressed by eq. (9.3).

If there is no kinetic reactions in the matrix, i.e. $k_1=k_2=0$, eq. (75) simplifies to eq. (69.2), whereas for ideal tracer to eq. (71.2).

This model (eq. 75) is especially applicable when the tracer flows through a thin aquifer situated in a infinitely thick aquiclude. In such a case the fissure parameters are replaced by the aquifer parameters, i.e. the fissure aperture (2b) is replaced by $n_e m$, where n_e is the aquifer porosity, and the matrix parameters (n_p, D_p) are replaced by the aquitard parameters (n_a, D_a). If the aquifer is of large extents, it may be necessary to consider a transient state. Then, the solution of the transport equation is sought as a function of time and space. However, as the experimental data are distributed in space, the solution is sought as a function of space for a given time. An example of such a solution obtained by the author can be found in NOLTE et al. (1991).

2.5 Summary of the models developed for artificial tracer experiments

The main models developed by the author and discussed in previous Chapters are summarized in Table 1 together with their fitting parameters represented by the physical parameters.

Table 1 Summarizing of the main developed models and their parameters

MODEL	Eq.	PARAMETERS			
PFDM					
with instantaneous equilibrium reaction in fissures and in the matrix	(6)	$t_o'=t_o/R_{af}$	Pe	$a=n_p(D_pR_{ap})^{1/2}/(2bR_{af})$	$p=2b\sqrt{R_{ap}}/(2n_f\sqrt{D_p})$
with instantaneous reaction in the matrix	(6)	t_o	Pe	$a=n_p(D_pR_{ap})^{1/2}/(2b)$	$p=2b\sqrt{R_{ap}}/(2n_f\sqrt{D_p})$
without reactions	(6)	t_o	Pe	$a=n_p(D_p)^{1/2}/(2b)$	$p=2b/(2n_f\sqrt{D_p})$
PFPFM					
with instantaneous equilibrium reaction in fissures and in the matrix	(16.1)	$t_o'=t_o/R_{af}$		$a=n_p(D_pR_{ap})^{1/2}/(2bR_{af})$	$p=2b\sqrt{R_{ap}}/(2n_f\sqrt{D_p})$
with instantaneous reaction in the matrix	(16.1)	t_o		$a=n_p(D_pR_{ap})^{1/2}/(2b)$	$p=2b\sqrt{R_{ap}}/(2n_f\sqrt{D_p})$
without reactions	(16.1)	t_o		$a=n_p(D_p)^{1/2}/(2b)$	$p=2b/(2n_f\sqrt{D_p})$

Table 1 continued

SFDM	Eq.	PARAMETERS				
with instantaneous equilibrium reaction in fissures and combined reactions in the matrix	(23)	$t_o'=t_o/R_{af}$	Pe	$a=n_p(D_pR_{ap})^{1/2}/(2bR_{af})$	$k_1'=k_1/R_{ap}$	k_2
with instantaneous reaction in the matrix and in fissures	(25)	$t_o'=t_o/R_{af}$	Pe	$a=n_p(D_pR_{ap})^{1/2}/(2bR_{af})$	-	-
with combined reaction in the matrix (without reaction in fissures)	(23)	t_o	Pe	$a=n_p(D_pR_{ap})^{1/2}/(2b)$	$k_1'=k_1/R_{ap}$	k_2
without kinetic reactions in the matrix and reactions in fissures	(25)	t_o	Pe	$a=n_p(D_pR_{ap})^{1/2}/(2b)$	-	-
without any reactions	(25)	t_o	Pe	$a=n_p(D_p)^{1/2}/(2b)$	-	-

3 Theoretical tracer concentration curves: the direct problem

Direct problems are solved by calculating the tracer concentration curves with the aid of the solutions to the transport equation for assumed values of parameters. Within this chapter, tracer concentration curves produced with the aid of the Parallel Fissure Dispersion Model (PFDM - see Chapter 2.1.1) are shown and compared with the curves obtained from the Dispersion Model (DM) and the Single Fissure Dispersion Model (SFDM). The curves obtained with the aid of the Parallel Fissure Piston Flow Model (PFPFM) are also shown. For graphical presentation of the results, the normalized tracer concentration $[C_f(t)Qt_o/M=C_f(t)V_f/M]$ and the normalized time (t/t_o) are used. This way of normalization is well known in chemical engineering and was introduced to hydrogeology by ZUBER (1971). For porous aquifers, the normalized concentration curves are independent of the mass of tracer injected (M), the volumetric flow rate (Q), and the mean transit time (t_o). In the case of fissured aquifers, it is not possible to eliminate the influence of t_o on the theoretical curves, however, this way of normalization seems to be still very convenient for a concise presentation of different curves obtained for different sets of parameters.

3.1 Parallel fissure models in the case of an instantaneous injection

Figures 5, 6 and 7 present concentration curves calculated with the aid of the PFDM (eq. 6) for an ideal tracer. Examples of the values of physical parameters which can be combined to obtain the model parameters a and p are given in Table 2. In Table 2 there are also shown the retardation factors, which as mentioned are equal to the mean relative transit time of tracer ($R=t_t/t_o$; eq. 43), and the normalized time variance of the concentration curve, i.e. the dispersion parameter of tracer $(P_D)^*=(\sigma_t)^2/[2(t_t)^2]$, calculated from a, p and P_D, by making use of eq. (47.1).

Figure 5 shows the influence of the model parameters a and p (eqs 11.1 and 11.2, respectively) for a constant value of $t_o=1$ year and a constant value of the dispersion parameter ($P_D=0.005$). The mean transit time of water (t_o) is relatively long and because of that the curves have a tendency to be symmetrically distributed around the mean relative transit time of tracer, i.e around $t_t/t_o \approx R_p$. It means, that the transport of tracer in the comparison to the mean transit time of water is R_p-times delayed. The curves show that when the a-parameter increases for a constant p, p increases for a constant a, a larger value of R_p is produced, which means a stronger delay of tracer (compare curves 1, 2 and 3 for a constant value of a, and 1 with 4, or 5 with 2 for two constant values of p). At the same time, for greater values of a, and/or p, the curves are more strongly dispersed (compare curves 1 and 4 for an increased value of a in the case of a constant p, and curves 1, 2 and 3 for larger value of p in the case of a constant value of a).

It is interesting to analyze directly the influence of the physical paramaters, which are hidden under the model parameters. Their values are summarized in Table 2. An increase in the matrix porosity (n_p) for other parameters being constant, increases the a-parameter, and consequently the R_p factor, which yields a greater delay (curves 1 and 4). The same effect is observed for decreased fissure porosity (n_f), which increases the value of the p-parameter, and produces a

greater retardation factor (compare curves 1, 2 and 3). By changing either the fissure apperture (2b) or the diffusion coefficient in the matrix (D_p), both a and p will be changed in the same way but in the oposite directions. In consequence, the retardation factor (R_p) remains unchanged (see eq. 45). However, a decreased fissure apperture or diffusion coefficient produce more asymmetrical curves, i.e. more dispersed, as it is shown by comparison of curves 1 with 5, or 4 with 2.

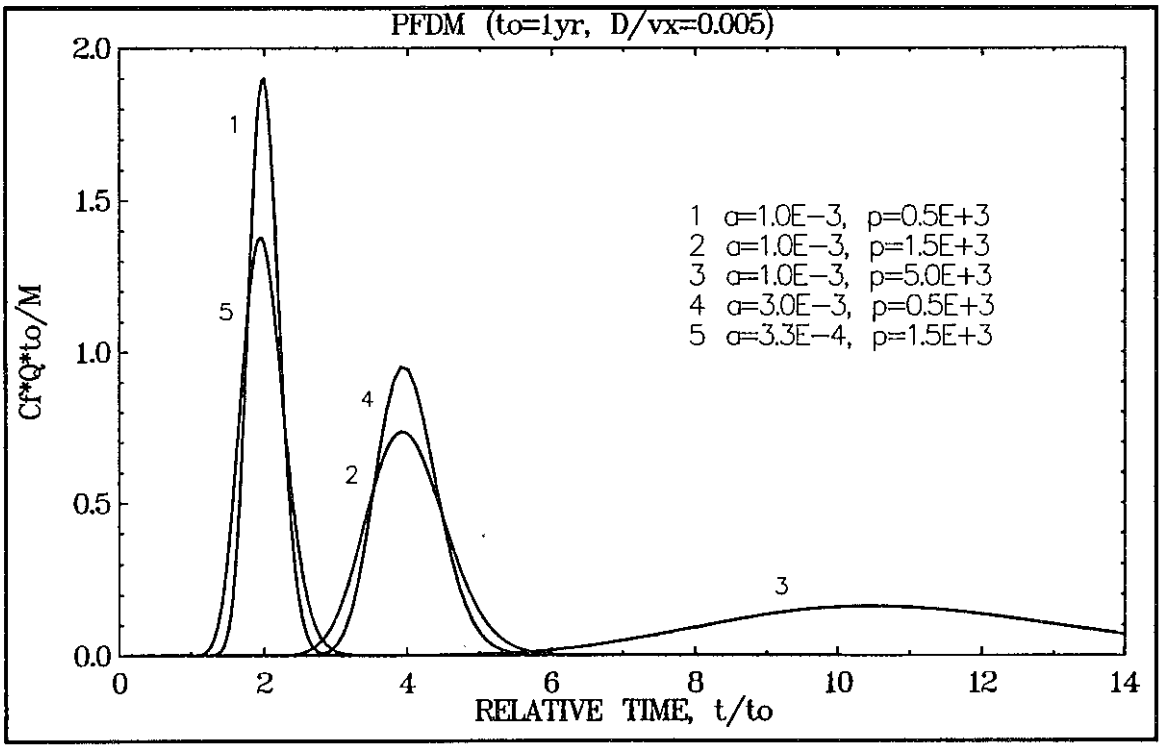

Fig. 5 **The influence of the a and p parameters on the shape of tracer concentration curves calculated from the PFDM (for physical parameters see Table 1)**

Figures 6 and 7 demonstrate the influence of the mean transit time of water (t_o) on the shape of the tracer concentration curves calculated when all the other parameters remain unchanged. The curves in Fig. 7 are calculated for greater p-parameter value than those in Fig. 6. A decrease of the mean transit time of water, for a constant value of the dispersion parameter (P_D) means an increase of water velocity (v). In such a case the tracer concentration curve is more dispersed, i.e. more asymmetrical (compare curve 1 with others in Fig. 6 or in Fig. 7). This effect increases with an increased value of p (e.g., with a decrease of fissure porosity, n_f), what is easy to observe by comparison of curves 1 in Figs 6 and 7.

A relatively good symmetry of the concentration curves at long transit times (long-term tracer experiments) suggests the applicability of the ordinary dispersion model (DM) with t_t and $(P_D)^*$, as it was described by MALOSZEWSKI & ZUBER (1984, 1985) and was also discussed in Chapter 2.3. For the sake of simplicity, contrary to MALOSZEWSKI & ZUBER (1984, 1985), the dispersion model was not fitted to the PFDM-curves but calculated directly for known values of parameters. In that way it is possible to check if the DM-curves calculated with the exact

values of tracer parameters agree with the PFDM-curves. The exact values of tracer parameters t_t and $(P_D)^*$ were found from the model parameters (a, p, t_o and P_D) by making use of eqs (43) and (49.1). It is evident that for comparing the DM-curves with the PFDM-curves, the concentrations calculated using eq. (41) with apparent parameters have to be normalized in the same way as the PFDM-curves. It has to be done by introducing directly Rt_o (eq. 43) instead of t_t in eq. 41 (it was not clearly described in MALOSZEWSKI & ZUBER 1985; in their eq. 24).

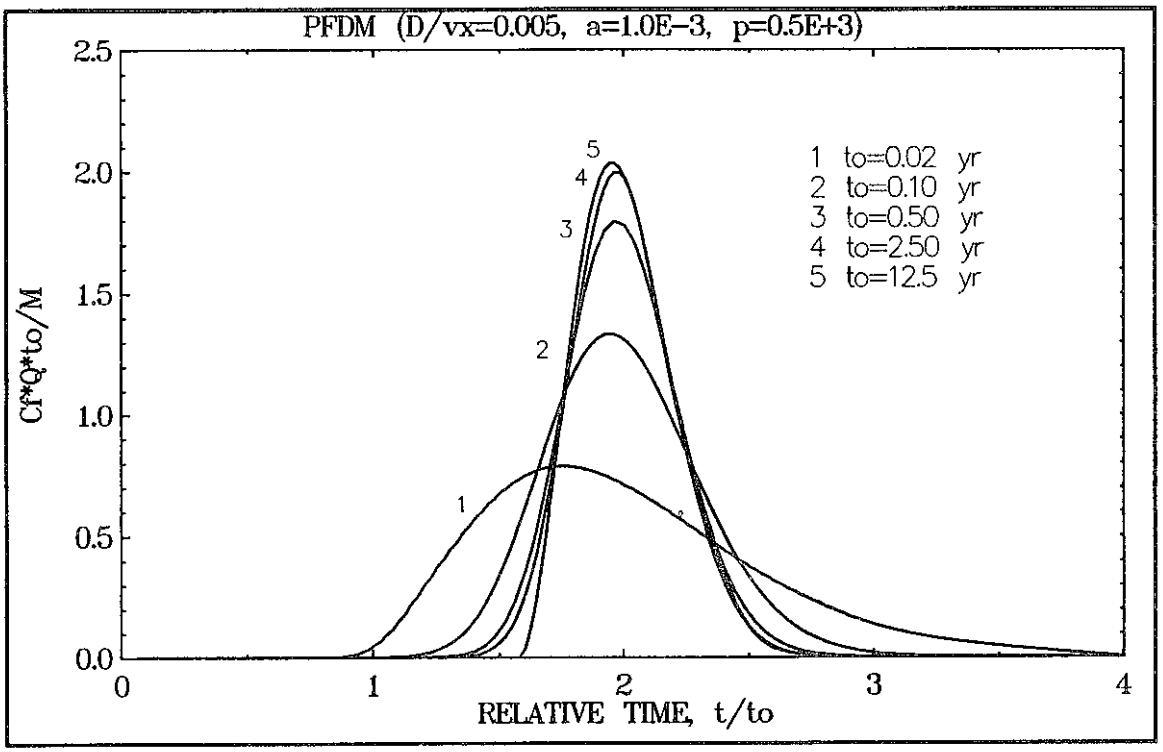

Fig. 6 **The influence of the mean transit time of water on the shape of tracer concentration curves calculated from the PFDM for a small value of the p-parameter (for physical parameters see Table 2)**

For the parameters shown in Figs 5-7 all the DM-curves obtained for the mean transit time of water $t_o > 0.5$ yr are exactly the same as those from the PFDM, whereas for $t_o < 0.1$ yr they are slightly different for $p = 0.5 \cdot 10^3$ $s^{1/2}$ and they are completely different for $p = 1.5 \cdot 10^3$ $s^{1/2}$ (the DM-curves are not shown in Figs 6 and 7). The differences between the DM and PFDM curves are demonstrated in Fig. 8. For $a = 5 \cdot 10^{-3}$ $s^{1/2}$ and $p = 5 \cdot 10^3$ $s^{1/2}$, the DM-curves become nearly the same as the PFDM-curves, when the mean transit time of water is greater than 2.5 yr.

The numerical findings presented above, prove that in long-term tracer experiments it is possible to describe the concentration curves by applying the ordinary dispersion model with tracer parameters related to physical parameters. It means that for a long transit time of water through the system, the tracer has enough time to diffuse into the porous matrix to occupy the whole space between the fissures. In such a case, the tracer transport can be described similarly to the tracer transport in porous systems, but with a delay given by eq. (45). This finding is of great importance due to two reasons. First, it proves that the DM can be used for solving the

inverse problem. Second, the applicability of the DM instead of the PFDM demonstrates the interplay of the PFDM parameters. In other words, it is not possible to solve in a unique way the inverse problem by making use of the PFDM. The parameters t_t and $(P_D)^*$ are the combinations of the real PFDM parameters (t_o, P_D, a and p) as it is shown by eqs (43) and (49.1). It means, that for given values of t_t and $(P_D)^*$, the same tracer curve can be obtained for different combinations of t_o, P_D, a and p parameter values. Their values have to satisfy only eqs (45) and (49.1).

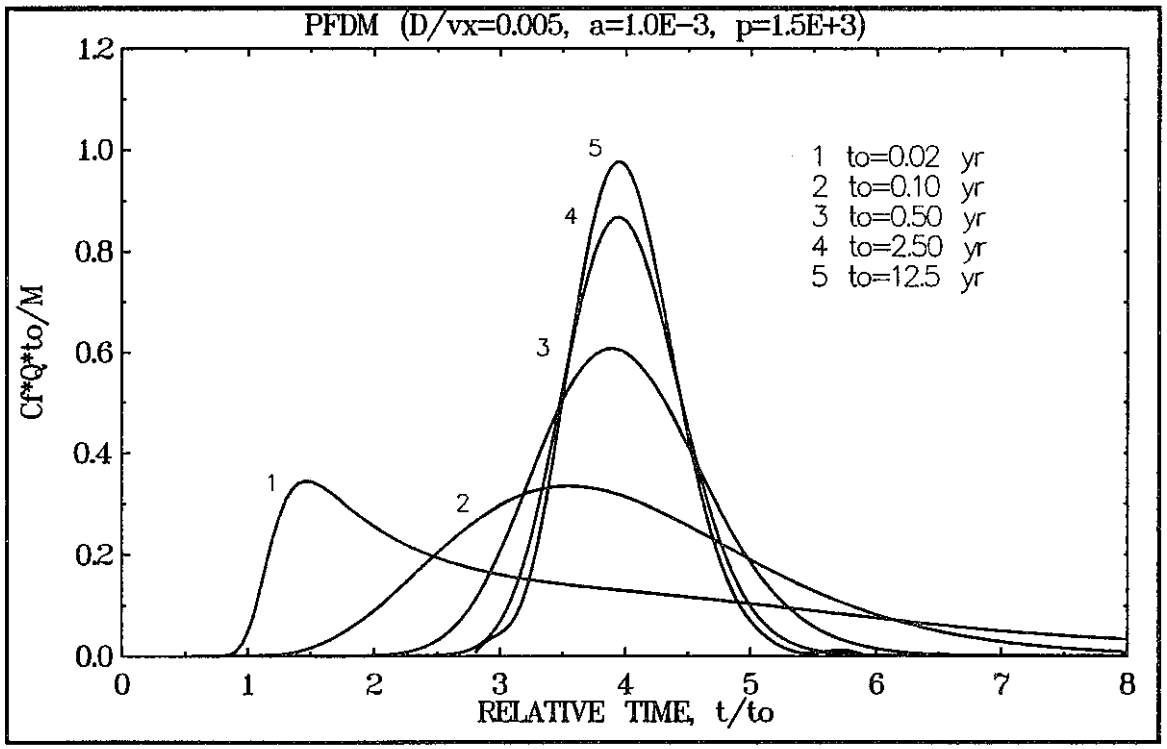

Fig. 7 **The influence of the mean transit time of water on the shape of tracer concentration curves calculated from the PFDM for the p-parameter three times larger than that in Fig. 6 (for physical parameters see Table 2)**

Another problem is the definition of a long-term experiment, or the mean transit time of water for which an equilibrium of tracer distribution between the fissures and matrix is obtained. In Chapter 2.3.1 a rough approximation represented by eq. (39.1) or (39.2) was given. This equation requires the mean transit time to satisfy the condition $(t_o)_{min} > t_{min}$. The numerical examination of that formula for the examples shown in Table 2 proves its satisfactory applicability. By the mean transit time of water $t_o = 1$ yr the curves given in Fig. 5 yield the largest value of $t_{min} = 304$ days for $a = 10^{-3}$ $s^{-1/2}$ and $p = 5 \cdot 10^3$ $s^{1/2}$ (curve 3). In Fig. 6 the transit time $(t_o)_{min} \geq 23$ days is needed, whereas the DM-curves for $t_o = 30$ days are still slightly different. For $a = 10^{-3}$ $s^{-1/2}$ and $p = 1.5 \cdot 10^3$ $s^{1/2}$ shown in Fig. 7, $(t_o)_{min}$ should be greater than 104 days what agrees very well. For $a = 5 \cdot 10^{-3}$ $s^{-1/2}$ and $p = 5 \cdot 10^3$ $s^{1/2}$ shown in Fig. 8, $(t_o)_{min} > 100$ days is required, however $t_o = 2.5$ years does not yet produce an exact agreement

between the PFDM and DM curves. It seems that the greater the value of p and the smaller the value of a, the better the approximation given by eq. (39.1).

Table 2 **Parameters used for the calculation of theoretical concentration curves shown in Figs 5-8 and tracer parameters calculated by making use of eqs (43) and (49.1). The values of n_p, n_f, D_p and 2b can be recalculated to other parameters by making use of eqs (11.1) and (11.2). For all cases P_D=0.005, except for 8.1 - 8.3 where P_D=0.05.**

Parameters									
	Model		Physical					Tracer	
Fig/ Curve	a	p	n_p	n_f	D_p	2b	t_o	R	$(P_D)^*$
	$s^{-1/2}$	$s^{1/2}$	-	-	m^2/s	μm	yr	-	-
5/1	10^{-3}	$0.5 \cdot 10^3$	0.01	0.01	10^{-10}	100	1	2	0.0058
5/2	10^{-3}	$1.5 \cdot 10^3$	0.01	0.0033	10^{-10}	100	1	4	0.0106
5/3	10^{-3}	$5.0 \cdot 10^3$	0.01	0.001	10^{-10}	100	1	11	0.0320
5/4	$3 \cdot 10^{-3}$	$0.5 \cdot 10^3$	0.03	0.01	10^{-10}	100	1	4	0.0056
	$3 \cdot 10^{-3}$	$0.5 \cdot 10^3$	0.01	0.0033	10^{-10}	33	1	4	0.0056
5/5	$10^{-3}/3$	$1.5 \cdot 10^3$	0.01	0.01	10^{-11}	100	1	2	0.0124
6/1	10^{-3}	$0.5 \cdot 10^3$	0.01	0.01	10^{-10}	100	0.02	2	0.0462
6/2	10^{-3}	$0.5 \cdot 10^3$	0.01	0.01	10^{-10}	100	0.10	2	0.0132
6/3	10^{-3}	$0.5 \cdot 10^3$	0.01	0.01	10^{-10}	100	0.50	2	0.0067
6/4	10^{-3}	$0.5 \cdot 10^3$	0.01	0.01	10^{-10}	100	2.5	2	0.0053
6/5	10^{-3}	$0.5 \cdot 10^3$	0.01	0.01	10^{-10}	100	12.5	2	0.0051
7/1	10^{-3}	$1.5 \cdot 10^3$	0.01	0.0033	10^{-10}	100	0.02	4	0.2840
7/2	10^{-3}	$1.5 \cdot 10^3$	0.01	0.0033	10^{-10}	100	0.10	4	0.0612
7/3	10^{-3}	$1.5 \cdot 10^3$	0.01	0.0033	10^{-10}	100	0.50	4	0.0161
7/4	10^{-3}	$1.5 \cdot 10^3$	0.01	0.0033	10^{-10}	100	2.5	4	0.0072
7/5	10^{-3}	$1.5 \cdot 10^3$	0.01	0.0033	10^{-10}	100	12.5	4	0.0054
8/1	$5 \cdot 10^{-3}$	$5.0 \cdot 10^3$	0.05	0.001	10^{-10}	100	0.10	51	0.1134
8/2	$5 \cdot 10^{-3}$	$5.0 \cdot 10^3$	0.05	0.001	10^{-10}	100	0.50	51	0.0627
8/3	$5 \cdot 10^{-3}$	$5.0 \cdot 10^3$	0.05	0.001	10^{-10}	100	2.5	51	0.0525

One may expect that in the oposite case, i.e., if the mean transit time of water is relatively short, it should be possible to replace the PFDM by the Single Fissure Dispersion Model (SFDM). Physically it means that the tracer has not enough time for diffusion, and, consequently for the penetration of the porous matrix deep enough to be influenced by adjacent fissures (see Chapter 2.2.1). Mathematically, it means that the tracer concentration curves produced by the PFDM are the same as those yielded by the SFDM (eq. 25). For an ideal tracer, this phenomena is graphically demonstrated in Figs 9 and 10. The curves are calculated for the parameter values which are often met in natural systems, i.e. $a=5\cdot10^{-3}$ $s^{-1/2}$ and $p=5\cdot10^{3}$ $s^{1/2}$. For instance, they correspond to $D_p=10^{-10}$ m^2/s, $2b=100\mu m$, $n_p=0.05$ and $n_f=0.001$. In Figs 9 and 10, $P_D=0.05$ and $P_D=0.1$ are used, respectively. In both figures the tracer concentration curves (1 and 1') obtained with the PFDM and the SFDM agree perfectly for the mean transit time of water (t_o) of 1.8 days and for the observation time up to 90 days ($50t_o$) after the injection. The SFDM-curves which were calculated for greater transit times (curve 2' for 3.6 and curve 3' for 18 days, respectively), begin earlier to differ from those of the PFDM (cuves 2 and 3).

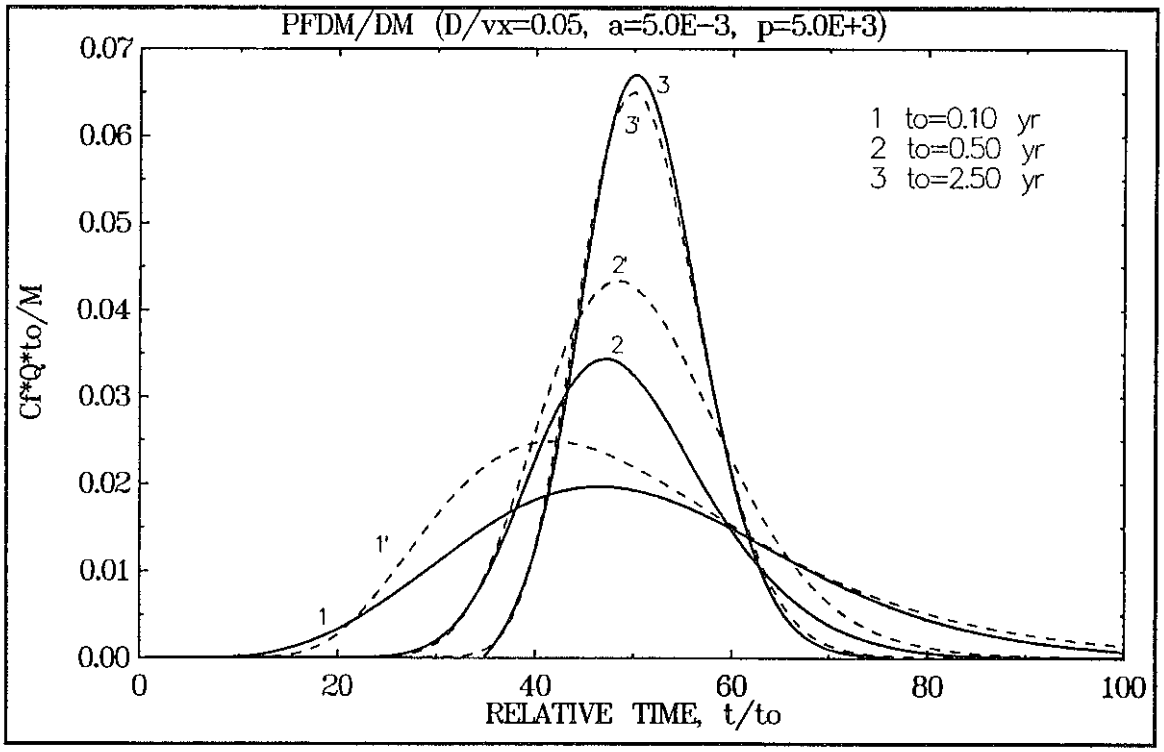

Fig. 8 **The comparison of tracer concentration curves obtained from the PFDM (solid lines) with those of the DM (dashed lines) in the case of different values of the mean transit time of water (see also Table 2), which demonstrates that in long-term tracer experiment the DM yields nearly the same curve as the PFDM (for physical parameters see Table 2)**

The concentration curves calculated for $t_o=3.6$ days are the same up to $6t_o$ (25 days), and reasonably close to each other up to $20t_o$ (72 days). The SFDM tracer curve up to $20t_o$ seems to be still good enough for applying that model for the inverse modelling. For the mean transit time

of water $t_o = 18$ days, the curves of the PFDM and the SFDM are completely different after $5t_o$ for $P_D = 0.1$ (Fig. 10) and after $10t_o$ for $P_D = 0.05$ (Fig. 9).

In conclusion, for interpreting the short-term tracer experiments the PFDM can successfully be replaced by the SFDM. The main problem is how to define mathematically a short-term tracer experiment. Examples shown in Figs 9 and 10 suggest that the mean transit time of water should be shorter than approximately 2-3 days. The upper limit of t_o strongly depends on the values of the parameters a and p. In Chapter 2.2.1, eq. (18.1) was introduced, which allows to estimate the time t_k, up to which the curves obtained from the PFDM and SFDM are nearly the same. It is evident that only a part of the experimental curve, which is measured up to that time after the injection is then applicable for the inverse modelling with the SFDM. Unfortunately, the time limit, t_k, is not directly related to the mean transit time of water. Due to the tailing effect of the tracer concentration curve, which depends on the value of the a-parameter, it is difficult to estimate if the observation time up to, say, $t_k = 20t_o$ is long enough for the inverse modelling of the observation curve. It is also evident that in order to calculate t_k one needs to know the value of p. Nevertheless, it is interesting to calculate the values of t_k for the examples shown in Figs 9 and 10. By introducing $p = 5 \cdot 10^3$ $s^{1/2}$ into eq. (18.1) one obtains $t_k < 72$ days. This corresponds to the relative times $t_k/t_o = 40$, 20 and 4 for the mean transit times of water 1.8, 3.6 and 18 days, respectively. This values agree very well with the values found from direct comparisons of the PFDM and SFDM curves as described above.

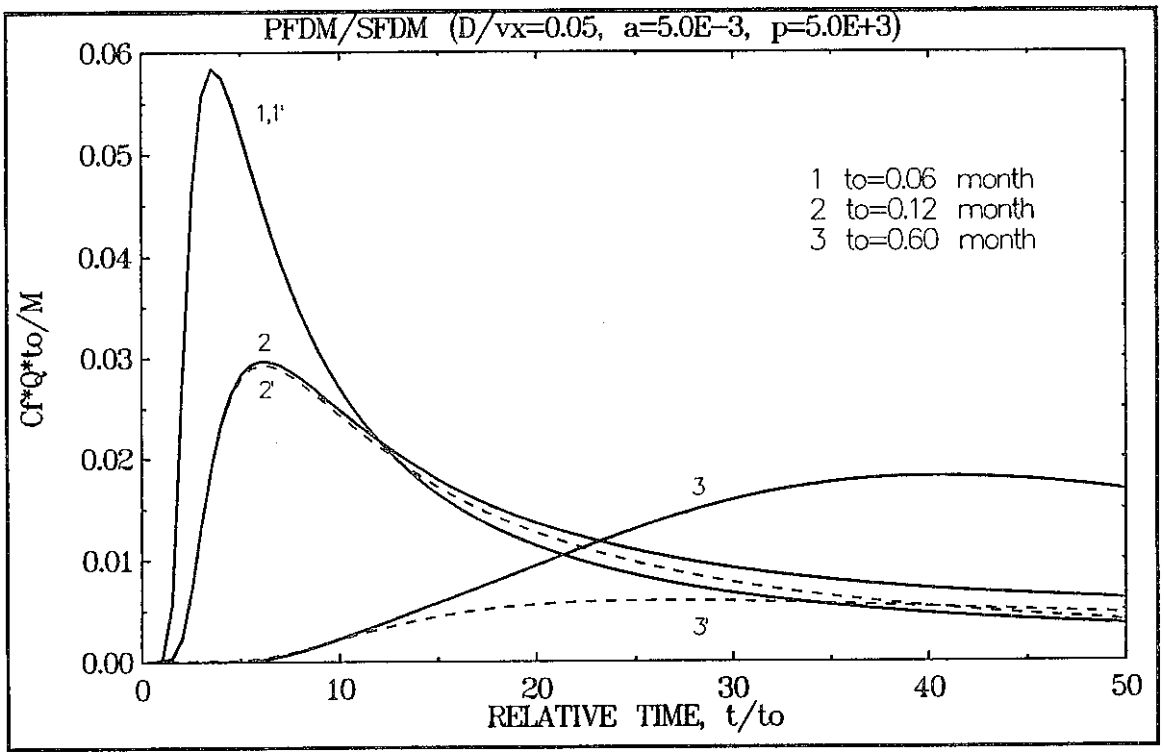

Fig. 9 **An example showing that in short-term tracer experiments the tracer concentration curves calculated from the PFDM and SFDM are nearly the same**

It seems that eq. (18.1) can successfully be applied to estimate the applicability of the SFDM for the interpretation of tracer experiments in fissured aquifers. That equation is applicable only after an experiment has already been performed, or when some independent information on the physical parameters of the system is available in advance. The SFDM is further disscussed in Chapter 3.2.

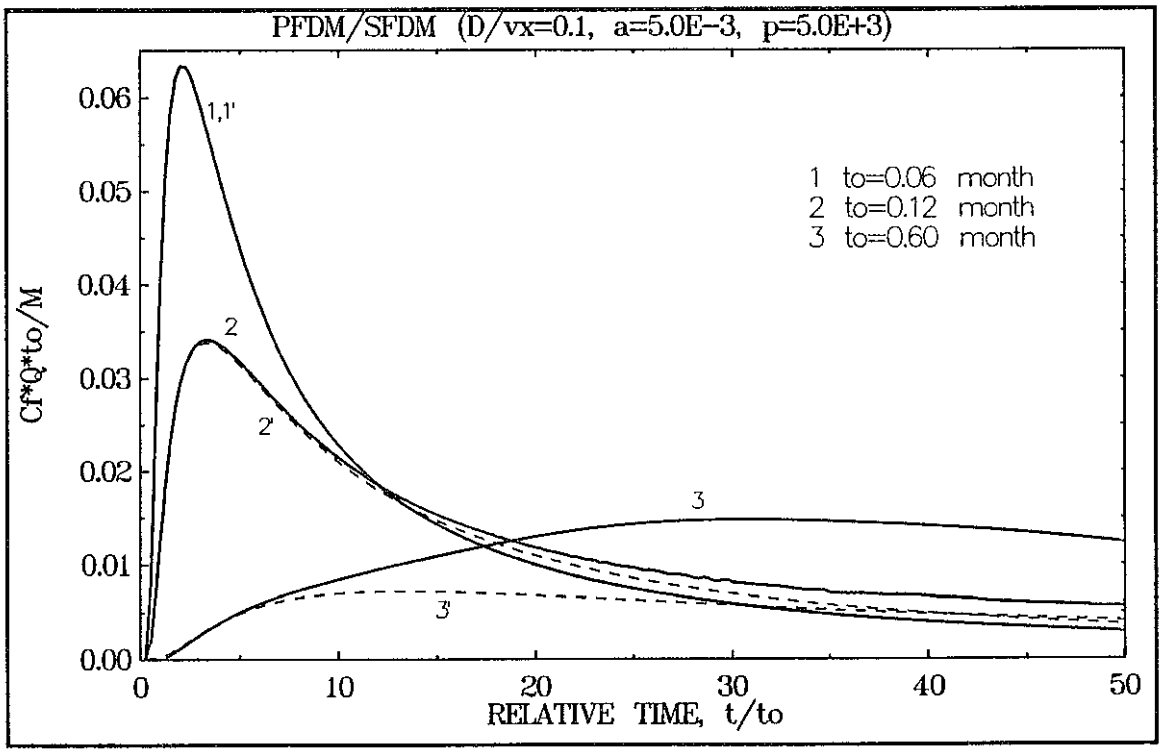

Fig. 10 **An example showing that in short-term tracer experiments the tracer concentration curves calculated from the PFDM and SFDM are nearly the same (D/vx value two times greater than in Fig. 9)**

From the data given in Table 2 one may expect that in some cases perhaps the Parallel Fissure Piston Flow Model (PFPFM) is applicable instead of PFDM. In Figs 11-12 the theoretical concentrations curves calculated for an ideal tracer by making use of the PFPFM are shown. In Fig. 13 some of them are compared with the curves obtained from the PFDM. The model parameters a and p, and the corresponding values of physical parameters are summarized in Table 3. The retardation factor R (eq. 43) and the normalized time variance of the curves, $(P_D)^*$, expressed by eq. (47.2), are also shown in that table. The influence of physical parameters, and, consequently, of the model parameters (a and p) on the shape of the tracer concentration curves is similar to that for the PFDM.

Another problem is to find out when the piston flow approach (PFPFM) can properly describe the dispersive flow in the fissures (PFDM). In Fig. 13 it is shown that for the parameters given, the PFPFM-curves (dashed lines) agree well with the PFDM-curves (solid lines) only for large redardation factors ($R > 11$). In MALOSZEWSKI & ZUBER (1985) it was shown that for a relatively small retardation factor ($R = 4$) the PFDM and PFPFM curves agreed

well, but for short transit times. This problem can be explained mathematically by comparing the time variances of the concentration distributions produced by both models (eqs 47.1 and 47.2). Generally, one has to consider two situations. First, if one assumes that the dispersion parameter (P_D) is assumed to be constant, i.e. independent of the flow distance. Then, the agreement between theoeretical curves of both models is possible if:

$$P_D << 5ap^3/(6t_oR^2) \qquad (76.1)$$

what is satisfied for: (1) decreased a (R decreases) and/or t_o (p remains constant); (2) increased p (a and t_o remain constant); and (3) conditions (1) and (2) together.

Table 3 **Parameters used for the calculation of theoretical concentration curves shown in Figs 11-13 and tracer parameters calculated by making use of eqs (43) and (49.2). The physical parameters (n_p, n_f, D_p and 2b) can be recalculated to other parameters by making use of eqs (11.1) and (11.2).**

Parameters									
	Model		Physical					Tracer	
Fig/ Curve	a	p	n_p	n_f	D_p	2b	t_o	R	$(P_D)^*$
	$s^{-1/2}$	$s^{1/2}$	-	-	m^2/s	μm	yr	-	-
11/1	10^{-3}	$0.5 \cdot 10^3$	0.01	0.01	10^{-10}	100	1	2	0.0008
11/2	10^{-3}	$1.5 \cdot 10^3$	0.01	0.0033	10^{-10}	100	1	4	0.0056
11/3	$3 \cdot 10^{-3}$	$0.5 \cdot 10^3$	0.03	0.01	10^{-10}	100	1	4	0.0006
	$3 \cdot 10^{-3}$	$0.5 \cdot 10^3$	0.01	0.0033	10^{-10}	333	1	4	0.0006
11/4	$10^{-3}/3$	$1.5 \cdot 10^3$	0.01	0.01	10^{-11}	100	1	2	0.0074
12/1	10^{-3}	$0.5 \cdot 10^3$	0.01	0.01	10^{-10}	100	0.02	2	0.0412
12/2	10^{-3}	$0.5 \cdot 10^3$	0.01	0.01	10^{-10}	100	0.10	2	0.0082
12/3	10^{-3}	$0.5 \cdot 10^3$	0.01	0.01	10^{-10}	100	0.50	2	0.0017
12/4	10^{-3}	$0.5 \cdot 10^3$	0.01	0.01	10^{-10}	100	2.5	2	0.0003
13/1	10^{-3}	$0.5 \cdot 10^3$	0.01	0.01	10^{-10}	100	1	2	0.0008
13/2	10^{-3}	$1.5 \cdot 10^3$	0.01	0.0033	10^{-10}	100	1	4	0.0056
13/3	10^{-3}	$5.0 \cdot 10^3$	0.01	0.001	10^{-10}	100	1	11	0.0270

Table 4 Comparison of tracer parameters calculated by making use of eqs (43), (49.1) and (49.2) for the piston flow (PFPFM) and dispersive (PFDM) approaches

	Parameters				Tracer parameters			
	Model		Physical		PFDM		PFPFM	
Fig/ Curve	a	p	t_o	D/vx	R	$(P_D)^*$	R	$(P_D)^*$
	$s^{-1/2}$	$s^{1/2}$	yr	-	-	-	-	-
11/1	10^{-3}	$0.5 \cdot 10^3$	1	0.005	2	0.0058	2	0.0008
11/2	10^{-3}	$1.5 \cdot 10^3$	1	0.005	4	0.0106	4	0.0056
11/3	$3 \cdot 10^{-3}$	$0.5 \cdot 10^3$	1	0.005	4	0.0056	4	0.0006
11/4	$10^{-3}/3$	$1.5 \cdot 10^3$	1	0.005	2	0.0124	2	0.0074
12/1	10^{-3}	$0.5 \cdot 10^3$	0.02	0.005	2	0.0462	2	0.0412
12/2	10^{-3}	$0.5 \cdot 10^3$	0.10	0.005	2	0.0132	2	0.0082
12/3	10^{-3}	$0.5 \cdot 10^3$	0.50	0.005	2	0.0067	2	0.0017
12/4	10^{-3}	$0.5 \cdot 10^3$	2.50	0.005	2	0.0053	2	0.0003
13/1	10^{-3}	$0.5 \cdot 10^3$	1	0.005	2	0.0058	2	0.0008
13/2	10^{-3}	$1.5 \cdot 10^3$	1	0.005	4	0.0056	4	0.0006
13/3	10^{-3}	$5.0 \cdot 10^3$	1	0.005	11	0.0320	11	0.0270

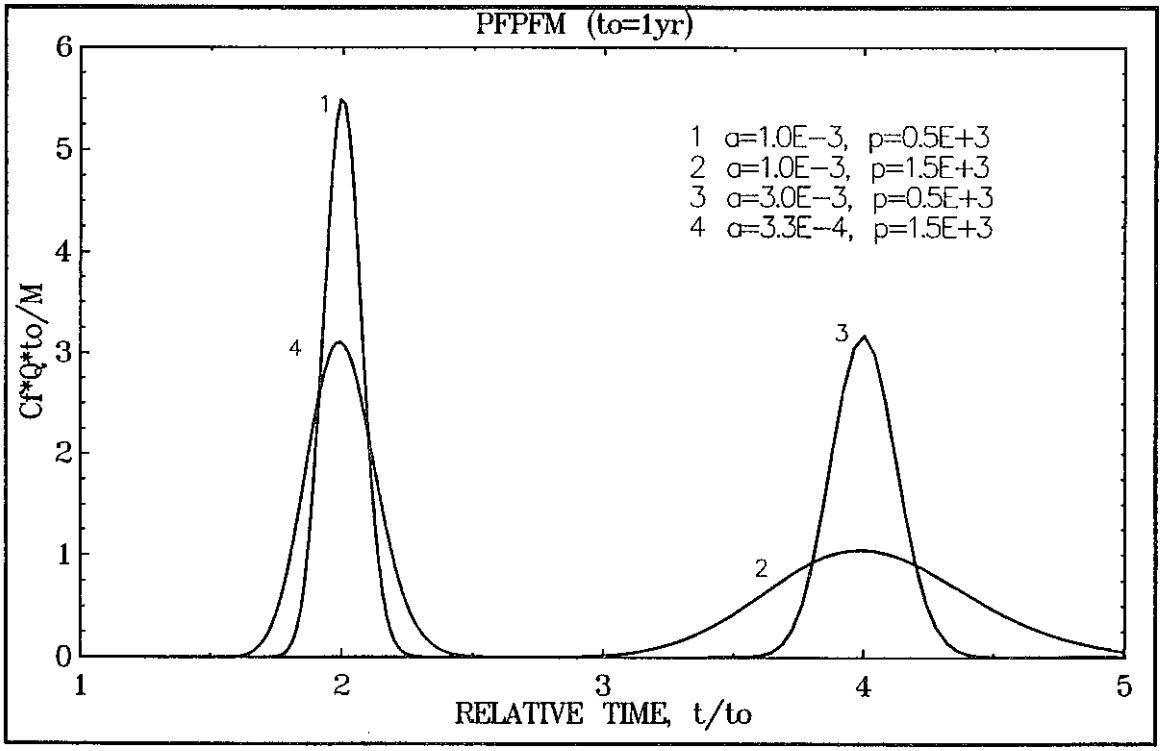

Fig. 11 The influence of the a and p values on the shape of tracer concentration curves calculated from the PFPFM (for physical parameters see Table 3)

Second, if one assumes that dispersivity (D/v) is constant and independent of the flow distance. Then, the following condition exists:

$$D/v << 5avp^3/(6R^2) \qquad (76.2)$$

which is satisfied for: (1) decreased a (R decreases for a constant p); (2) increased water velocity v and/or parameter p; (3) conditions (1) and (2) together. The eqs (76.1) or (76.2) describe mathematically, the condition which must be satisfied to apply the piston flow approach instead of the dispersive one.

Table 4 summarizes the normalized time variances for the curves shown in Figs 11-13, which were calculated from the model parameters (a and p) with the aid of eqs (49.1) for the PFDM, and (49.2) for the PFPFM. The comparison of the results confirms the findings of MALOSZEWSKI & ZUBER (1985), that if $(P_D)^*$ values are similar the concentration curves are also similar (compare results for the PFDM with those for the PFPFM in the case of curves 12/1 and 13/3 in Table 4; compare also curves 3 and 3' in Fig. 13).

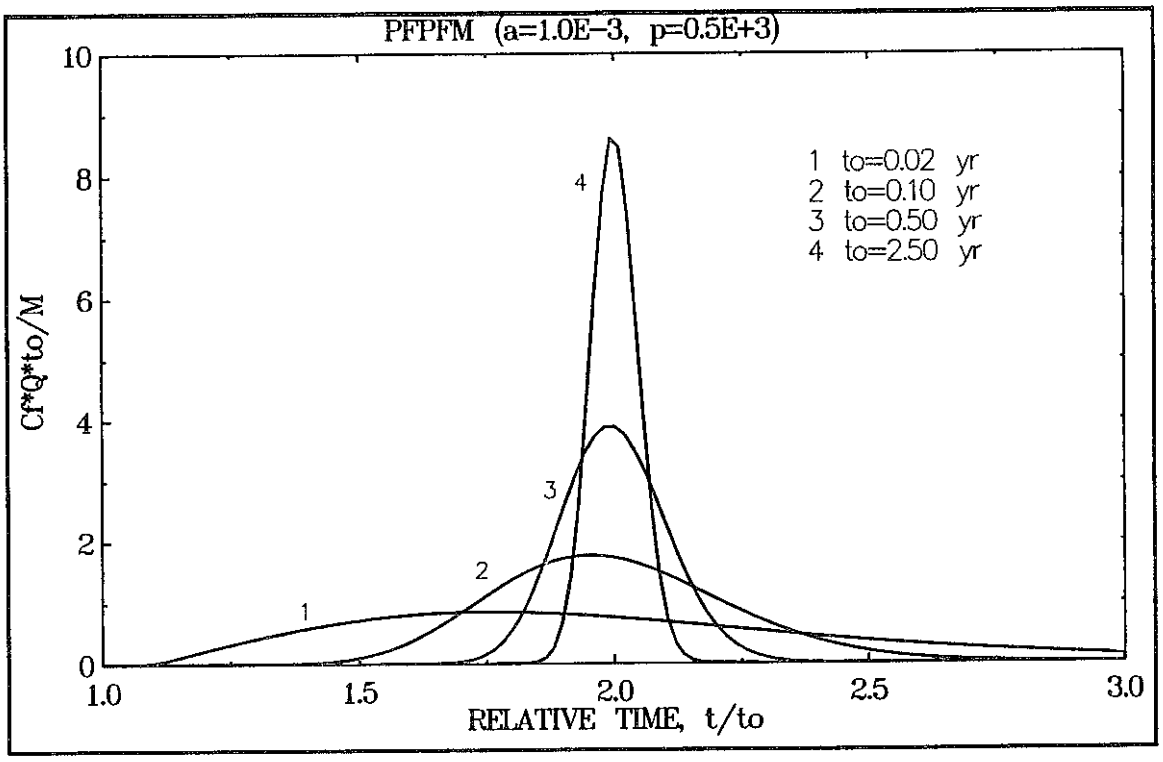

Fig. 12 **The influence of the mean transit time of water on the shape of tracer concentration curves calculated from the PFPFM (for physical parameters see Table 3)**

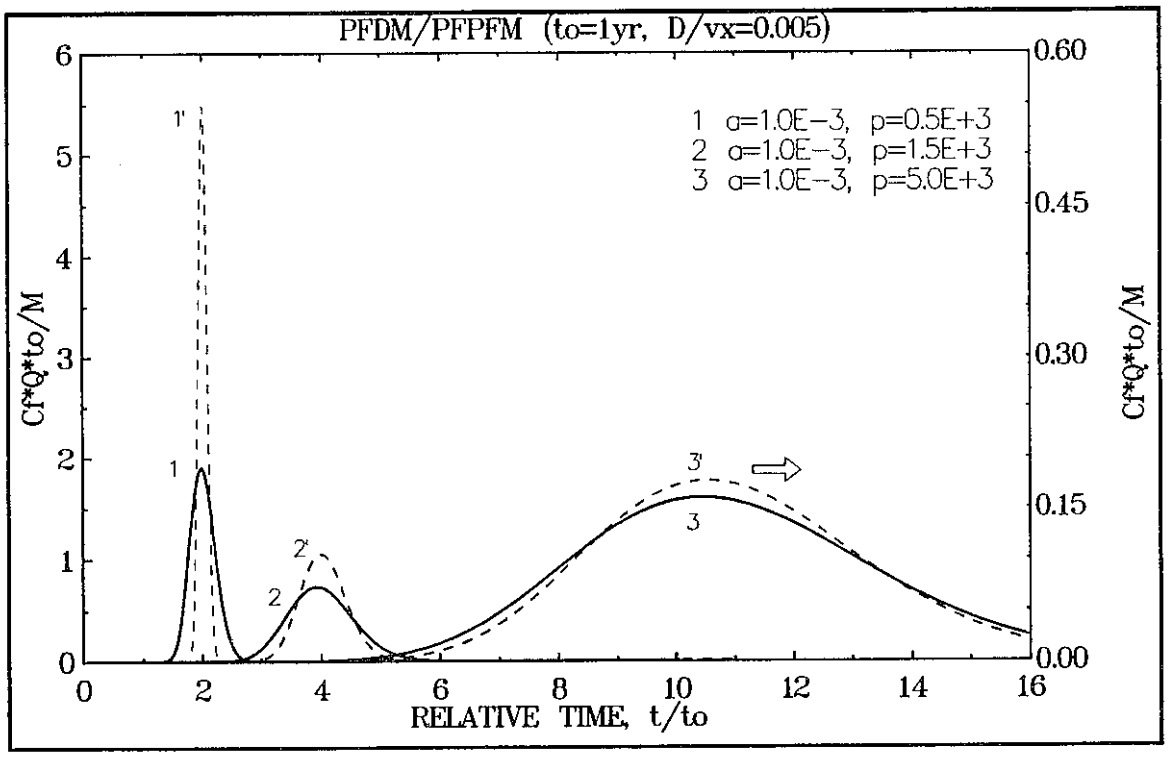

Fig. 13 **For a sufficiently large value of the p-parameter, the concentration curves calculated from the PFDM and PFPFM are nearly the same (for physical parameter see Table 3)**

3.2 Single fissure model for an instantaneous injection

The Single Fissure Dispersion Model (SFDM) was introduced in Chapter 2.2.1. Within this chapter the model is employed for solving the direct problems in short-term tracer experiments. Figures 14-17 show the concentration and recovery curves calculated for different values of model parameters in the case of an ideal tracer (eqs 25 and 35, respectively). An increased value of the a-parameter produces: (1) a greater tailing effect (asymmetry of the curve is larger); (2) a lower maximum of the tracer concetration curve; and (3) a more delayed time of the maximal concentration in comparison with the mean transit time of water. These effects are clearly demonstrated by curves 1, 2 and 3 in Fig. 14, and by curves 1 and 2 in Fig. 15. An increased value of the a-parameter, also results in a lower recovery for a given time after the injection. Even as low value of the a-parameter as $5 \cdot 10^{-4}$ $s^{-1/2}$ and the mean transit time of water as short as 12 hrs, produce a visible tailing, and, consequently, the mass recovery obtained after the time $t=4t_0$ (48 hrs), is only about 88% (see curve 3 in Fig. 14). If the mean transit time of water is decreased for a constant value of the a-parameter, one observes similar effects as in the case of decreased value of the a-parameter for a constant t_0 value (see curves 3, 2 and 1 in Fig. 16). In Fig. 17, curves calculated for different values of the dispersion parameter (P_D) are shown. An increased value of P_D, for constant values of other parameters, yields more asymmetrical curves

(more dispersed), with the maximum concentration appearing at shorter times than t_o. In general, the higher the dispersion parameter, the ealier the appearance of the maximum concentration in respect to the mean transit time of water.

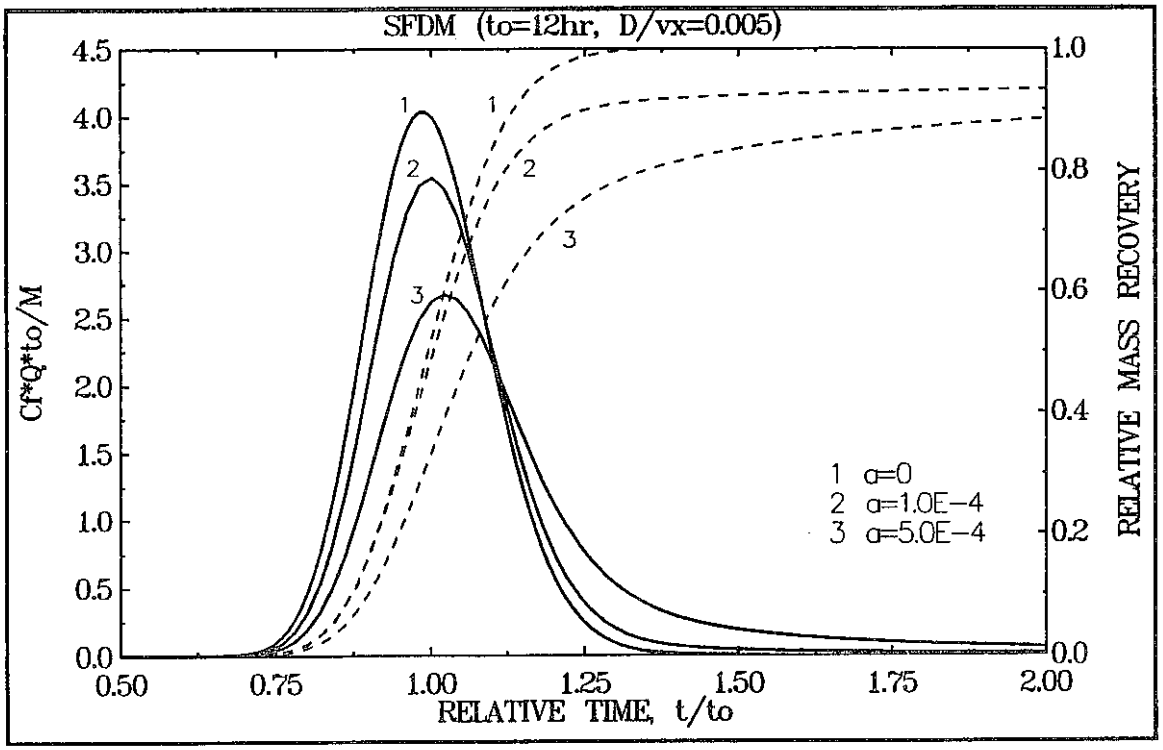

Fig. 14 **The influence of the a-value on the shape of tracer concentration and recovery curves for the SFDM**

For very low values of the a-parameter, say, for $a < 10^{-4}$ $s^{-1/2}$, the curves are similar to those without matrix diffusion, i.e., with a=0 (compare curve 2 with 1 in Fig. 14). This effect was also obtained by MALOSZEWSKI & ZUBER (1985) for the same value of the a-parameter and for different values of the mean transit times (t_o=3, 12 and 24 hrs), and for different values of the dispersion parameter (P_D=0.005, 0.5 and 5.0). In such a situation the interpretation of the experimental curve can be done by making use of the ordinary dispersion model commonly applied for porous systems. Then, by fitting of the DM one may obtain directly the model parameters t_o and $\alpha_L = D/v$ with a satisfactory accuracy. Unfortunately, in such a case the information on the fissured medium contained in the a-parameter is not available. One should also remember that even for such a low value of the a-parameter, the curve can be characterized by a long tail. This effect is not easily identified on the concentration curve (solid line 2 in Fig. 14), but easy to discover from the tracer recovery curve (dashed line 2 in Fig. 14). The tracer recovery reaches only 94% after $4t_o$, whereas the curve without diffusion reaches 100% already after the time equal to $1.25t_o$ (dashed line 1 in Fig. 14). This example clearly demonstrates the importance of the mass recovery concept for the interpretation of tracer experiments.

For the a-parameter equal to 10^{-4} $s^{-1/2}$, the corresponding values of physical parameters can be, say, $D_p = 10^{-12}$ m^2/s, matrix porosity of 1% or smaller and fissure aperture of 100 μm. Such

a low diffusion coefficient can be observed when the constrictivity factor (δ) is much smaller than 1 (see eq. 30), as observed for magmatic rocks of low porosity (0.001 $\pm$ 0.003) by SKAGIUS & NERETNIEKS (1986). For most carbonate rocks and sandstones unchanged strongly by diagenesis, the constrictivity factor (δ) is probably close to 1. Then, the diffusion coefficients are about three orders of magnitudes greater, and the values of the a-parameter about 32 times larger. Consequently, the tracer curves must be characterized by long tails and low recoveries (e.g., in approximation curve 2 in Fig. 15). In conclusion, the matrix diffusion effects during tracer transport through fissured aquifers are seldom negligible.

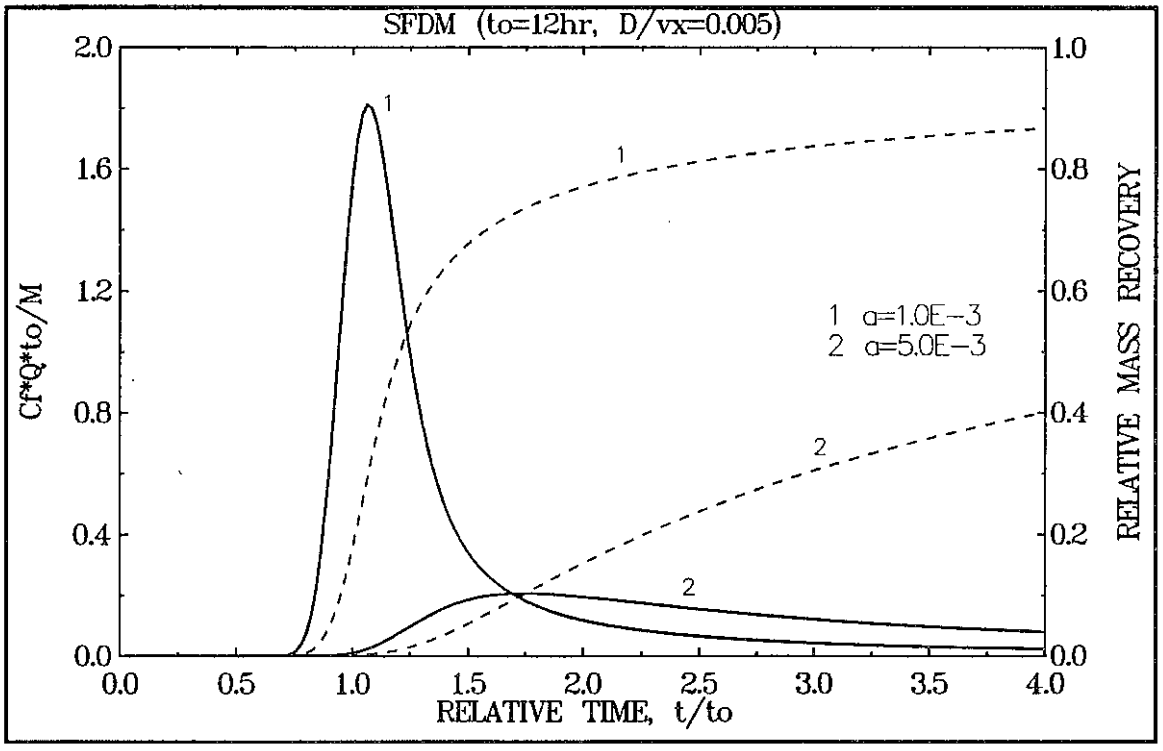

Fig. 15 **The influence of the a-value on the shape of tracer concentration and recovery curves for the SFDM (cont. of Fig. 14)**

In Figs 18 and 19 the curves for reactive tracers calculated by making use of eq. (23), under an assumption of no reaction in fissures ($R_{af}=1$), are presented. The influence of an instantaneous equilibrium reaction in the fissures is not shown because it can easily be deduced from eqs 9.2 and 9.3. The retardation factor R_{af} larger than 1 yields the same effect as a larger value of the mean transit time and a lower value of the a-parameter.

Behaviour of a tracer which follows only kinetic exchange reactions in the porous matrix is demonstrated in Fig. 18. The tracer curves (solid lines 2 and 3) are compared with that for an ideal tracer (solid line 1). An increased value of the kinetic-reaction rate-constants (k_1 and k_2) yields stronger tailing effect and lower peaks (maximum). Note that, for low values of the reaction rate constants the peak may be shifted to the earlier times in comparison with the case of no reaction. For larger values of k_1 and k_2 a reversal shift to greater times is observed (not

shown here). The mass recovery curves (dashed lines) become lower for larger values of the kinetic rate constants.

In Fig. 19 the influence of an instantaneous equilibrium reaction in the matrix is shown. In the case of $k_1=k_2=0$, the retardation factor R_{ap} greater than 1 yields a larger value of the a-parameter, as it is evident from eq. (10.2), and the effects discussed earlier are observed (compare curve 2 with 1). If, additionally, kinetic reactions take place in the matrix, the peak of the tracer curve (solid line 3) and the mass recovery curve (dashed line 3) will be lower, as well as the shape of the curve changed.

Examples disscussed above show that the mass recovery curves considered together with the concentration curves give a better insight into the behaviour of tracer, especially at the tailling parts, and allow to detect reversible and/or nonreversible losses.

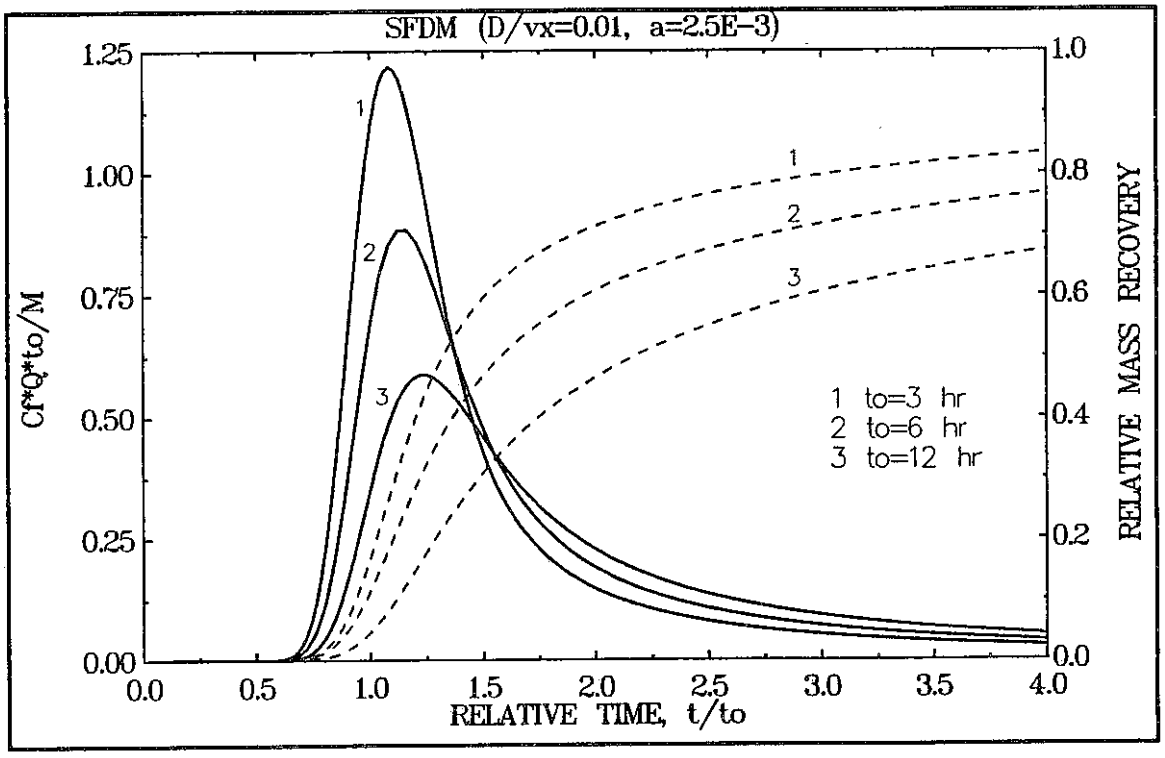

Fig. 16 **The influence of the mean transit time of water on the shape of tracer concentration and recovery curves for the SFDM**

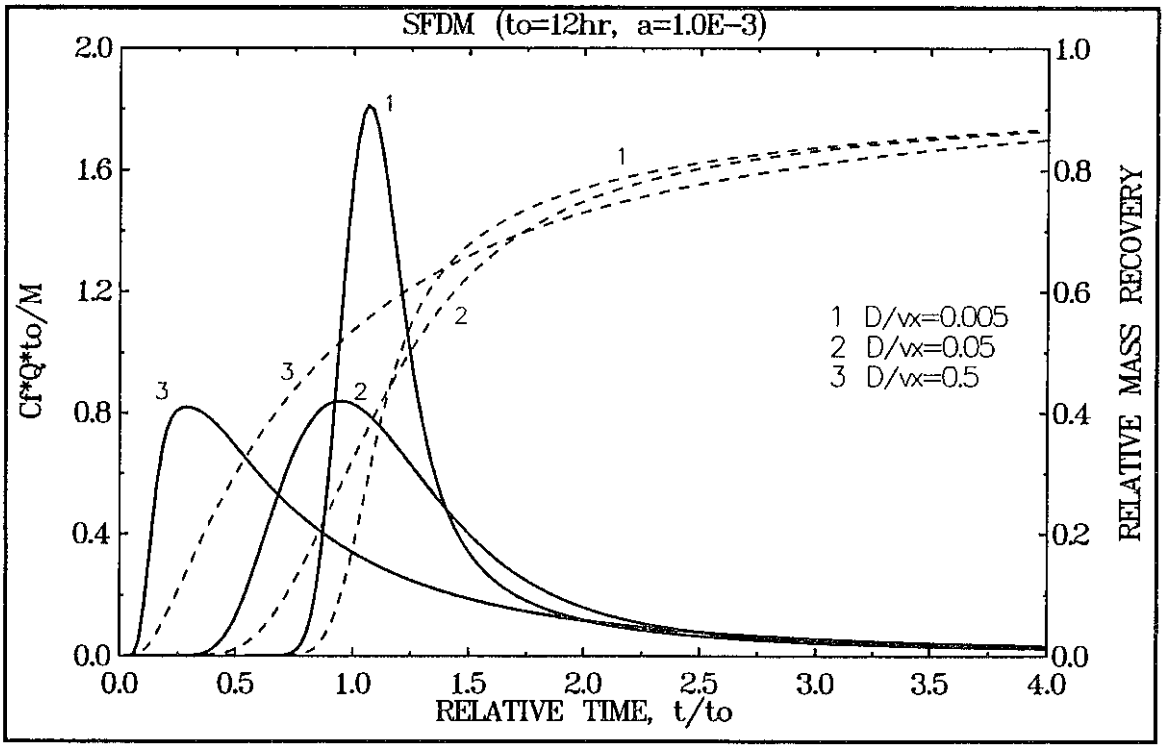

Fig. 17 The influence of the dispersion parameter on the shape of tracer concentration and recovery curves for the SFDM

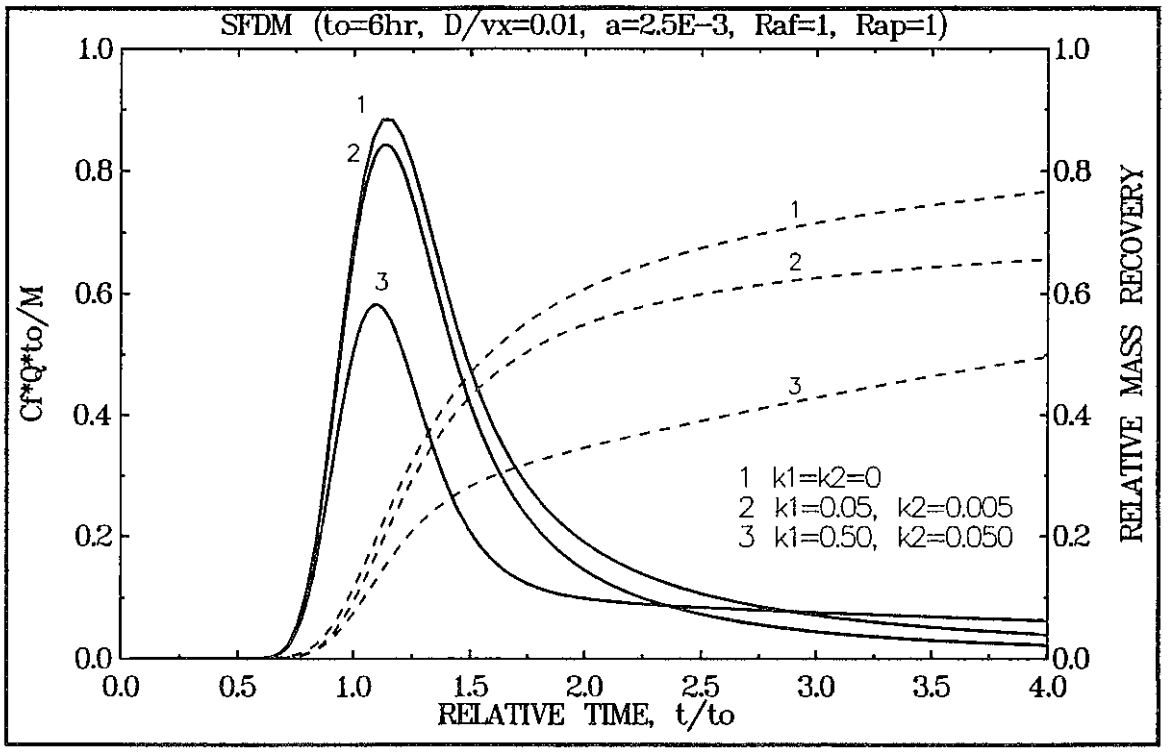

Fig. 18 The influence of increased values of the reaction rate constants for the first order kinetic exchange reaction in porous matrix on the shape of tracer concentration and recovery curves in the case of the SFDM (k_1 and k_2 in hrs^{-1})

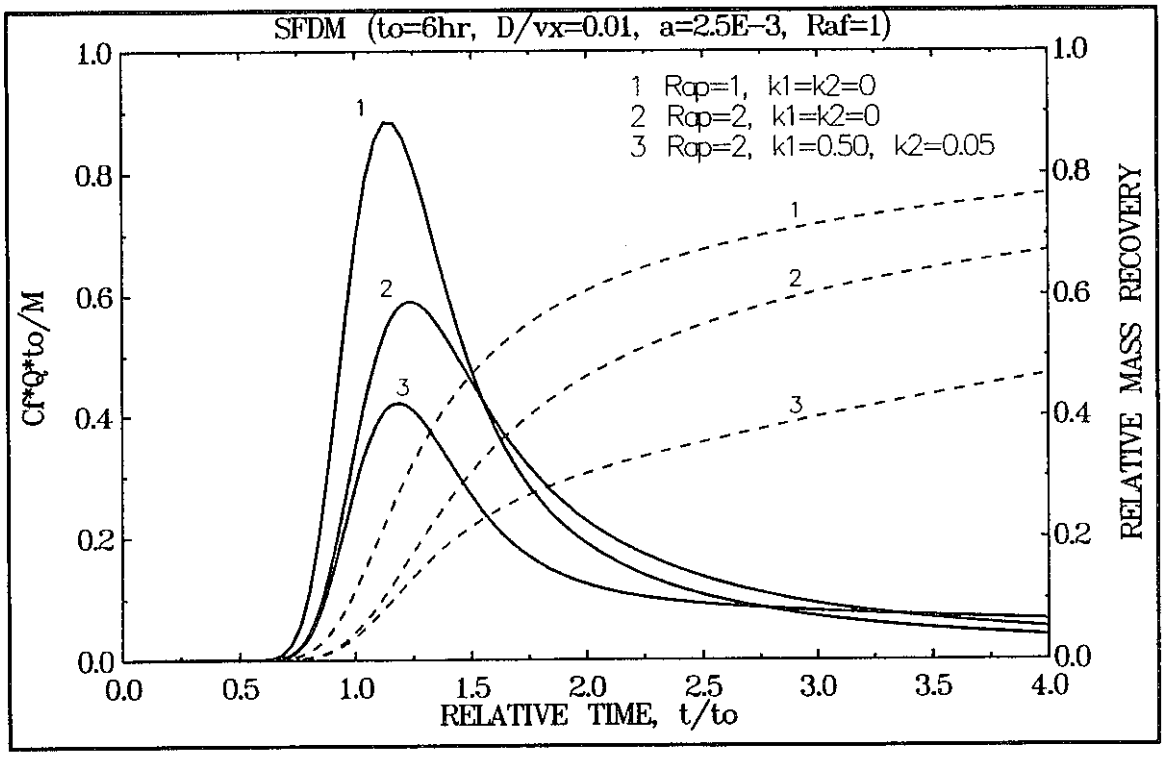

Fig. 19 The influence of an instantaneous equilibrium reaction (2), and an instantaneous equilibrium reaction coupled with the first order kinetic reactions (3) on the shape of tracer concentration and recovery curves in the case of the SFDM (k_1 and k_2 in hrs^{-1})

4 Case studies: the inverse problem

As mentioned earlier, solving the inverse problem is a process in which a mathematical model is fitted to the experimental data in order to obtain the values of parameters which describe the investigated system. This process is also called calibration of the model (e.g., MALOSZEWSKI & ZUBER 1992). The fitting parameters (other terms: model, nondisposable, or sought parameters), are varied till the best fit of the theoretical solution to the experimental data is obtained. The best fit is quantitatively described by the goodness of fit, i.e. the sum of the square roots of the differences between calculated and measured values must reach a minimum. In tracer hydrology some approximate methods to determine the system parameters are known, like the method of cumulative curve or the method of moments. These methods are based mainly on the ordinary dispersion model (see MALOSZEWSKI & ZUBER 1990b; or MALOSZEWSKI 1992). Difficulties appear when the investigator does not check if the parameters estimated in a simple way yield the curve which is supposed to fit to the experimental data. MALOSZEWSKI & ZUBER (1990b, 1992) have shown that the parameters obtained in a simple way are usually little related to the reality. Therefore, it is always of great importance to check the model parameters, i.e. to calibrate the model properly. However, the best fit, i.e. a calibrated model, does not guarantee that the parameters obtained have a proper values. The model should not only be calilibrated but, if possible, also validated. The definitions of calibration and validation, and the applicability of these processes for the mathematical modelling of groundwater tracer experiments were given by MALOSZEWSKI & ZUBER (1992). Validation can be performed by comparison of the values of parameters obtained with those obtainable independently (e.g., matrix porosity obtained from the tracer test should agree with that measured on core samples). It is self-evident that a model which is not calibrated cannot be validated. Some of these problems are exemplified in next Chapters.

4.1 Applications of the Single Fissure Dispersion Model (SFDM) in short-term tracer experiments

4.1.1 Tracer experiments in chalk aquifers

A unique possibility to compare the behaviour of several tracers and to examine the SFDM has so far been offered by the multitracer experiment of GARNIER et al. (1985). The experiment was performed between two wells in a radial-convergent flow in a fissured chalk formation overlain by clays and silts. The distance between the wells was 10.22 m, and the pumping rate of 20.8 m^3/h was obtained. Four tracers, heavy water (D_2O), Iodide (I^-), disodium-fluoresceine (Uranine) and $H^{13}CO_3^-$, were instantaneously injected in one well, and their concentrations measured in water withdrawn from another well. The transmissivity of that chalk is about $1.75 \cdot 10^{-3}$ m^2/s (J.M. Garnier, private information), which for the aquifer thickness (m) of 32.8 m yields the hydraulic conductivity (k) of $5.3 \cdot 10^{-5}$ m^2/s = 4.6 m/d. The injection and pumping wells were screened over the depth of 19.9-29.9 m (10m), and 19.2-34.2 m (15m), respectively. The four tracer concentration curves were presented by GARNIER et al. (1985) in the commonly used method, i.e. each curve was normalized to its maximum concentration value.

As it was mentioned in Chapter 2.2.2, such a normalization is necessary for the experiments performed under natural flow conditions, where the volumetric flow rate remains unspecified. In the case of radial flow, when the system is well defined and the flow rates controlled, the normalization to maximum leads to the loss of information. Especially, in multi-tracer experiments, the normalization of each tracer curve to its own maximum is an error of art. For the comparison of behaviour of different tracers one should normalize each tracer curve to its mass injected (MALOSZEWSKI & ZUBER 1990a). In the case of a combined pumping and tracer test, the mass recovery curves should also be examined, as it was discussed in Chapter 3.2. The tracer curves obtained in Garnier's experiment, normalized in a proper way, and the mass recovery curves are shown in Fig. 20, after MALOSZEWSKI & ZUBER (1990a). From Fig. 20, it is clear that particular tracer and recovery curves differ considerably from one another. This was not visible in the original work of GARNIER et al. (1985), where each curve was normalized to its maximum concentration.

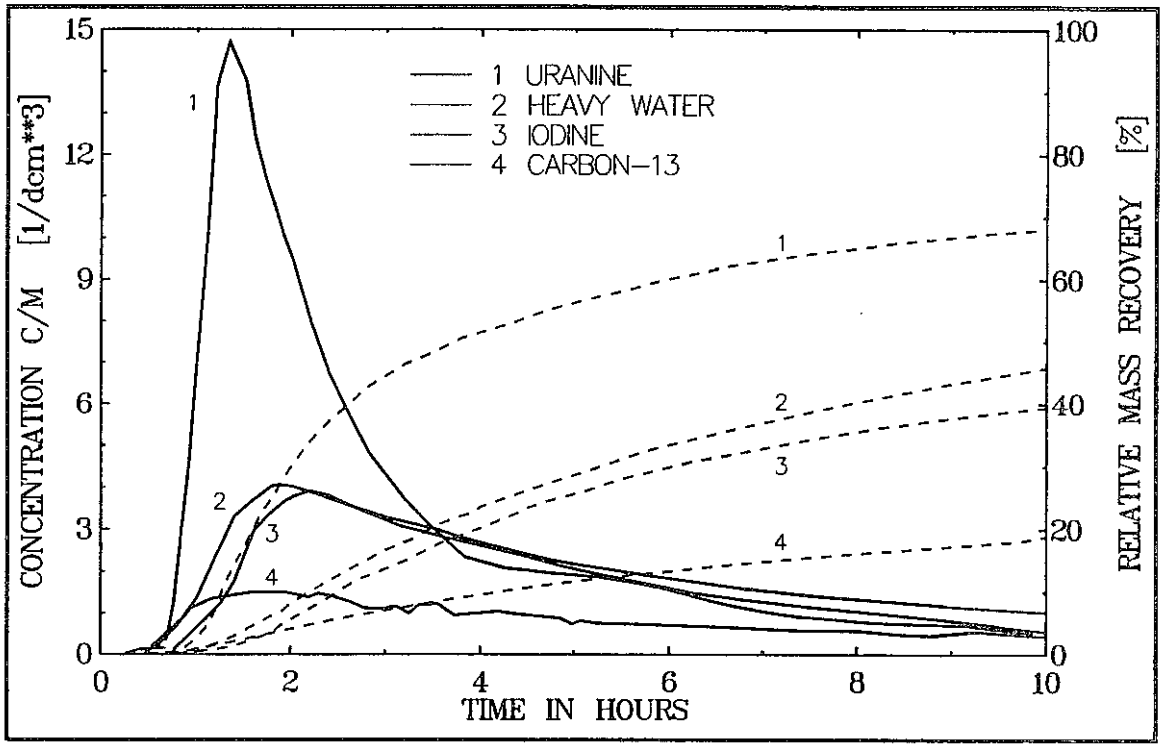

Fig. 20 **Tracer concentration curves normalized to the mass injected and the mass recovery curves for a multi-tracer experiment performed in a fissured chalk (original data after GARNIER et al. 1985)**

Qualitatively one can immediately say that if the system under consideration is a double porosity medium, then the highest peak and the highest recovery observed for the Uranine may result only from the lowest diffusion coefficient of that tracer. Both, heavy water and Iodide have much lower peaks and recoveries than the Uranine, which suggest greater diffusion rates of these two tracers into porous matrix.

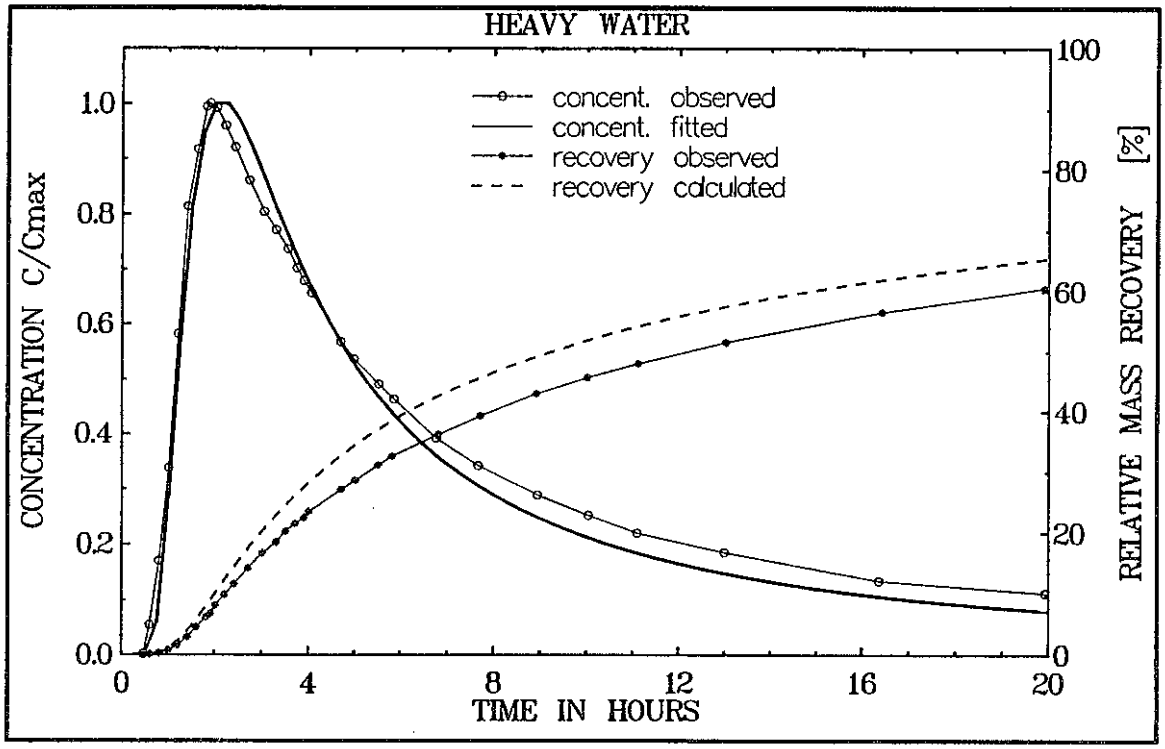

Fig. 21 **The best fit of the SFDM obtained for D_2O, without fitting the mass recovery curve (experimental points after GARNIER et al. 1985)**

The first quantitative interpretation with the aid of the SFDM (eq. 25) was performed by MALOSZEWSKI & ZUBER (1989) without including the concept of tracer recovery. It was assumed Uranine, heavy water and Iodide behaved as ideal tracers (the a-parameter is given by eq. 11.1) and $H^{13}CO_3^-$ follows an instantaneous equilibrium reaction in the porous matrix (the a-parameter is given by eq. 10.2). The best fits obtained by the calibration of the model to such curves are shown in Figs 21-24. Within this work, the experimental and calculated (eq. 35.2) tracer recovery curves are also given to demonstrate the differences between them when they are not calibrated. The model parameters obtained by MALOSZEWSKI & ZUBER (1989) are summarized in Table 5. The conclusion drawn from the analysis of these parameters were:

- the SFDM (eq. 25) works well for three nonreactive tracers because the model parameters (which do not dependent on the tracer used, i.e. flow parameters: the mean transit times of water, and the dispersion parameter) obtained in the fitting procedure are nearly the same (compare values of t_0 and P_D in Table 5);

- as the matrix porosity and the fissure aperture do not depend on the tracer used, the differences in the a-parameter result from different values of the diffusion coefficients of the tracers;

- the reaction model applied for the interpretation of $H^{13}CO_3^-$ does not work. Though, a resonably good fit was obtained (see Fig. 24), its parameters appeared to be inconsistent with those obtained for the other three tracers, particularly the dispersion parameter was four times

larger. It was suggested that the P_D was in that case an apparent parameter which covered some other processes. It means that though the SFDM with an instantaneous reaction model was calibrated properly, it was not validated.

Table 5 **The SFDM parameters obtained for a fractured chalk from the experiment of GARNIER et al. (1985), with an instantaneous equilibrium reaction in the matrix assumed for the reactive tracer ($H^{13}CO_3^-$), and without fitting of the mass recovery curves**

Tracer	t_o	a	P_D
	hr	$s^{-1/2}$	-
D_2O	1.00	$23.3 \cdot 10^{-3}$	0.03
Uranine	1.15	$7.5 \cdot 10^{-3}$	0.03
Iodide	1.25	$15.8 \cdot 10^{-3}$	0.03
$H^{13}CO_3^-$	0.90	$33.3 \cdot 10^{-3}$	0.12

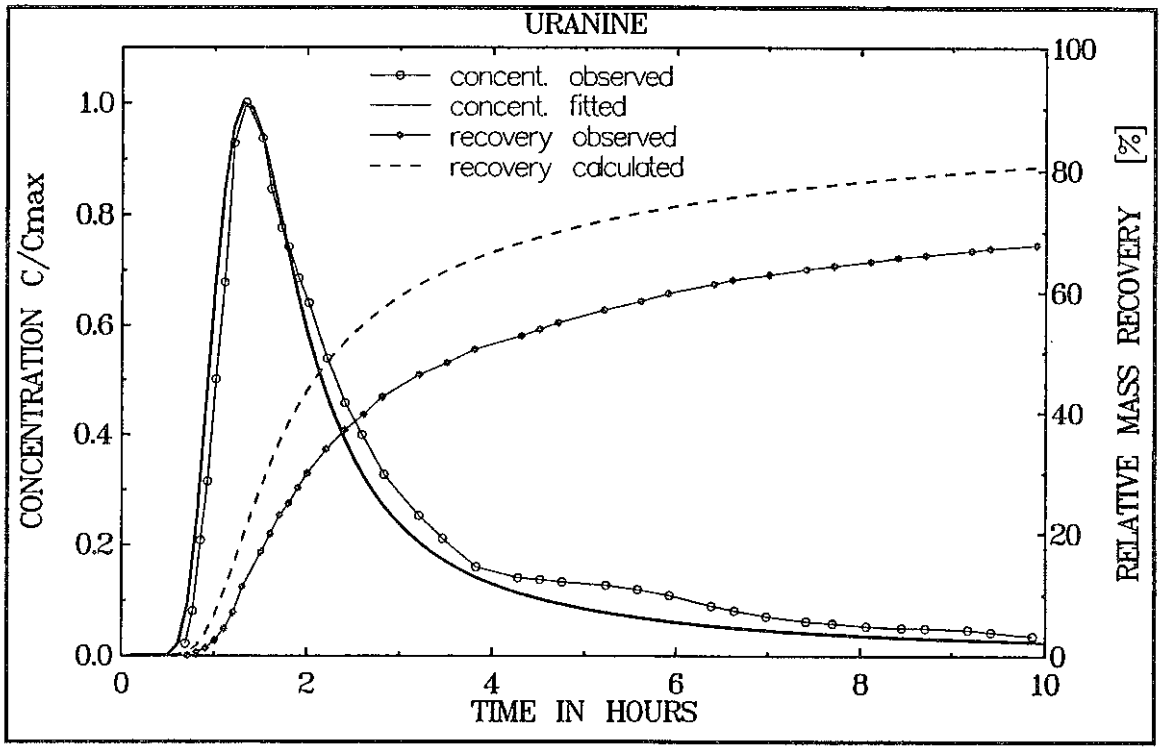

Fig. 22 **The best fit of the SFDM obtained for Uranine, without fitting the mass recovery curve (experimental points after GARNIER et al. 1985)**

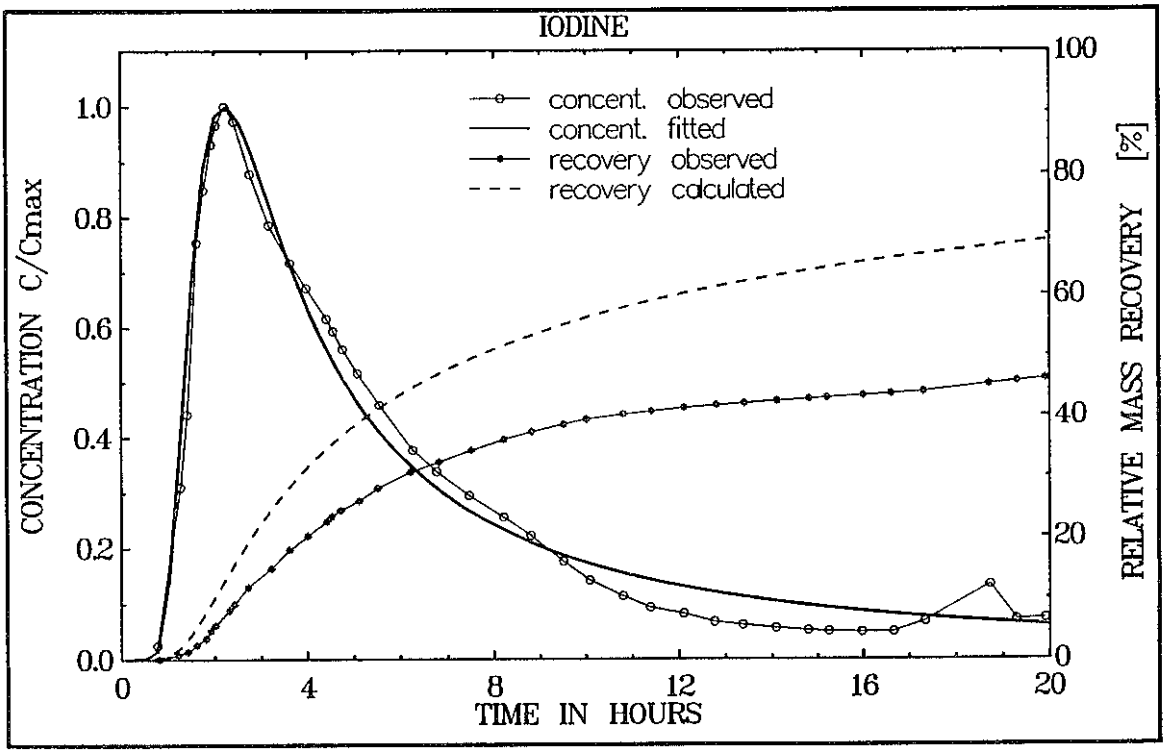

Fig. 23 **The best fit of the SFDM obtained for Iodide, without fitting the mass recovery curve (experimental points after GARNIER et al. 1985)**

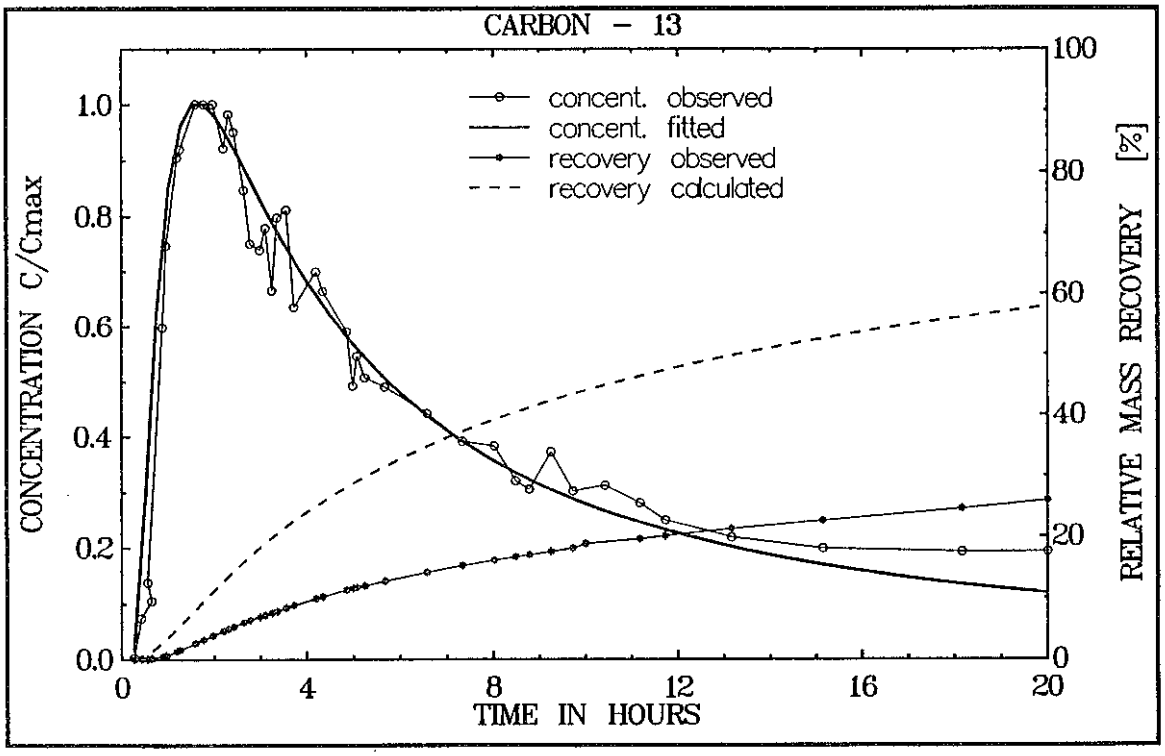

Fig. 24 **The best fit of the SFDM obtained for $H^{13}CO_3^-$, without fitting the mass recovery curve (experimental points after GARNIER et al. 1985)**

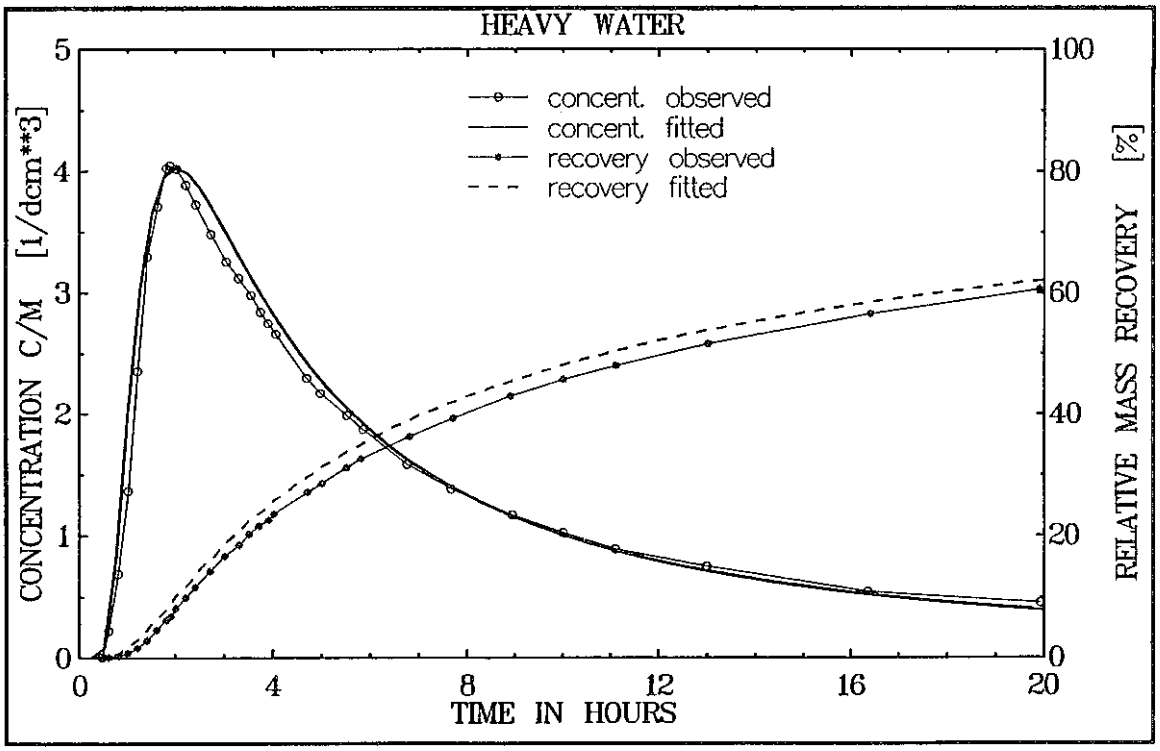

Fig. 25 **The best fit the SFDM obtained for D_2O, with an additional fit of the mass recovery curve (experimental points after GARNIER et al. 1985)**

A search for a better exchange reaction model disclosed another inconsistency manifested by the lack of a good fit for the mass recovery curves as demonstrated in Figs 21-24. The discrepancy between the observed mass recoveries of Uranine and heavy water were not very large. However, the new calibration procedure consisting of the fitting of both concentration and recovery curves for these two tracers improved the fit, as it is presented in Figs 25 and 26. Unfortunatelly, it was not possible to obtain a good fit without assuming that 9% of each tracer was missing. Most probably this 9% of tracer mass was trapped in the unscreened part of the injection well. For the consistency of the data the other two tracers were also corrected for the same lost amount.

The new fitting procedure still did not yield the same values of the mean transit time of water (t_o) for Uranine and heavy water. Assuming that the reaction model described in Chapter 2.1.2 is the proper one, the discrepancy between both tracers cannot be explained by the retardation of Uranine in the fissures ($R_{af}=1.5$), because an unreasonably high distribution coefficient in the fissures would then appear (from eq. 12: $k_a \approx 200$ μm for $2b=270$ μm found from D_2O). This, in turn, would yield a very high R_{ap} value for any assumed diameter of micropores (see eq. 14), and, consequently, an unreasonably large value of the a-parameter. The origin of this discrepancy remains unknown. Most probably it results from inaccuracies in determinations of t_o, which means that R_{af} cannot be found with an acceptable accuracy.

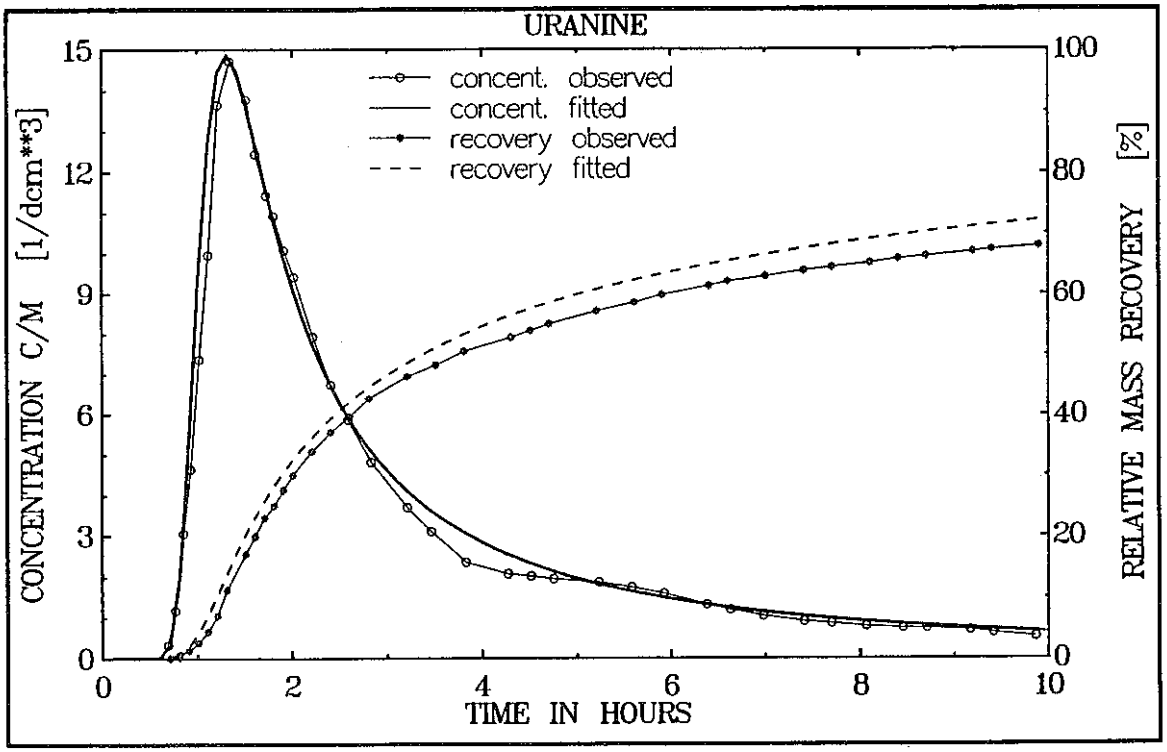

Fig. 26 **The best fit of the SFDM obtained for Uranine with an additional fit of the mass recovery curve (experimental points after GARNIER et al. 1985)**

The most striking feature is the decrease of both t_o and P_D for these two good tracers in the comparison with the previous calibration, though in both cases the same eq. (25) was applied. Therefore, it can be supposed that a good fit of the mass recovery improves the interpretation procedure considerably. As mentioned earlier, the normalization to the maximum concentration causes a loss of information on the mass recovery. It appears that in practice, a good fit of the concentration curve is a necessary, though not sufficient, condition for a good fit of the mass recovery as it will be shown below for the Iodide curve.

The recovery of Iodide was so low that it was not possible to obtain the best fits simultaneously for the concentration and recovery curves. Consequently, it was necessary to assume that this tracer, contrary to the common opinion, cannot be considered as a nonreactive one. This finding is in accordance with some earlier works (e.g., BEHRENS 1985; or MALOSZEWSKI et al. 1980). To solve the problem, a more refined version of the SFDM represented by eq. (23) which includes additionally the first order kinetic reactions in the porous matrix was used for the interpretation of the both reactive tracers (MALOSZEWSKI & ZUBER 1990a). The best fits obtained with that version of the SFDM for Iodide and $H^{13}CO_3^-$ are shown in Figs 27 and 28. It is self-evident that by calibration of the SFDM (eq. 23) for a reactive tracer (five fitting parameters), one has to take the flow parameters (t_o and P_D) from an experiment with an ideal tracer (see Chapter 2.2.2.2) in order to reduce the number of nondisposable (fitted) parameters to three. In that case the flow parameters found for the heavy water were used. However, one can deduce from MALOSZEWSKI & ZUBER (1990a) difficulties encountered, if an instantaneous equilibrium reaction in the fissures occurs. Then t_o is not a known parameter

(disposable), but it is a fitting parameter (t_o'), and, consequently the number of fitting parameters increases to four. In the case of Iodide, MALOSZEWSKI & ZUBER (1990a) have shown another possible calibration, with a larger value of the mean transit time (t_o=0.8 hr), a smaller value of the a-parameter ($a=31.7 \cdot 10^{-3}$ $s^{-1/2}$), and nearly the same values of P_D and kinetic reaction rate constants. The larger value of t_o obtained in the second fit can be explained as a result of the retardation of Iodide in the fissures (R_{af}=1.25). The t_o and a parameters recalculated to be separated from the R_{af} factor are shown as the second set of parameters in Table 6. Note very close values of the a-parameter found in both fits for the Iodide. However, in the second set of parameters for R_{af}=1.25 an unacceptable high value of k_a results, as it was disscussed earlier for Uranine. For these reasons the second set of parameters can be rejected from further discussions.

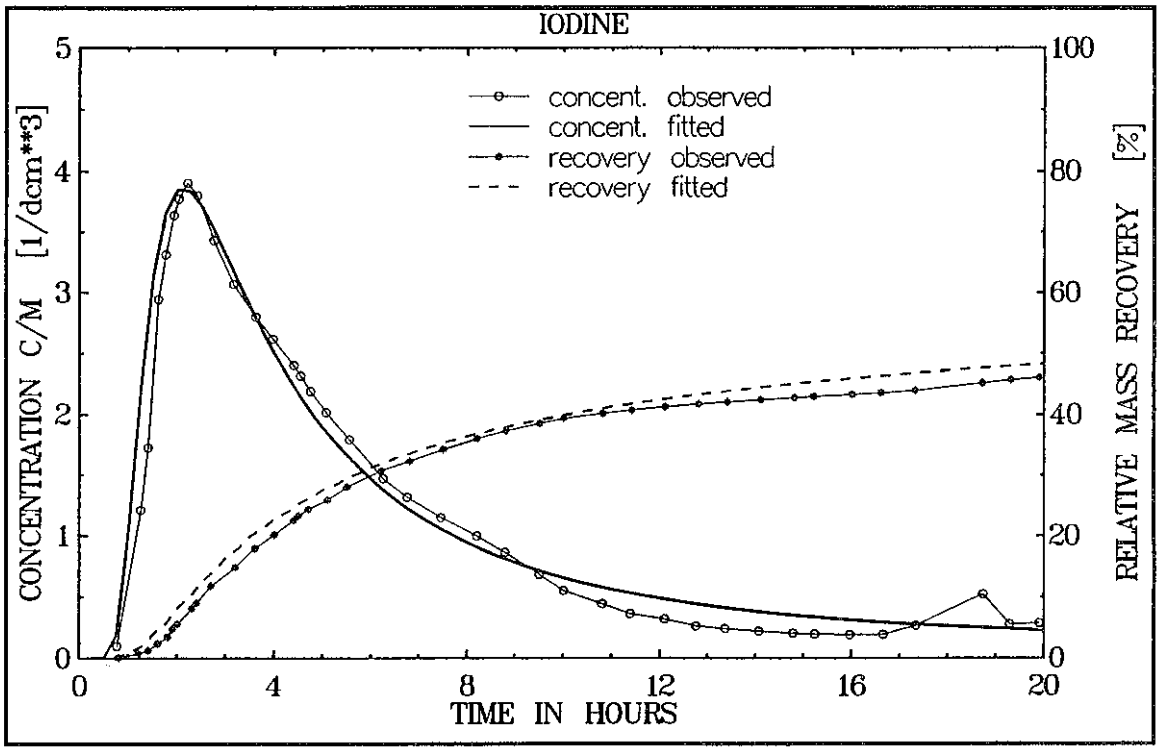

Fig. 27 **The best fit of the SFDM obtained for Iodide, with an additional fit of the mass recovery curve (experimental points after GARNIER et al. 1985)**

The above example demonstrates that the calibration of a multi-parameter model is a relatively easy though not unambiguous process. An independent information is required, which can only be obtained from a multitracer experiments and/or from laboratory determinations of some parameters in order to change nondisposable parameters to disposable ones.

The parameters obtained for all four tracers from the new fitting procedure are summarized in Table 6. From the parameters found for ideal tracers (D_2O, and Uranine in approximation), the physical parameters of the system can be calculated by making use of the equations introduced in Chapter 2.2.2.1. MALOSZEWSKI & ZUBER (1990a) assumed that the micropores in the chalk are sufficiently large to ensure the constrictivity factor to be equal to unity and that the tortuosity

factors for the fissures and microporous matrix are equal to 1.5. The following values of diffusion coefficients in free water (D_m) were used: $2.5 \cdot 10^{-9}$ m^2/s for D_2O, $4.5 \cdot 10^{-10}$ m^2/s for Uranine, $1.6 \cdot 10^{-9}$ m^2/s for Iodide, and 10^{-9} m^2/s for $H^{13}CO_3^-$.

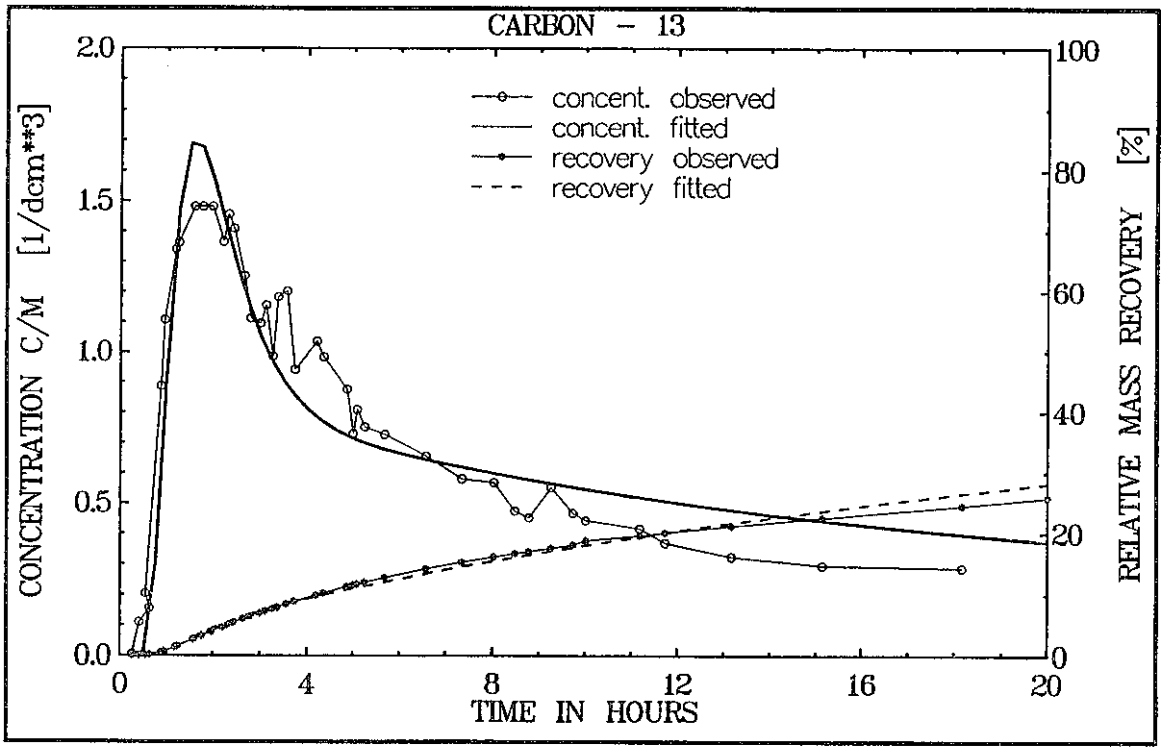

Fig. 28 **The best fit of the SFDM obtained for $H^{13}CO_3^-$, with an additional fit of the mass recovery curve (experimental points after GARNIER et al. 1985)**

The fissure porosity (n_f) is calculated from eq. (27) for found t_o, known pumping rate (Q), and distance between the wells (X). Following MALOSZEWSKI & ZUBER (1990a), instead of the aquifer thickness, the lenght of the screen in the pumping well (15 m) was used. This realistic assumption yielded quite reasonable values of n_f: 0.0027 and 0.004, for D_2O and Uranine, respectivelly. Next, for known hydraulic conductivity (4.6 m/d), and the values of n_f, the fissure appertures (2b) obtained from eq. (29) were 270 μm and 220 μm, respectively. Finally, from eq. (30), (in MALOSZEWSKI & ZUBER 1990a) that equation was given in a wrong form, which however did not yield a great error], the matrix porosity of 0.29 and 0.17 results from the heavy water and Uranine data, respectively. The matrix porosity found from the D_2O curves is closer to typical values of matrix porosity for chalks and marls (PRICE 1987), than the value yielded by Uranine. However, if one assumes $R_{af}=1.5$ and $R_{ap}=1$, the physical parameters of the system found from Uranine are: $n_f=0.0027$ and $2b=270\mu m$, and $n_p=0.31$, i.e., nearly identical to those found from heavy water. In other words it seems that the Uranine is distinctly delayed in the fissures ($R_{af}=1.5$) but does not react strongly in the matrix. This phenomena remains unclarified.

For reactive tracers an additional interpretation of the retardation factors (R_{ap}) is possible from the a-parameter by making use of eq. (10.2). The diffusion coefficients in free water (D_m)

given earlier, the matrix porosity of 0.29 and the fissure aperture of 2b=270 μm found from D_2O curve yield from eq. (10.2) $R_{ap}=1.4$ and $R_{ap}=2.3$, for Iodide and $H^{13}CO_3^-$, respectivelly.

The physical and reaction parameters calculated from the parameters given in Table 6 are summarized in Table 7.

Table 6 **The SFDM parameters obtained for a fractured chalk from the experiment of GARNIER et al. (1985), by making use of the combined model of reactions in the matrix (eq. 23), and with additional fitting of the mass recovery curves. The a-parameter is expressed by eq. 11.1 for ideal tracers and by eq. 10.2 for reactive tracers.**

Tracer	t_o	a	P_D	R_{af}	k_1'	k_2
	hr	$s^{-1/2}$	-	-	1/hr	1/hr
D_2O	0.64	$40.0\cdot10^{-3}$	0.02	-	-	-
Uranine	0.95	$13.3\cdot10^{-3}$	0.015	1.0[1]	-	-
Iodide	0.64[1]	$41.7\cdot10^{-3}$	0.02[1]	1.0[1]	0.05	0.007
Iodide[2]	0.64[1]	$39.6\cdot10^{-3}$	0.02[1]	1.25	0.06	0.01
$H^{13}CO_3^-$	0.64[1]	$41.7\cdot10^{-3}$	0.02[1]	1.0[1]	0.72	0.1

1) Assumed

2) a-parameter is calculated from fitted value of a by using $R_{af}=1.25$ (eqs 9 and 9.3 combined with 10.2)

Table 7 **The physical and reaction parameters calculated from the fitted parameters given in Table 6**

Tracer	n_f	2b	n_p	R_{ap}	k_1	k_2
	%	μm	%	-	1/hr	1/hr
D_2O	0.27	270	29	-	-	-
Uranine	0.40	220[1]	17	1.0[2]	-	-
Uranine[3]	0.27	270	31	1.0[2]	-	-
Iodide	0.27[1]	270[1]	29[1]	1.4	0.07	0.007
Iodide	0.27[1]	270[1]	29[1]	1.4	0.08	0.01
$H^{13}CO_3^-$	0.27[1]	270[1]	29[1]	2.3	1.66	0.1

1) Assumed from the parameters found from D_2O

2) Assumed

3) Parameters obtained under the assumption of abnormal behaviour of Uranine, i.e., adsorption in fissures ($R_{af}=1.5$) and no reactions in the porous matrix ($R_{ap}=1.0$)

It is interesting to calculate the p-parameter for an ideal tracer (eq. 11.2) to check if the condition for applying the SFDM instead of the PFDM (eq. 18.1) was satisfied in that experiment. From both porosities and the value of the a-parameter one obtains $p=1.34 \cdot 10^3$ $s^{1/2}$ $=22$ $hr^{1/2}$ for heavy water or $p=1.6 \cdot 10^3$ $s^{1/2}=27$ $hr^{1/2}$ for Uranine, and eq. (18.1) yields approximately $t_k < 120$ hrs, which was very well satisfied (see Figs 25 through 28).

The above case study has documented that in spite of its simplicity, the SFDM works surprisingly well. The SFDM was not only calibrated, but was also shown to yield reasonable values of the physical parameters, which can be regarded as a partial validation process. A more complete validation would require determination of n_p and reaction constants on rock samples.

Another experiment performed in the English Chalk by IVANOVICH & SMITH (1978) and reinterpreted by MALOSZEWSKI & ZUBER (1985) is mentioned here for the comparison of parameters obtained for similar formations in different field experiments. The experiment was done with a radioactive tracer ($^{82}Br^-$) in a radial-convergent flow on the distance of 8 m with the pumping rate of 3.85 m^3/hr. The thickness of aquifer was 13 m. The hydraulic conductivity of 0.7 m/d was estimated by KREFT & ZUBER (1979). The model parameters obtained by fit of the SFDM (eq. 25) given by MALOSZEWSKI & ZUBER (1985) were $t_0 = 1.5$ hr, $P_D = 0.08$ and $a=21 \cdot 10^{-3}$ $s^{-1/2}$. The calculated fissure porosity of 0.0022 (eq. 27) is close to that found in France. The fissure aperture $2b=115$ μm (eq. 29) is smaller than that in France, but qualitatively agrees with lower hydraulic conductivity, and agrees well with 100 μm estimated by FOSTER (1975). MALOSZEWSKI & ZUBER (1985) assumed the diffusion coefficient of bromide in the matrix to be equal to 10^{-10} m^2/s and obtained the matrix porosity of 23%. However, if $D_p = 10^{-9}$ m^2/s is assumed, the matrix porosity is only about 8%, definetely too low for a chalk formation. Therefore, it can be concluded that without independent determinations of n_p and/or D_p, the accuracy of physical parameters is limited by a factor of 2 to 3.

4.1.2 Tracer experiments in a fractured ore-dike of granite

In a gallery (observation tunnel) of a test site at Lindau, Schwarzwald, Germany, several tracer experiments and hydraulic tests have recently been performed in a fractured zone of the Hermann ore dike in the Albtal granite. A relatively high permable zone is a result of fracturing by tectonic shear processes and of weathering through descendant meteoric waters. This fractured zone is nearly tight at the depths of more than 80 m below the surface (HIMMELSBACH 1991, 1992; HIMMELSBACH & MALOSZEWSKI 1992). Tracer experiments were carried out just above the tight zone in radial-convergent (monopole tests) and injection-withdrawal (dipole tests) flow conditions. The SFDM model was applied in both types of tests in the way described in Chapter 2.2.2.1 (HIMMELSBACH & MALOSZEWSKI 1992). The results obtained are recalled here to compare monopole and dipole tests performed between the same pairs of two wells. The concept of the mass recovery was included in the fitting procedure. All the tracer used (Uranine, Eosine, Pyranine and deuterium) are regarder here as ideal ones. The tortousity factor in fissures was assumed to be $\tau_f = 1.5$.

Two monopole tests were performed between wells BL8 and BL10 for a distance of 11.2 m. In the first experiment (Monopole I with $Q=0.353$ m^3/hr) Pyranine was injected in well BL8 and observed in BL10. In the second experiment performed several months later (Monopol VI with $Q=0.346$ m^3/hr) two tracers: Pyranine and deuterium (heavy water) were injected simultaneously in well BL10 and their concentrations were observed in well BL8. In the fitting procedure it was necessary to assume that in both experiments a part of tracers were partialy lost. In the firts test the loss was about 15% whereas in the second about 10%. The fitting

parameters obtained for Pyranine were nearly the same in both experiments: t_o=1.58 and 1.62 hrs, P_D=0.03 and 0.02, a=11.6·10^{-3} and 10.3·10^{-3} s$^{-1/2}$ for Monopole I and VI, respectively. The best fit curves of Pyranine are shown in Fig. 29. For the sake of the comparison of the results, the concentration curves were normalized to be independent from the volumetric flow rates and the masses of tracers used (CQ/M). The fissure porosity calculated (eq. 27) for the permeable zone thickness of 1.53 m was in both cases the same and equal to about 0.001. Similarly, the mean fissure aperture calculated for k=0.89·10^{-5} m/s (found for the injection well from the hydraulic tests) was the same, i.e. 184 μm (eq. 29). The matrix porosities calculated from eq. (30) for D_m=1.3·10^{-9} m^2/s, were 7.3% and 6.5% for the first and second experiment, respectively. The justification for the accepted value of D_m is given further.

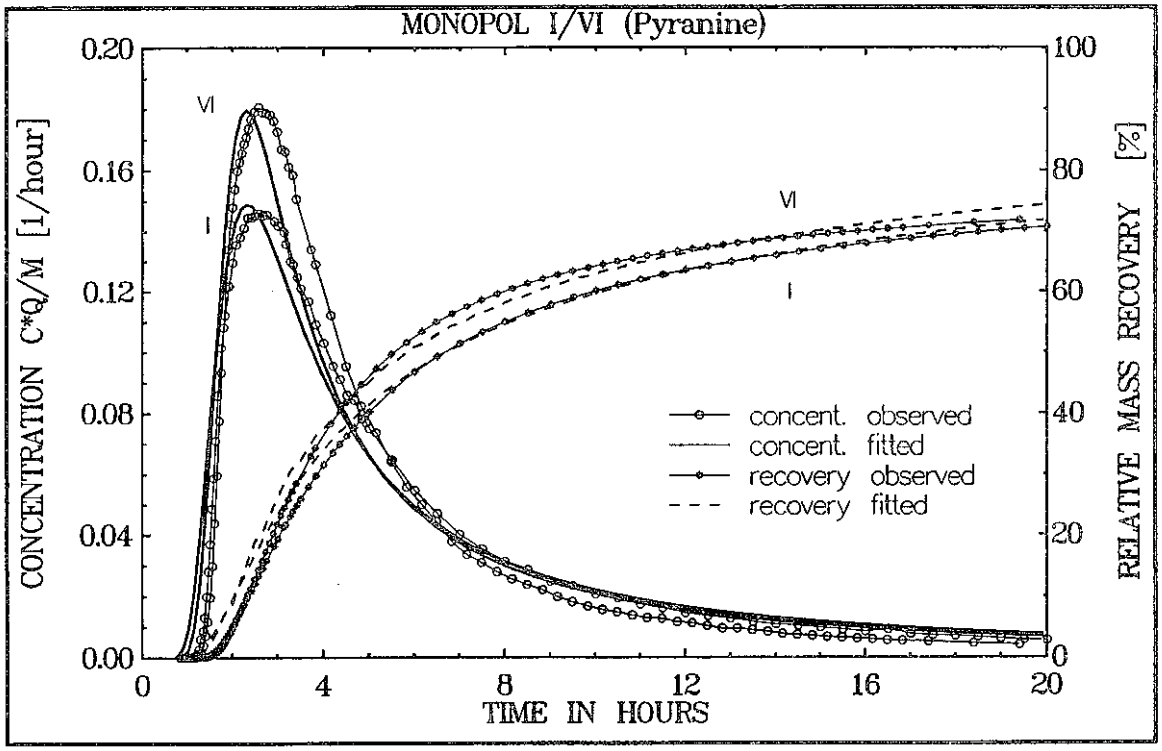

Fig. 29 **The best fits of the SFDM to tracer concentration and recovery curves in two monopole tests performed between the same pair of wells (BL8-BL10) in an ore-dike of fractured granite at the test site of Lindau**

The modelling of deuterium was only possible for the tracer concentration curve normalized to the maximum concentration. The difficulty encountered was probably related to a low concentration of tracer and poor determination of the mass injected [the maximal concentration measured (about 200 ppm) was only 30% higher than the natural background concentration (about 150 ppm)]. In spite of that difficulty, the two fitting parameters, which should be independent of the tracer used, agreed well with values obtained from Pyranine (t_o = 1.52 hrs and P_D=0.02 versus t_o=1.58 and 1.62 hrs, and P_D=0.02 and 0.03 for Pyranine). The diffusion parameter, a=14.2·10^{-3} s$^{-1/2}$, found for deuterium is about 1.4 times larger than that found for Pyranine in the same experiment. Equation (11.1) shows that the ratio of a^2 for both tracers is equal to the ratio of molecular diffusion coefficients in the matrix for both tracers. In this way

(see MALOSZEWSKI & ZUBER 1989), the molecular diffusion coefficient for Pyranine can easily be estimated from the known molecular diffusion coefficient for deuterium, if both values of δ are equal to 1.0 (see eq. 30). Then, D_m (Pyranine) = $2.5 \cdot 10^{-9}/(1.4)^2 = 1.3 \cdot 10^{-9}$ m^2/s. If the values of δ were larger than 1, the D_p values should differ more and different tracers should yield greatly different values of η_p.

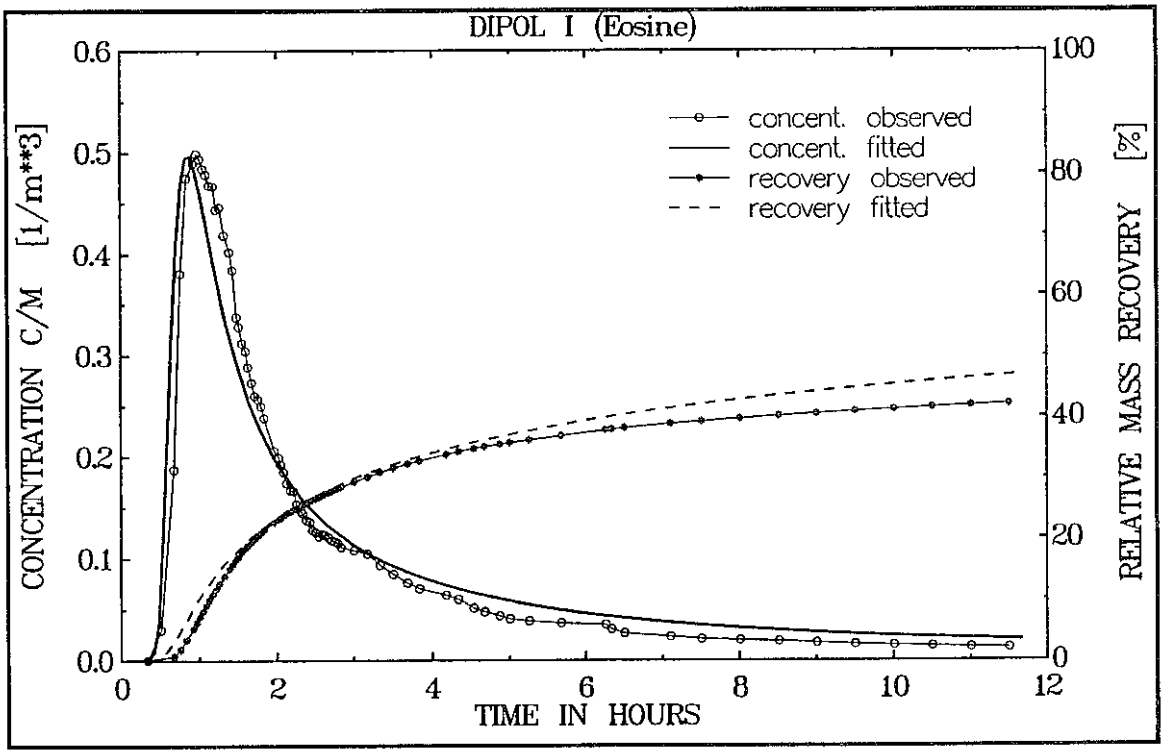

Fig. 30 **The best fits of the SFDM to tracer concentration and recovery curves in dipole test performed between the same pair of wells as in Fig. 29 (BL8-BL10)**

Between the same wells an injection-withdrawal test (Dipole I) was also performed with Eosine and the pumping rate of 0.457 m^3/hr. The injection was performed in well BL8. The best fit obtained with fitting parameters: $t_{o1}=0.6$ hr (eq. 34.1), $Pe_1=67$ (eq. 34.2) and $a=11 \cdot 10^{-3}$ $s^{-1/2}$ is shown in Fig. 30. The resulting parameters, i.e. fissure porosity of 0.0029 and the fissure aperture of 105 μm obtained are of the same order as those found from the monopole tests. The matrix porosity of 6.6%, calculated assuming the diffusion coefficient for Eosine to be the same as for Uranine, agrees well with 7.3% and 6.5% found in monopole tests with Pyranine and D_2O (see Table 9).

Another radial-convergent test (Monopole IV) was performed between two wells BL11 and BL9 for the distance of 16.2 m, pumping rate of 0.457 m^3/hr, and BL11 as an injection well. The calibration of the SFDM to the Uranine curve was obtained for $t_o=1.25$ hr, $P_D=0.075$ and $a=5.66 \cdot 10^{-3}$ $s^{-1/2}$. The best fit curves are shown in Fig. 31. For the known mean thickness of the water bearing layer of 2.15 m, the fissure porosity was calculated to be 0.0005. The hydraulic conductivity of $1.1 \cdot 10^{-5}$ m/s (0.95 m/d) found from the hydraulic test (transmissivity,

$T=2.47\cdot10^{-5}$ m^2/s) yields the mean fissure aperture of 280 μm. Matrix porosity obtained from eq. (30) was 9.3%, for assumed $D_m=4.5\cdot10^{-10}$ m^2/s.

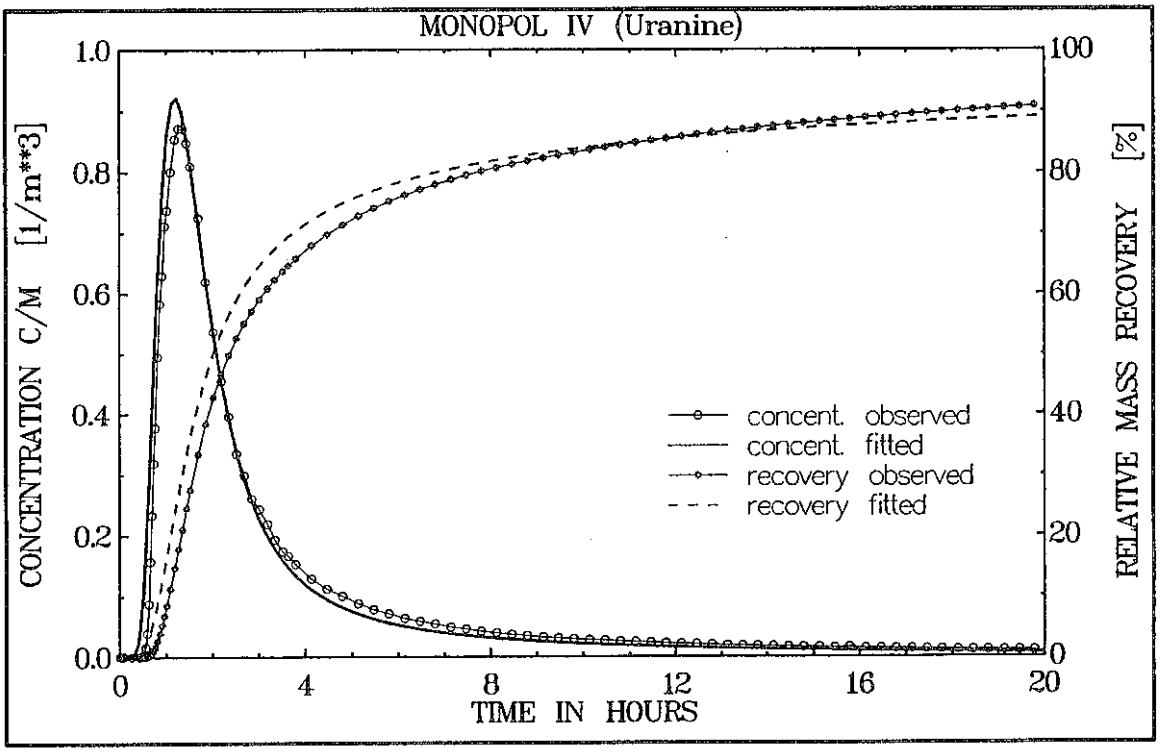

Fig. 31 **The best fits of the SFDM to tracer concentration and recovery curves in monopole test performed between the wells BL9 and BL11 in ore-dike of fractured granite at the test site of Lindau**

The injection-withdrawal test (Dipole III) was performed between the same wells with the flow rate of 0.396 m^3/hr. Pyranine was injected in well BL11 and observed in BL9. The best fit, shown in Fig. 32, was obtained for $t_{o1}=0.7$ hr, $Pe_1=67$ and $a=4.91\cdot10^{-3}$ $s^{-1/2}$. The calculated fissure porosity and aperture ($n_f=0.0005$ and $2b=280$ μm) were exactly the same as in monopole test. Taking $D_m=1.3\cdot10^{-9}$ m^2/s, the matrix porosity of 4.8% was obtained. This value is about two times smaller than that obtained for Uranine. The fitting parameters for all experiments are summarized in Table 8, whereas resulting physical parameters of the system in Table 9.

The SFDM works very well both in monopole and dipole tracer test yielding quite realistic physical parameters of the system. Unfortunately, laboratory measurements of the matrix porosity have not been performed so far, and, therefore, a direct validation of the model is unavailable. However, a good agreement of the physical parameters obtained in a number of experiments performed with several tracers of different diffusion coefficients can perhaps be considered as an indirect validation.

It is interesting to calculate the fissure spacing, and consequently the number of fissures between the wells in the ore dike by making use of eq. (80) for the known fissure porosity,

fissure aperture and thickness of the aquifer [$N = mn_f/(2b\tau_f)$, see next Chapter]. In monopole tests between wells BL8 and BL10 one obtains 5-6 fissures, in agreement with 5 fissures visually observed in BL10 (HIMMELSBACH 1992). However, for the dipole experiment with Eosine, the number of fissures is in a disagreement with the value observed. Of the five tests performed only the test with Eosine appeared to differ from all the other test (Table 8). The reason for that discrepancy is not known. Perhaps Eosine cannot be regarded as an "ideal" tracer in that case due to some retardation in the fissures.

Table 8 **Pumping rates used and model parameters obtained in ore dike zone of fissured granite at the Lindau test site by making use of the SFDM under radial-convergent and injection-withdrawal flow conditions (eqs 23 and 31.2 with 32, respectively)**

Tracer	Experiment	Q	t_o	a	P_D
		m^3/hr	hr	$s^{-1/2}$	-
Pyranine	BL8-10 Mon.I	0.353	1.58	$11.6 \cdot 10^{-3}$	0.03
Pyranine	BL8-10 Mon.VI	0.346	1.62	$10.3 \cdot 10^{-3}$	0.02
D_2O	BL8-10 Mon.VI	0.346	1.52	$14.2 \cdot 10^{-3}$	0.02
Eosine	BL8-10 Dip.I	0.457	0.60	$11.0 \cdot 10^{-3}$	0.015
Uranine	BL11-9 Mon.IV	0.457	1.25	$5.7 \cdot 10^{-3}$	0.075
Pyranine	BL11-9 Dip.III	0.396	0.70	$4.9 \cdot 10^{-3}$	0.015

Table 9 **The physical parameters obtained for the ore dike zone of granite at the Lindau test site from the parameters of SFDM, and calculated and observed numbers of fissures**

Tracer	Experiment	2b	n_f	n_p	N	N
		µm	%	%	calc.	obs.
Pyranine	BL8-10 Mon.I	184	0.10	7.3	5-6	5
Pyranine	BL8-10 Mon.VI	184	0.10	6.5	5-6	5
D_2O	BL8-10 Mon.VI	184	0.10	6.5	5-6	5
Eosine	BL8-10 Dip.I	105	0.29	6.6	25	5
Uranine	BL11-9 Mon.IV	280	0.05	9.3	3	3-4
Pyranine	BL11-9 Dip.III	280	0.05	4.8	3	3-4

In monopole and dipole tests performed between BL11 and BL9 the number of fissures was the same N=3, and agrees surprisingly well with 4 and 3 observed in BL11 and BL9, respectively. Additionally, the fissure apertures obtained from the dipole tracer experiments agreed reasonably with those found from dipole hydraulic tests [105 μm and 280 μm against 88 μm and 306 μm (HIMMELSBACH; private information) for BL8-BL10 and BL11-BL9, respectively]. Concluding, one can say that the SFDM was not only calibrated but also indirectly validated in the test field of fractured zone of ore dike in granite formation.

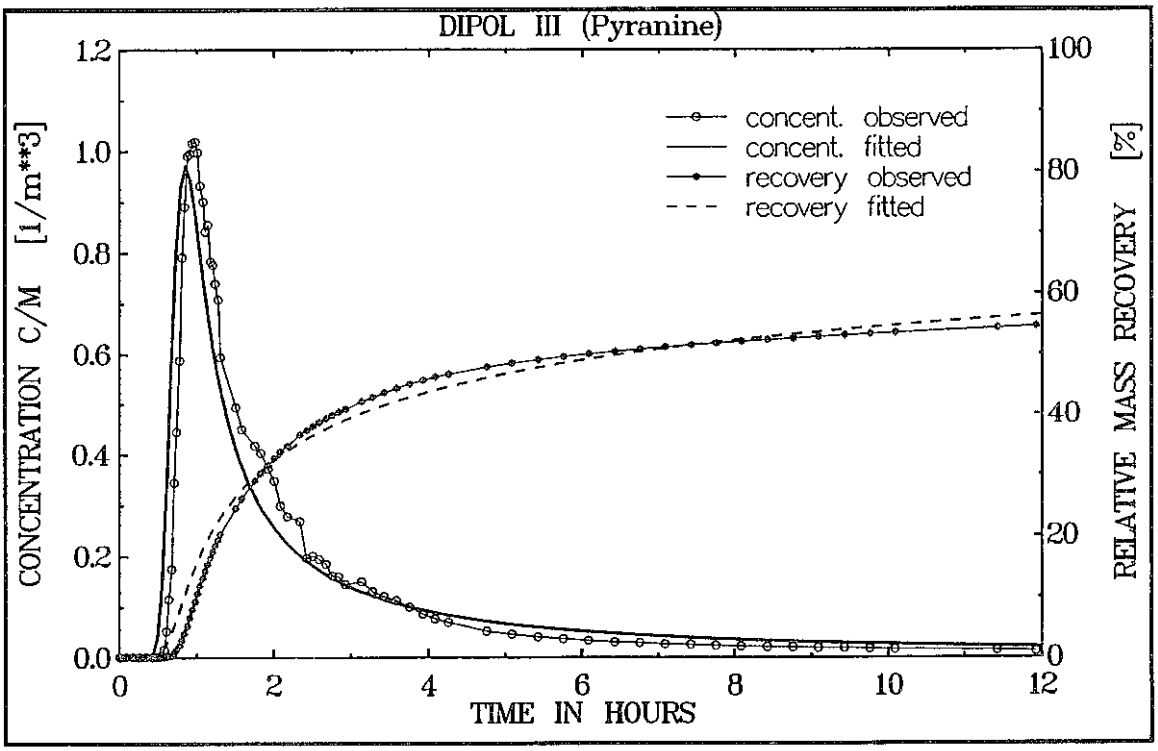

Fig. 32 **The best fits of the SFDM to tracer concentration and recovery curves obtained in dipole test performed between the same pair of wells as in Fig. 31 (BL9 and BL11)**

4.1.3 Tracer experiments in fractured dolomite

Two examples shown here are taken from KREFT et al. (1974) and LENDA & ZUBER (1970). Both experiments were performed in radial-convergent flow (pumping test) in the same geological formation of a fractured dolomite in order to determine the effective porosity of Zn-Pb deposits. Unfortunatelly, due to an uncontrolled loss of tracer in stagnant zones of the injection wells, the concept of the tracer recovery cannot be included.

The first experiment was performed on a distance of 21.3 m with the mean thicknees of water bearing layer equal to 48 m. The pumping rate was 120 m^3/hr. The hydraulic conductivity obtained from pumping tests was about 50 m/d (ZUBER 1974). The radioactive $^{131}I^-$ with a carrier was considered as an ideal tracer. By applying the SFDM (eq. 25), the best fit (see Fig. 10 in MALOSZEWSKI & ZUBER 1985) was obtained for the following model parameters:

t_o=8.7 hrs, P_D=0.11 and a=10^{-3} $s^{-1/2}$. Assuming, as previously, that the tortuosity factor for the fissures is equal to 1.5, the model parameters yield fissure porosity of 0.016, fissure aperture of 360 μm and matrix porosity of 3.4%. This last value is a rough estimate because it was calculated from eq. (11.1) for an assumed value of the diffusion coefficient in the matrix, $D_p=10^{-10}$ m^2/s.

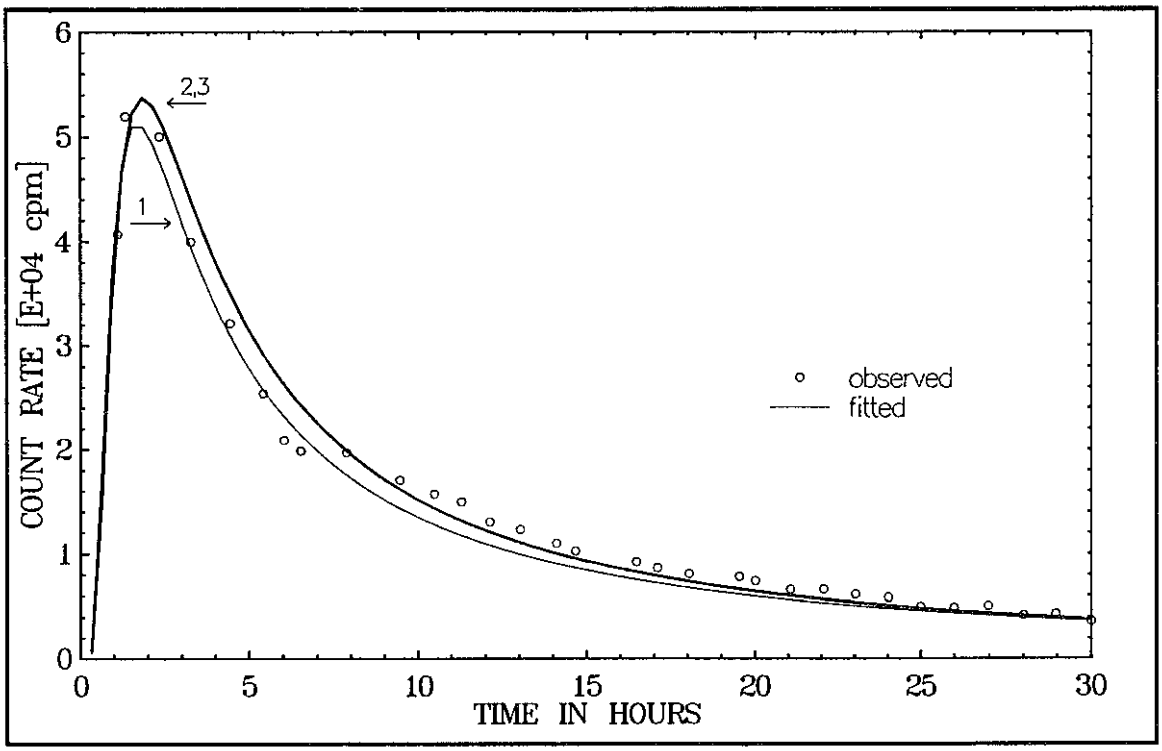

Fig. 33 **Three best fits of the SFDM to the tracer concentration curve obtained in the experiment performed in a highly dispersive fractured dolomite (experimental points after LENDA & ZUBER 1970)**

In the second experiment, at another site situated several kms from the first one, the same tracer was used, for the distance between injection and pumping wells of 22 m, the thickness of the water bearing layer of 57 m, and the pumping rate of 1.7 m^3/hr. The hydraulic conductivity obtained from pumping tests was 41 m/d. The best fit of the SFDM was obtained by MALOSZEWSKI & ZUBER (1985) for t_o=28.8 hrs, P_D=3.0 and a=$3.2 \cdot 10^{-3}$ $s^{1/2}$ (see curve 1 in Fig. 33). These parameters gave: n_f=3.5%, 2b=225 μm and matrix porosity, n_p=7.1%. Both porosities are two times greater as those found in the first experiment.

As mentioned in Chapter 4.1.1, when a fitting procedure includes only the concentration curve (i.e. the concept of recovery cannot be applied), it may happen, that the solution is not unique. Two additional fits were found here with exactly the same accuracy as for the first one. The second fit was obtained for the following parameters: t_o=5.3 hrs, P_D=0.5 and a=$6 \cdot 10^{-3}$ $s^{1/2}$ (curve 2 in Fig. 33), which in turn yield n_f=0.006, 2b=524 μm and n_p=31%. The third fit was obtained for: t_o=11.1 hrs, P_D=1.0 and a=$2.6 \cdot 10^{-3}$ $s^{1/2}$ (curve 3 in Fig. 33), and yielded: n_f=0.013, 2b=362 μm and n_p=9.4%. Without an independent information it is not possible to

decide which set of parameters is the adequate one. However, an unrealistic value of matrix porosity found from fit 2 shows that this set of parameters can be eliminated.

The results obtained in both experiments are summarized in Table 10. In both experiments the SFDM was properly calibrated, however in the second experiment three fits were obtained, two of them physically acceptable. Several equally good fits in the second experiment result from a strong asymmetry of the tracer concentration curve expressed by extremly high values of the dispersion parameter, P_D. This problem was explained by KREFT (1983) who showed that in the cases of high dispersion, unique solutions are not available. In the situation considered the first and third fits yield, at least, results of the same order of magnitude. The matrix porosity interpreted from the parameters found in both fits agrees well with the mean value of matrix porosity equal to 6.4% found by J. MOTYKA (private information) for core samples of the same formation taken from a well at the distance of about 2 km, which can perhaps be regarded as a kind of direct validation.

Table 10 **The physical parameters obtained for a fractured dolomite in Poland as a result of fitting the SFDM (eq. 25) to the experimental data of KREFT et al. (1974) and LENDA & ZUBER (1970) performed in the same formation, but at different sites**

Tracer	n_f	2b	n_p
	%	μm	%
1th Exper.	1.6	360	3.4
2nd Exper.			
Fit 1	3.5	225	7.1
Fit 2	0.6	524	31.0
Fit 3	1.3	362	9.4

Another possibility for the selection of a more adequate set of parameters seems to be offered by eq. (18.1), which serves for the examination of the applicability of the SFDM. The p-parameter (eq. 11.3) calculated from the model parameters was $p=1.06 \cdot 10^3$ $s^{1/2}$ and $p=2.3 \cdot 10^3$ $s^{1/2}$ for the first experiment and for fit 3 in the second experiment, respectively. These values of p produce $t_k < 78$ hrs and $t_k < 367$ hrs, respectively, which is well satisfied in both cases. The parameters obtained by MALOSZEWSKI & ZUBER (1985), fit 1 in second experiment, yield $p=0.33 \cdot 10^3$ $s^{1/2}$ and consequently $t_k < 8$ hrs, which is not satisfied in the experiment, if the system parameters are properly found. It means that this set of parameters (fit 1) should not be taken into account. The above procedure, consisting of checking the internal consistency of data seems to be sound. However, further experience is needed to find out if such a procedure is generally applicable for tracer experiments interpreted with the aid of the SFDM.

4.1.4 Tracer experiments in fractured gneiss

RAVEN et al. (1981) performed five tracer experiments in the test field of Chalk River Nuclear Laboratories in Canada, described in detail by NOWAKOWSKI et al. (1985). RAVEN

et al. (1981) in their tests, tried to separate a single fracture with packers, and, consequently, they applied a model adequate to that assumption, and based on negligible matrix diffusion. MALOSZEWSKI & ZUBER (1993a) questioned both assumptions as shown below.

For the interpretation of tracer experiments in a single fissure some additional equations are needed (e.g., MALOSZEWSKI & ZUBER 1993a).

In a classical hydraulic pumping test the transmisivity of the water bearing layer (in confined aquifer), T, is equal to

$$T = Q\ln(X/r_w)/(2\pi\Delta H) \tag{77}$$

where r_w is the diameter of the pumping well, ΔH is the net imposed hydraulic head between the tracer injection and pumping wells, X is the distance between the wells, and Q is the pumping rate.

The transmisivity of the single fissure, T_s, is described by, the so-called cubic law (e.g., SNOW 1970; or GRISAK et al. 1980), which corrected by MALOSZEWSKI & ZUBER (1993a) for the fissure tortousity factor, τ_f, has the form

$$T_s = A(2b)^3/(\tau_f)^2 \tag{78.1}$$

where $A=qg/(12\mu)$ (q is the fluid density, g is the gravitational acceleration, μ is the dynamic viscosity). For water at 10°C, A is equal to $A=6.3\cdot10^5\ m^{-1}s^{-1}$.

The transmisivity of several unconnected fissures will be then

$$T = N \cdot T_s \tag{78.2}$$

where N=m/L is the number of fissures, i.e. the thickness of the fissured zone (m) divided by the fracture spacing (L).

By making use of eq. (10.1) the fissure aperture is:

$$2b = Qt_o/[\pi\tau_f(X)^2] \tag{79.1}$$

whereas, in the case of several fissures one obtains

$$2bN = Qt_o/[\pi\tau_f(X)^2] \tag{79.2}$$

For the model of parallel fractures, the matrix porosity (n_f) in a densely fissured rock is equal to (MALOSZEWSKI & ZUBER 1993a)

$$n_f = 2b\tau_f/L \tag{80}$$

and then eq. (79.2) can easily be simplified to eq. (27), which is normally used to calculate the fissure porosity in the system of fissures.

The fissure aperture can also be calculated from the transmissivity and the parameters of the pumping and tracer tests. By combining (78.1) with (79.1) and inserting into (77) one obtains

$$2b = X[\tau_f \ln(X/r_w)/(2\Delta H A t_o)]^{1/2} \qquad (81)$$

The above equation is valid for a single fissure and the system of N unconnected fissures, i.e., the fissure aperture calculated from eq. (81) is independent of the number of fissures.

Note that if tracer is transported through a single fissure, both equations (79.1) and (81) must produce the same result. Whereas, if the system of fissures exists, eqs (79.2) and (81) can be used to calculate the number of fissures (N).

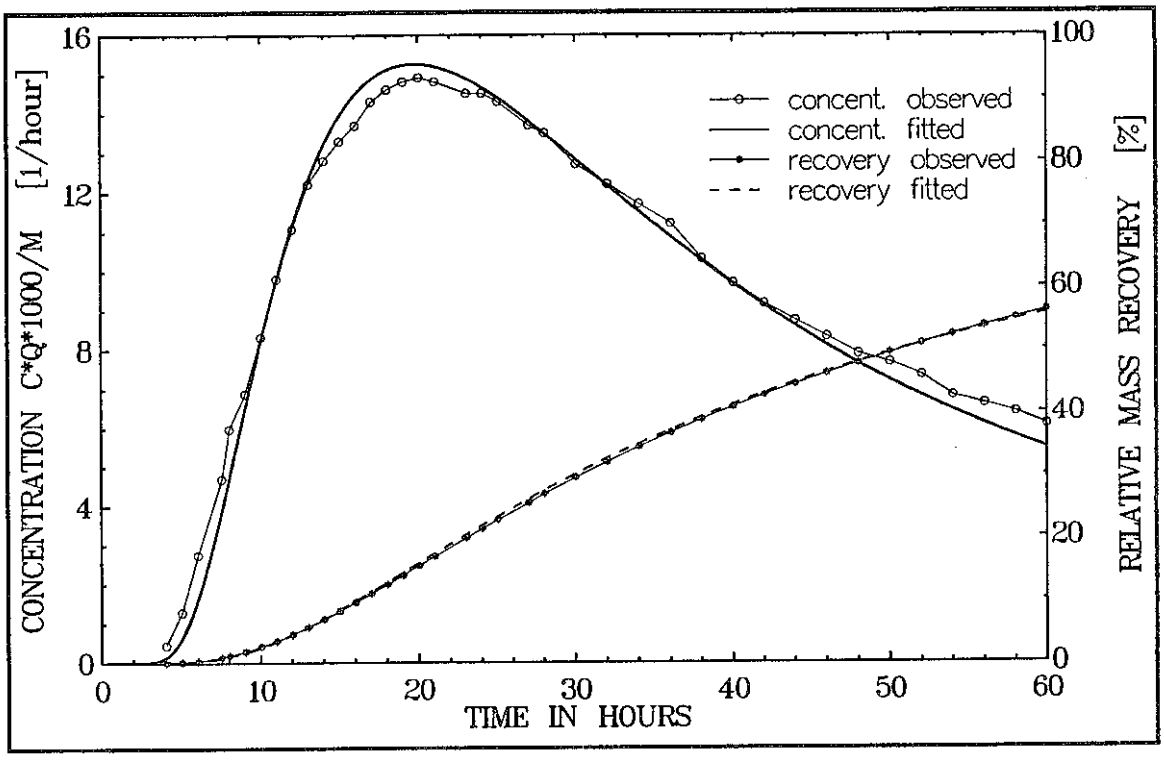

Fig. 34 **The best fits of the SFDM to tracer concentration and recovery curves obtained for experiment performed in fractured gneiss in Chalk River test site (experimental points after RAVEN et al. 1985)**

The following discusion is limited to the experiment performed in radial-convergent flow. The distance between the injection and observation wells was 12.7 m, and the pumping rate was 0.014 m^3/hr. The tracer used, radioactive $^{82}Br^-$ is an ideal tracer. The best fit curves obtained with $t_o=34.5$ hrs, $P_D=0.23$ and $a=10^{-3}$ $s^{-1/2}$ are shown in Fig. 34. The diameter of the pumping well was not given by RAVEN et al. (1988), but MALOSZEWSKI & ZUBER (1993a) assumed $r_w=7.5$ cm. The net imposed hydraulic head between the wells was $\Delta H=0.7$ m. Assuming the tortousity factor equal to 1.5, the fissure aperture (2b) calculated from eq. (81) is equal to $2b=110$ μm. This value agrees very well with the mean value of $2b=135$ μm found

from several hydraulic tests (RAVEN et al. 1988). In contrary to this value, eq. (79.1) yields $2b=635$ μm. MALOSZEWSKI & ZUBER (1993a), after analysing the hydrological situation presented in RAVEN et al. (1988), found that in reality the experiment was probably not performed in a single fracture, but in a system of several fractures. Consequently, eq. (79.2) is valid, and 635 μm coresponds to 2bN, which yields the number of fissures $N=635\mu m/110\mu m \approx 6$. Now taking the spacing of packers, $m=0.64$ m, as the thickness of the investigated part of aquifer, the fissure porosity of 0.0015 is easily obtained from eq. (29). For known n_f and 2b, eq. (80) yields the fissure spacing of 0.11 m. Such a fissure spacing produces, for the assumed above fissured zone, the number of fissures equal to $N=0.64/0.11=6$, which agrees surprisingly well with N calculated by making use of eqs (81) and (79.2). The parameter $p=2.67 \cdot 10^3$ $s^{1/2}$ yields $t_k < 490$ hrs, which means that the condition for the applicability of the SFDM was well satisfied.

This example shows that the SFDM also works in fissured rocks of low matrix porosity and that matrix diffusion can play an important role in such formations. It should be noted that RAVEN et al. (1988) underestimated five times the value of the a-parameter ($2 \cdot 10^{-4}$ $s^{-1/2}$) and concluded that such a small value permits to neglect the influence of matrix diffusion. However, the theoretical curves shown in Fig. 14 (Chapter 3.2) demonstrate that even for such small value of a, the matrix diffusion should be taken into account.

Detailed discussion and reinterpretation of other experiments performed by RAVEN et al. (1988) can be found in MALOSZEWSKI & ZUBER (1993a).

4.1.5 Tracer experiments in fractured granite of uranium mine

CACAS et al. (1990a) presented a stochastic model of a dense network of fractures consisting of discs. CACAS et al. (1990b) used that model of flow coupled with the particle tracking method for the interpretation of tracer experiments performed in highly fractured granite. The test field was situated about 150 m below the surface in a 100 m long drift in Fanay-Augeres uranium mine in France. The tracer passages were observed between the sections of wells drilled from the drift and the drift which drains water locally. The transport model applied by CACAS et al. (1990b) was based on negligible diffusion of tracer into the porous matrix. On the other hand, MALOSZEWSKI & ZUBER (1992, 1993a) showed that the SFDM yielded much better fit than the model of CACAS et al. (1990b), and the values of its parameters were reasonable. As the experiments lasted up to three months they are recalled here to show how the SFDM works in such a case. Due to the conditions of the experiments the concept of the mass recovery could not be applied, and, therefore, the tracers used, fluorescent dyes, Iodide and Cr-EDTA were assumed to be ideal tracers. The best fits obtained for four experiments F3-CH6 ($X=14$ m), F3-CH4 ($X=18$ m), F3-CH3 ($X=26$ m) and F2-CH7 ($X=16$ m) are shown in Figs 35-38, whereas the model parameters obtained are summarized in Table 11 (the distances are those estimated by MALOSZEWSKI & ZUBER 1993a; from figures given by CACAS et. al 1990a, 1990b). Assuming the matrix porosity of about 0.02 (BAUDRACCO et al. 1982) and $D_p=10^{-11}$ m^2/s (SKAGIUS & NERETNIEKS 1986), the fissure aperture (2b) can be calculated from the a-parameter by making use of eq. (11.1). The values obtained vary between 23 μm and 40 μm for different experiments (see Table 11), with the mean value of about 33 μm. For the known values of hydraulic conductivity ($k=2 \cdot 10^{-8}$ m/s according to CACAS et al. 1990a) and fissure aperture (2b), one can apply eq. (29) to estimate the fissure porosity (n_f) as follows:

$$n_f = k(1260\tau_f)^2/(2b)^2 \qquad (82)$$

where k is expressed in [m/s] and 2b in [μm]. The fissure porosities calculated from eq. (82) are given in Table 12.

Table 11 **The SFDM parameters obtained for four experiments in fractured granite of uranium mine in Fanay-Augeres**

Experiment	X[1)]	t_o	a	P_D
	m	hr	$s^{-1/2}$	-
F3-CH6	14	190	$2.83 \cdot 10^{-3}$	0.08
F3-CH4	18	140	$1.58 \cdot 10^{-3}$	0.05
F3-CH3	26	150	$1.67 \cdot 10^{-3}$	0.08
F2-CH7	16	90	$2.00 \cdot 10^{-3}$	0.50

[1)] Distances estimated as explained in the text.

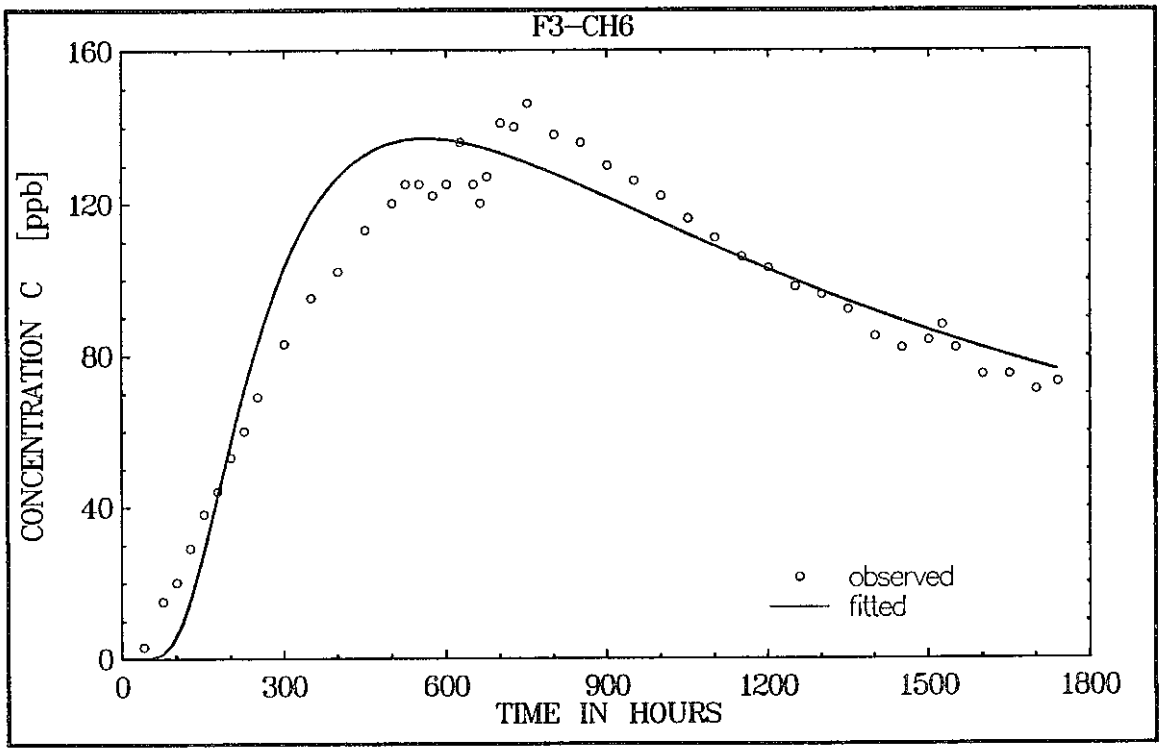

Fig. 35 **The best fit of the SFDM and tracer concentration data obtained in the experiment F3-CH6 of CACAS et al. (1990b)**

The fissure porosity can also be calculated from the Darcy law using the mean transit time of water (t_o) found from the SFDM, known hydraulic gradients (i), flow distances (X), and hydraulic conductivity (k):

$$n_f = ikt_o/X \qquad (83)$$

The above equation yields the fissure porosities about 2.5 times greater (see Table 12) than those obtained from eq. (82). Note that this difference can easily be eliminated by assuming other acceptable values of the diffusion coefficient in eq. (29). Consequently, by accepting the values from eq. (83), one obtains the mean fissure porosity of about 0.0002.

Table 12 **The physical parameters obtained from the parameters of the SFDM (a and t_o) given in Table 11, assuming the matrix porosity n_p=0.02 and by making use of eq. (11.1) for calculating 2b, and eqs (82) and (83) for calculating n_f**

Experiment	i	2b	n_f	
		μm	(eq. 82)	(eq. 83)
F3-CH6	0.4	23	0.00014	0.00039
F3-CH4	0.4	40	0.00005	0.00022
F3-CH3	0.4	38	0.00005	0.00016
F2-CH7	0.9	32	0.00007	0.00016

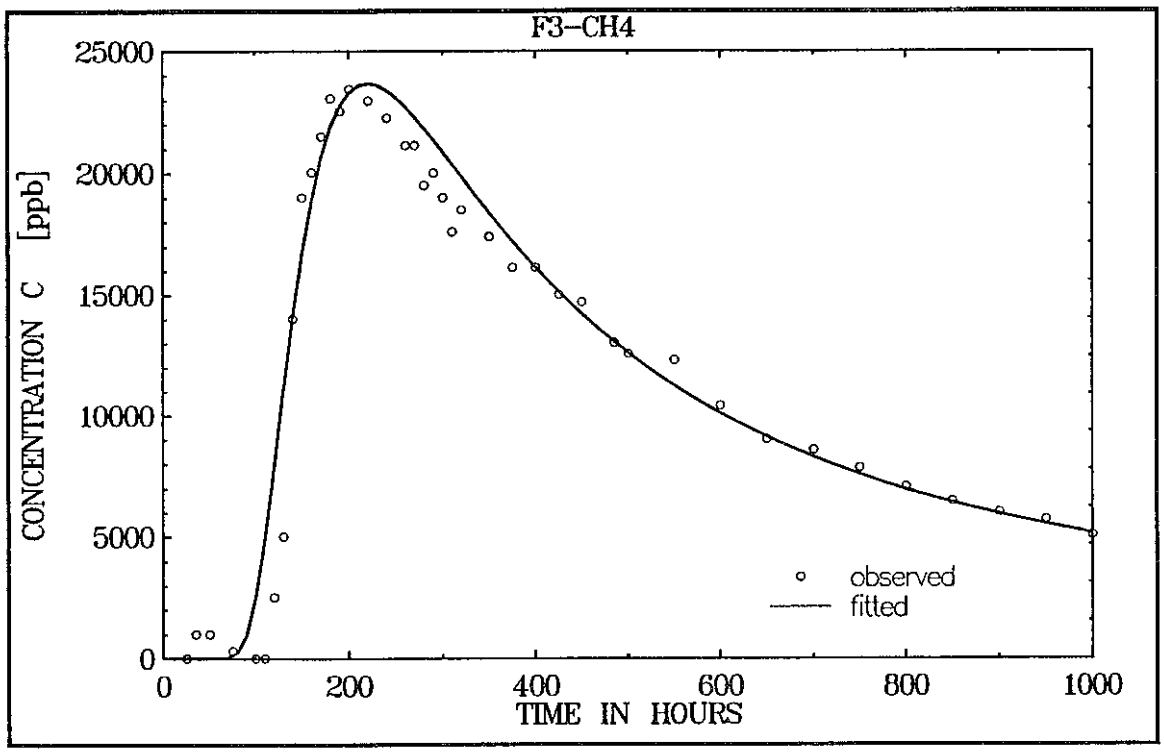

Fig. 36 **The best fit of the SFDM and tracer concentration data obtained in the experiment F3-CH4 of CACAS et al. (1990b)**

It is interesting to examine the condition given by eq. (18.1). On the basis of the mean values of parameters found above one obtains $p=2.6\cdot10^4$ $s^{1/2}$. This value yields $t_k < 5$ yrs, which is satisfied very well in all the experiements (in the longest one the concentration curve was measured till 2000 hrs, i.e. nearly three months). Such a value of t_k means that the tracer concentration curve observed in the outflow from the system up to 5 years after the injection can be interpreted by the SFDM. In other words, it means that for a low diffusion coefficient and a large fissure spacing (say, L=0.25 m as calculated from eq. 80), the tracer transport for a quite long time can be approximated by a single fissure model. A relatively high value of the a-parameter proves the necessity of taking into account the diffusion processes, even if the diffusion coefficient and the matrix porosity are so low.

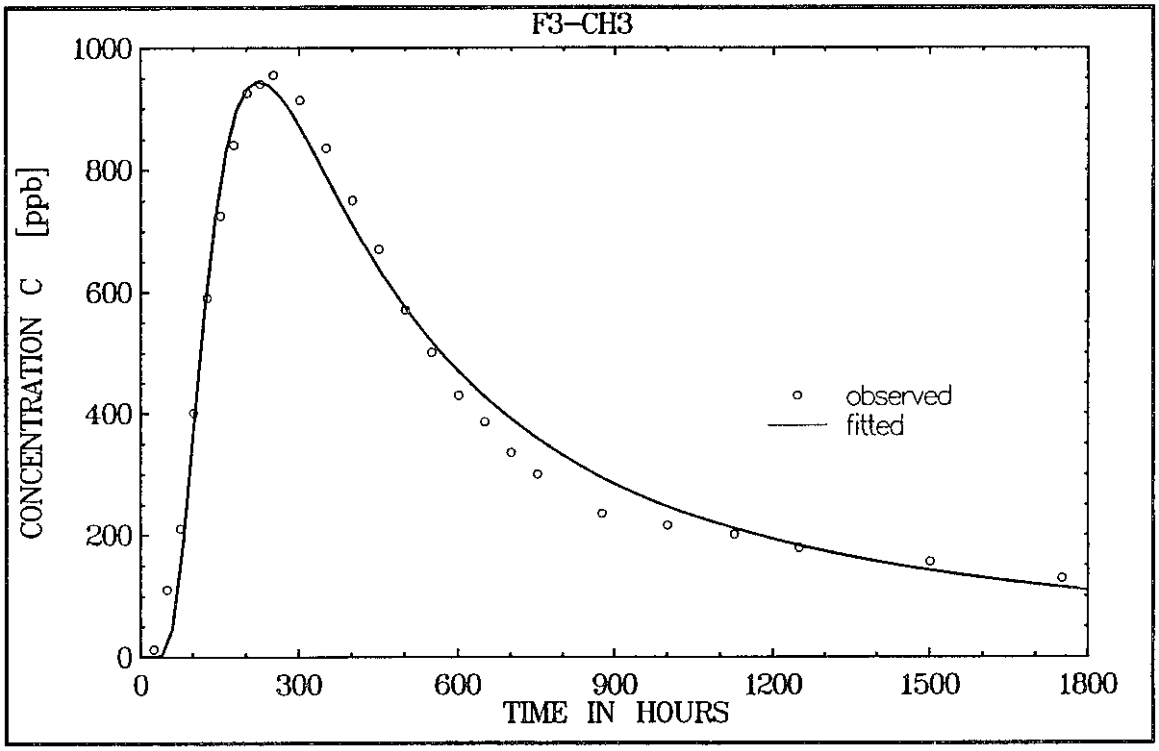

Fig. 37 **The best fit of the SFDM and tracer concentration data obtained in the experiment F3-CH3 of CACAS et al. (1990b)**

Imagine that the flow parameters, i.e. the mean transit time of water and the intrinsic dispersion parameter were determined independently by other methods (e.g., by a transport model based on the observed distribution of the fissure aperture and spacing). For such a case, the tracer curves obtained by calibration of the SFDM in F3-CH3 experiment (curve 1), with those calculated from dispersion model without diffusion, but for the same values of flow parameters t_o and P_D (curve 2) are compared in Fig. 39. That figure explicitly shows the consequences of neglecting a possible influences of diffusion [for a better demonstration the tracer recovery curves (3 and 4) are also compared].

Concluding, it is interesting to point out that the SFDM may work very well also in a long-term experiment in which the concentration curves have to be measured up to three months or more. In such a case, the model is applicable if the physical parameters of the system yield a large value of the model parameter p (as it happens for a very low fissure porosity).

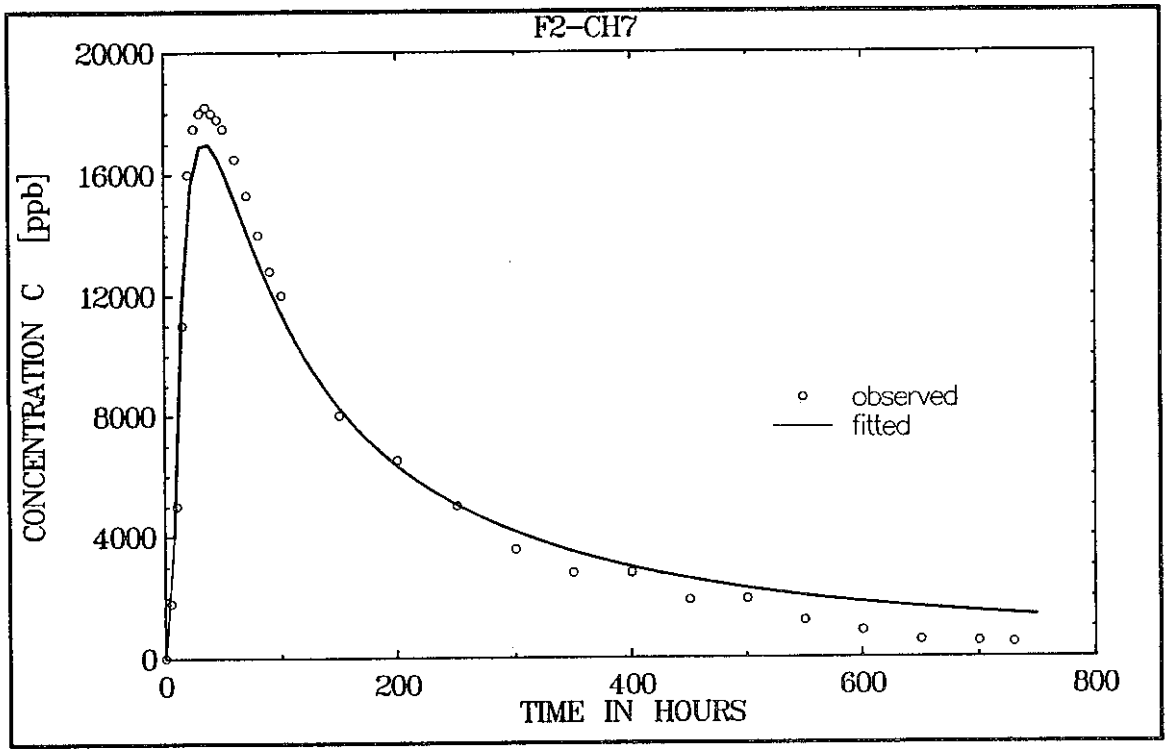

Fig. 38 **The best fit of the SFDM to tracer concentration data obtained in the experiment F2-CH7 of CACAS et al. (1990b)**

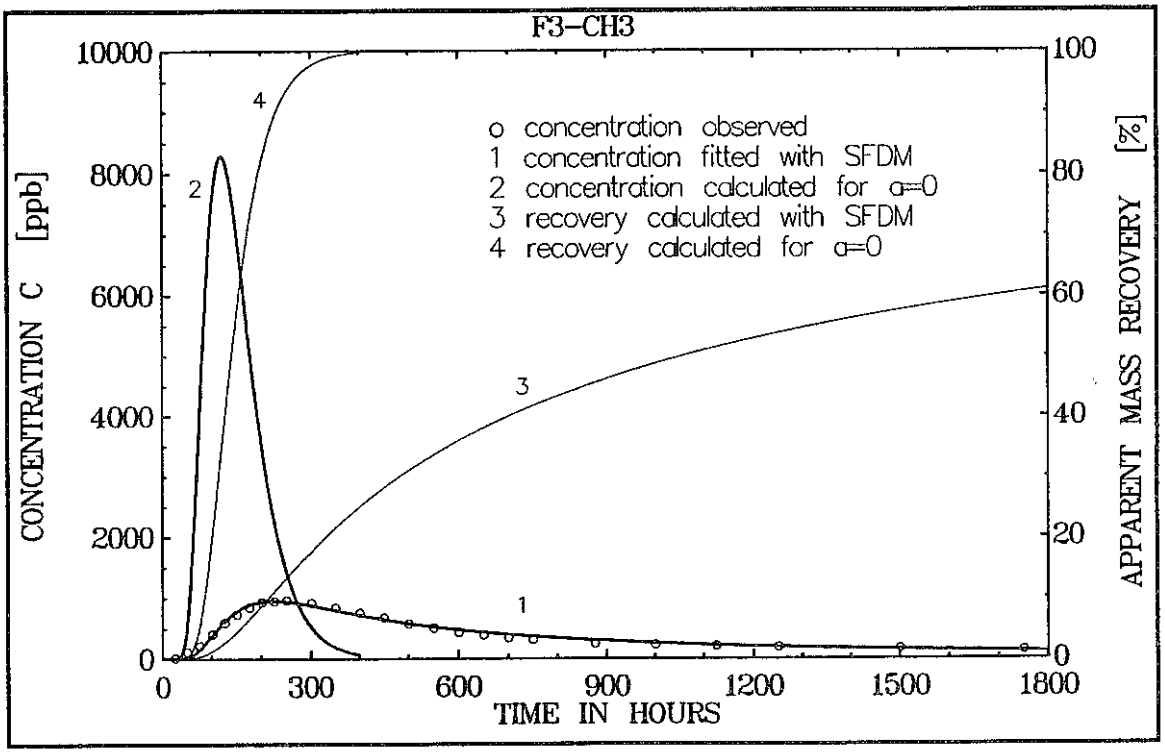

Fig. 39 **The comparison of the tracer concentration and recovery curves for the experiment F3-CH3 obtained by fitting SFDM (1, 3) and calculated for the same flow parameters under the assumption of no diffusion into porous matrix (2, 4)**

4.1.6 Summary of the rock parameters and the retardation factors

It is worth mentioning that the majority of experiments discussed in Chapter 4.1 were designed to predict a possible contaminant transport from planned nuclear waste depositories. Therefore, it should be of interest to see how the retardation factor (eq. 45) depends on the parameters found. Table 13 summarized the physical parameters of the investigated rocks and the calculated values of the retardation factor.

From the examples shown in Tab. 13 it is evident that the lowest value of the a-parameter found so far is $1.0 10^{-3}$ $s^{-1/2}$. In other words, a common practice of many researchers, especially in the U.S.A. and France, to neglect the matrix diffusion is not justified. All the models derived under an assumption of negligible matrix diffusion would yield $R_p=1$, which means overestimation of pollutant velocity at large scales.

Table 13 **The model and physical parameters obtained in different formations by using the SFDM and additional interpretation. In the case of several tracer experiments in the test site the mean values are given.**

	Model parameters		Physical parameters			Retar.
	a	p	n_f	n_p	2b	R_p
Formation	$s^{-1/2}$	$s^{1/2}$	%	%	µm	-
Chalk in France	$40.0 \cdot 10^{-3}$	$1.3 \cdot 10^{3}$	0.27	29	270	108
Chalk in England	$21.0 \cdot 10^{-3}$	$2.5 \cdot 10^{3}$	0.22	23	115	106
Dolomite/Olkusz Poland	$1.8 \cdot 10^{-3}$	$1.3 \cdot 10^{3}$	1.40	6.4	360	6
Ore dike in granite/Lindau	$8.6 \cdot 10^{-3}$	$4.9 \cdot 10^{3}$	0.08	6.8	210	86
Granite/uranium mine France	$2.0 \cdot 10^{-3}$	$25.0 \cdot 10^{3}$	0.02	2.0	33	101
Gneiss/Chalk R. Canada	$1.0 \cdot 10^{-3}$	$2.7 \cdot 10^{3}$	0.15	0.8	110	6

4.2 Interpretation of long-term tracer experiments using different models

4.2.1 Artificial tracer experiments

It will be shown within this Chapter that the DM fitted to data of a short-term experiment which from its duration may seem to be a long-term one, can neither be applied for the determinations of parameters nor for a prediction to a larger scale. The parameters obtained from the interpretation of the F3-CH3 experiment of CACAS et al. (1990b) are chosen here to demonstrate the problem.

Consider first a "classical" interpretation of the tracer concentration curve by applying: (1) the method of moments (MM); (2) the method of cumulative curve (MCC); and (3) the fitting of the ordinary dispersion model to the concentration curve measured. The first two methods are very often used in practice to calculate the parameters of a groundwater system directly from the concentration curves. For nonreactive tracers it is a common practice to assume the parameters found by making use of these methods to be the system parameters (i.e. the water velocity and dispersivity). The method of moments is described in Chapter 2.3. By applying eqs (42) and (46) directly to the concentrations observed one gets the mean transit time of tracer (centre of gravity) and the time variance of the concentration curve. From both, by making use of eq. (48), the dispersion parameter is obtained.

The method of cumulative curve is also very simple. One calculates the cumulative curve of a tracer concentration, next this curve is normalized to unity (apparent relative tracer recovery) and three values of time are found: $t_{0.16}$, $t_{0.5}$, $t_{0.84}$, which correspond to apparent relative recoveries of 0.16, 0.5 and 0.84, respectively. It is assumed that (FRIED 1975)

$$t_o = t_{0.5} \tag{84.1}$$

and

$$P_D = [(t_{0.84} - t_{0.16})/t_{0.5}]^2/8 \tag{84.2}$$

A critical discussion of both methods can be found in MALOSZEWSKI & ZUBER (1990b, 1992) or MALOSZEWSKI (1992).

Equations (42) and (46) used in the MM, require as a precondition the calculation of the integrals to infinity, which in practice means, up to the time moment in which the whole tracer curve has already passed the observation well. If the concentration curve is characterized by a strong tailing-effect (as in a double-porosity medium), the realization of this precondition is seldom possible. It should be noted that this condition is not required for fitting procedures (i.e. for a direct calibration of any model). The concentration curve in the experiment F3-CH3 has a long tail, which was not completely measured, and, therefore, the MM and the MCC cannot be directly used. To obtain an unbiased comparison, though not free of errors, the tailing part of the concentration curve was extrapolated up to 3600 hrs (i.e. twice the duration of the experiment) for the calulation of moments and the cumulative curve. The quality of the resulting parameters was checked by the calculation of the theoretical concentration curves from the model on which

the methods were based (i.e. from the DM), and by comparing them with the concentrations measured. The parameters employed for further comparisons are summarized in Table 14. Figure 40 shows the concentration curves calculated by using the DM with parameters from the MM (3) and MCC (4), as well as from the fitted DM (2) and SFDM (1). From that figure it is easy to conclude that both approximate methods are not able to yield a good fit of the model to the experimental data. One should mention that all the curves shown in Fig. 40 were obtained by normalizing the concentrations to the same maximal experimental concentration measured. From Fig. 40 it is self-evident that both aproximate methods (MM and MMC) yielded unacceptable results. One should not use the methods to obtain parameters which, in turn, do not yield a good fit. To demonstrate the real differences between the models or/and methods, in Fig. 41 are shown the tracer curves which would be observed when the mass of tracer is taken into account, i.e. without normalization to the maximal concentration.

The differences between the parameters of the MM, MMC and those obtained by calibration of the DM are not very large because the two methods are based on the DM, but they differ largely from those obtained for the SFDM (see Table 14). The mean transit time of water obtained from the SFDM is about five times smaller (150 hrs), and consequently the water velocity is five times larger (v=4.16 m/d), then those found from the DM (t_o=714 hrs and v=0.87 m/d). The dispersion parameters differ by a factor of about 6.

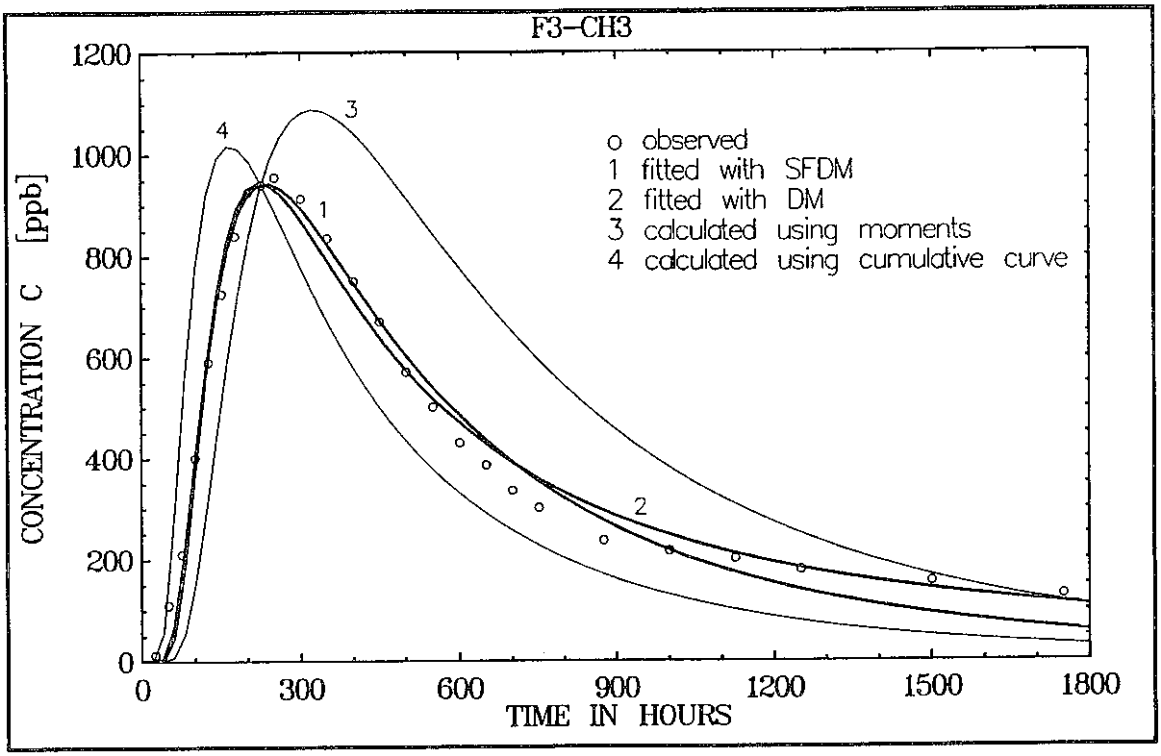

Fig. 40 **Comparison of concentration curves obtained by fitting the SFDM (1) and DM (2) as well as calculated by making use of parameters found from the method of moments(3) and the method of cumulative curve (4) for the experiment F3-CH3 of CACAS et al. (1990b) normalized to the maximum concentration observed**

Table 14 **Parameters obtained in fissured granite of the Fanay-Augeres test site for experiment F3-CH3 (X=26 m) by making use of different methods of interpretation and two models**

	Calculated or fitted		Calculated for known X	
	t_0	P_D	v	D/v
Method	hr	-	m/d	m
M.moments	838	0.37	0.745	9.6
M.cumu.curve	557	0.51	1.120	13.3
Fitted DM	714	0.46	0.874	12.0
Fitted SFDM	150	0.08	4.160	2.1

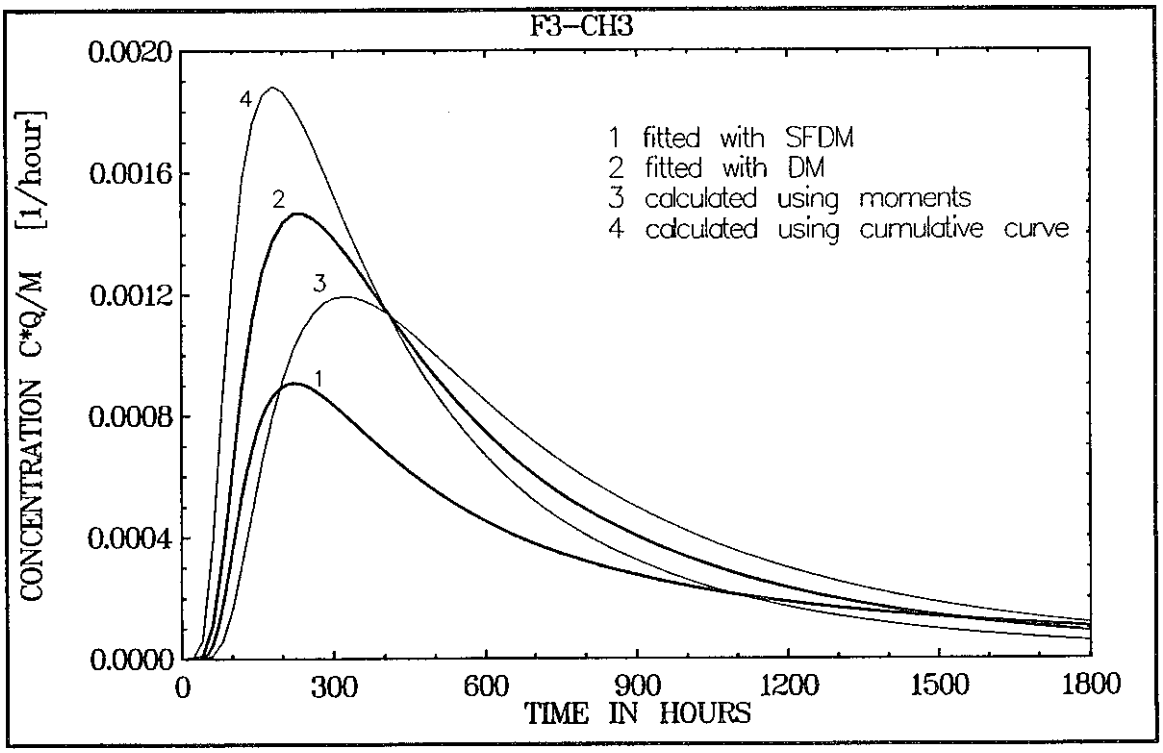

Fig. 41 **Comparison of concentration curves predicted from the parameters found for the experiment F3-CH3 by fitting the SFDM (1) and DM (2), as well as by the method of moments (3) and the method of cumulative curve (4)**

Imagine that the parameters obtained from the DM will be accepted by a researcher as flow parameters. He would support himself by a proper calibration of the DM and would follow the usual opinion about negligible diffusion in granitic rocks. The examination of the physical

parameters obtained from the DM parameters performed below proves that such an approach is unacceptable and that the diffusion is not negligible.

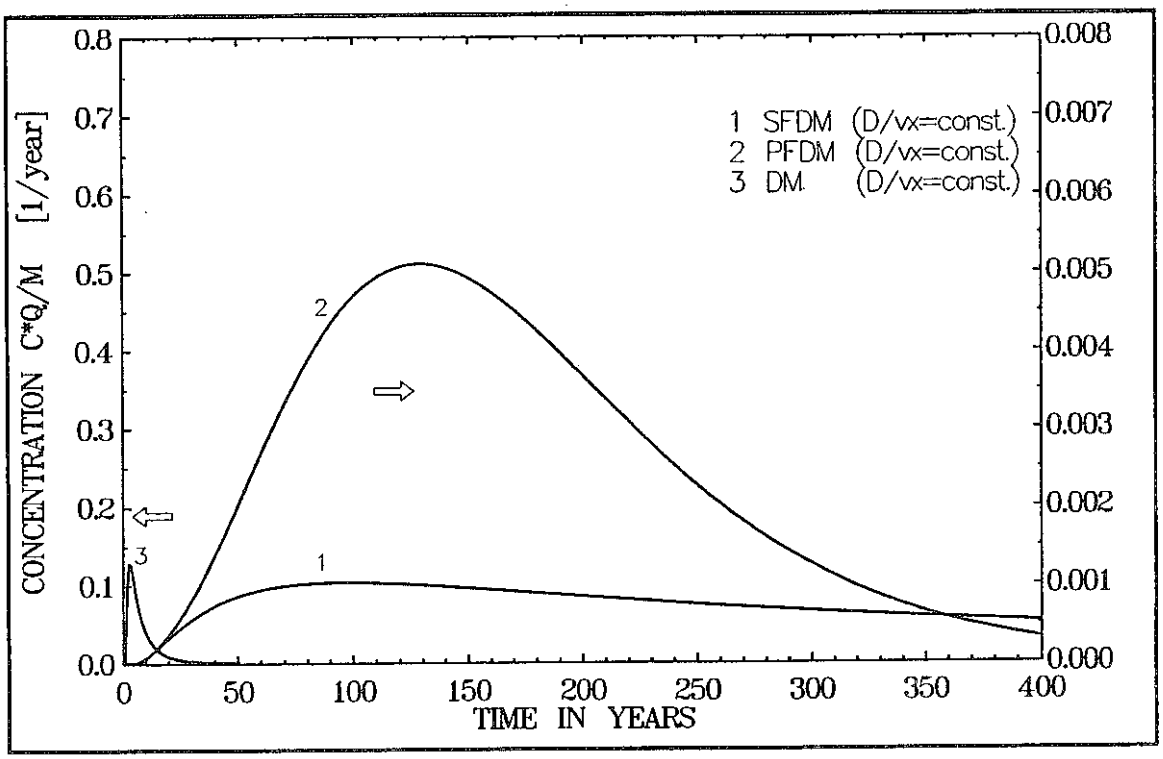

Fig. 42 **Predicted tracer concentration curves for a distance 100 times larger than in Fig. 40 for a constant dispersion parameter (P_D), by making use of the SFDM (1), DM (3) and PFDM (2)**

The common opinion about negligible diffusion into the microporous matrix for granitic rocks results from very low values of diffusion coefficient measured by SKAGIUS & NERETNIEKS (1986) and from expected low values of the a-parameter (eq. 11.1). In Table 11 (Chapter 4.1.5) it has already been shown that the calibration of the SFDM in experiment F3-CH3, yields relatively large value of $a=1.67 \cdot 10^{-3}$ $s^{-1/2}$ which does not permit to neglect the diffusion. The mean transit time of tracer interpreted from the DM, if assumed to be equal to the mean transit time of water and applied to Darcy law (eq. 83) yields the fracture porosity of 0.000034. This value seems to be unreasonably low, but in turn it produces (eq. 82) the fissure aperture of 17 μm, which may seem to be reasonable. However, that value of 2b for the previously used values of matrix porosity and diffusion coefficient yields the a-parameter even larger then the value found from the SFDM ($a=3.6 \cdot 10^{-3}$ $s^{-1/2}$), and, consequently, according to Figs 14-16 the diffusion effects should even be larger than those observed. In conclusion, the above consideration demonstrates that the mean transit time obtained from the DM should not be used as the mean transit time of water.

Another possible check of the hypothesis on a possible applicability of the DM (eq. 41, Chapter 2.3.1) is based on the comparison of the tracer parameters [t_t and $(P_D)^*$] with the PFDM parameters (eqs 45 and 49.2). Taking the real values of the parameters $a=1.67 \cdot 10^{-3}$ $s^{-1/2}$,

$p=3\cdot10^4$ $s^{1/2}$, $t_o=150$ hrs, and $P_D=0.08$, found from the calibration of the SFDM and its additional interpretation, one obtains $t_t=15150$ hrs, and $(P_D)^*=0.19$. These values disagree completely with those found by calibration of the DM (714 hrs and 0.46, respectively). It was already mentioned in Chapter 2.3, that DM can only be succesfully applied when the mean transit time of water is greater than about $16p^2/R_p$, i.e., in the considered experiment for $(t_o)_{min}>4.6$ yrs.

However, eq. (39.1) should be regarded as a rough approximation because example shown below suggest that for practical purposes shorter transit times of water (1.7 yrs) can be accepted (see Fig. 44).

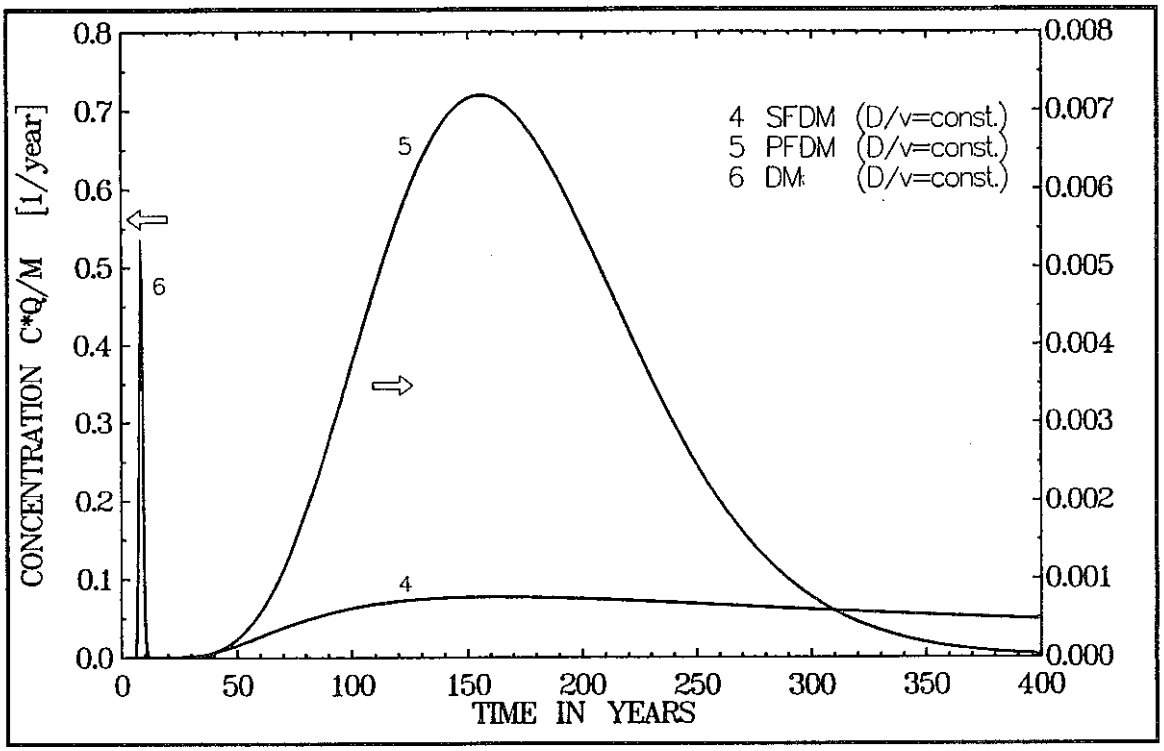

Fig. 43 **Predicted tracer concentration curves for a distance 100 times larger than in Fig. 40 for a constant dispersivity (D/v), by making use of the SFDM (1), DM (3) and PFDM (2)**

Consider a solution to the direct problem for the parameters obtained from both calibrated models. For example, for a flow distance 100 times larger than that in experiment F3-CH3, i.e. for X=2600 m. The results of calculations obtained with the aid of the DM, SFDM and PFDM are shown in Figs 42 and 43, whereas the parameters used are summarized in Table 15 (note that the data in Table 15 do not represent real predictions because they were calculated for flow velocities induced by the presence of drift). Figure 42 presents the predicted curves calculated for an assumed constant value of P_D, whereas in Fig. 43 a constant dispersivity (D/v) was used. The curves calculated with the DM, SFDM and PFDM are completly different (note that the concentration scale for both the SFDM and the PFDM is 100 times larger then that for the DM). The differences between the SFDM and PFDM were expected because the SFDM is not applicable at large scales. However, the figures demonstrate that the DM model, though it was

earlier calibrated at small scale, produces completely wrong predictions. To eliminate such errors it is required to use not only calibrated but also validated models. The SFDM was calibrated and validated as it was shown in Chapter 4.1.5. However, only parameters obtained from the SFDM can be used for futher predictions both in the DM and the PFDM, but not the model itself.

It is also very interesting to note that the assumption related either to a constant value of the dispersion parameter or dispersivity plays negligible role as it is shown in Fig. 44 (compare curves 2 with 4, or 1 with 3) (see also MALOSZEWSKI & ZUBER 1990b). In that figure the concentration curves predicted at large times are also shown for the ordinary dispersion model with properly calculated tracer parameters, i.e. from the values found from the SFDM (curves 1 and 3). The differences between the DM and the PFDM are not very large and probably acceptable for a period of hundreds years. It must be mentioned that for rocks with lower spacing of fissures, the applicability of the DM can be obtained for shorter times (at shorter distances), but its parameters must, of course, also be related to the physical parameters, e.g., found from the SFDM.

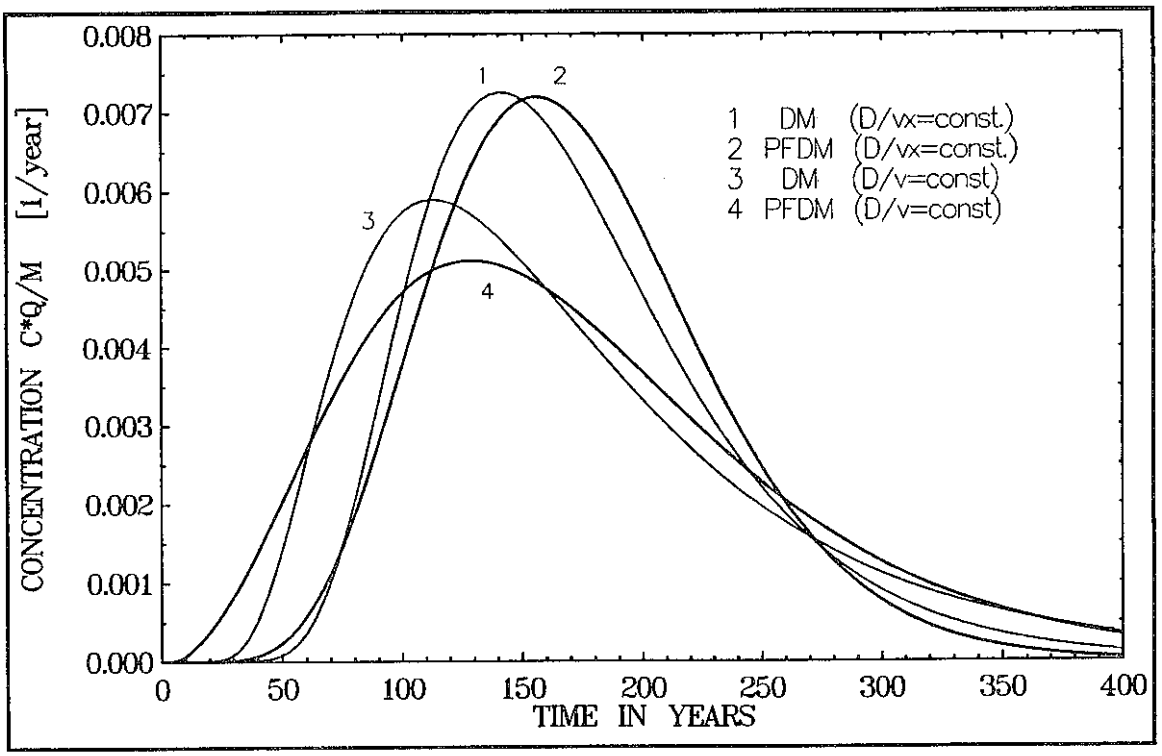

Fig. 44 **Comparison of tracer concentration curves for a distance 100 times larger than in Fig. 40 obtained taking constant (D/vx) and (D/v) in the PFDM (with four parameters) and the DM (with two tracer parameters predicted from the SFDM)**

Table 15 **The flow parameters to predict the polutant movement from model parameters of Table 14 for the flow distance X=2600 m**

	v or v_t	P_D or $(P_D)^*$	a	p
Model	m/yr	-	$s^{-1/2}$	$s^{1/2}$
Constant P_D				
DM (t_o, P_D)	319	0.460	-	-
DM [t_t, $(P_D)^*$]	15	0.148	-	-
SFDM	1518	0.080	$1.67 \cdot 10^{-3}$	-
PFDM	1518	0.080	$1.67 \cdot 10^{-3}$	$3.0 \cdot 10^{4}$
Constant D/v				
DM (t_o, P_D)	319	0.0046	-	-
DM [t_t, $(P_D)^*$]	15	0.0690	-	-
SFDM	1518	0.0008	$1.67 \cdot 10^{-3}$	-
PFDM	1518	0.0008	$1.67 \cdot 10^{-3}$	$3.0 \cdot 10^{4}$

4.2.2 Interpretation of environmental tracer tritium (variable input concentration)

The environmental tritium as an constituent of water molecule is generally regarded as an ideal tracer and often used for determining the hydrological parameters, i.e. water age, velocity or the volume of mobile water in groundwater systems. A review of lumped parameter (black-box) models was given by MALOSZEWSKI & ZUBER (1982, 1993b) and ZUBER (1986). The main fitting parameter directly interpreted from the relations between the input and output concentrations in the porous aquifers is the mean transit time of water t_o (eq. 10.1). Examples of the black-box approach for the interpretation of environmental tracer data in different aquifers are given in a number of papers, e.g., by MALOSZEWSKI & ZUBER (1982, 1993b), MALOSZEWSKI et al. (1983, 1990, 1992), HERRMANN et al. (1986), STICHLER et al. (1986), NOLTE et al. (1991) or RANK et al. (1992).

The crucial problem is related to the meaning of the main fitting parameter, i.e. t_t, in the weighting function (eq. 52) of the black-box model approach. Generally, it is assumed that due to the fact that tritium is an ideal tracer one obtains directly the mean transit time of water. It is true for saturated porous aquifers, but it is not true for a double-porosity medium like a fissured aquifer. Assuming that the mean transit time of water t_o is large enough to permit the application of the DM instead of the PFDM (see Chapter 2.3) one obtains as a result of fitting, the mean transit time of tracer, which for an ideal tracer and a large distance is R_p times larger than t_o (eq. 53). In other words, tritium behavies in fissured aquifer (when is transported for sufficiently long distances) as a tracer which has R_p times smaller velocity in comparison with the water flow velocity (MALOSZEWSKI & ZUBER 1985):

$$v_t = X/t_t = X/(t_o R_p) = v/R_p \approx vn_f/n \qquad (85)$$

where v_t is the tracer velocity, X is the flow distance and n is total porosity of the rock (fissure + matrix porosities).

The mean transit time of tracer observed for a whole system permits to estimate the total volume of water (stagnant and mobile) in that system (see eq. 54). If one erroneously identifies the mean transit time of tracer as the mean transit time of water to estimate the volume of mobile water in the groundwater system, the resulting value will be R_p times overestimated. To find the real volume of the mobile water, an independent information on both porosities is required (see Chapter 2.3.2). The problem was discussed in detail by MALOSZEWSKI et al. (1990, 1992) or MALOSZEWSKI & ZUBER (1993b).

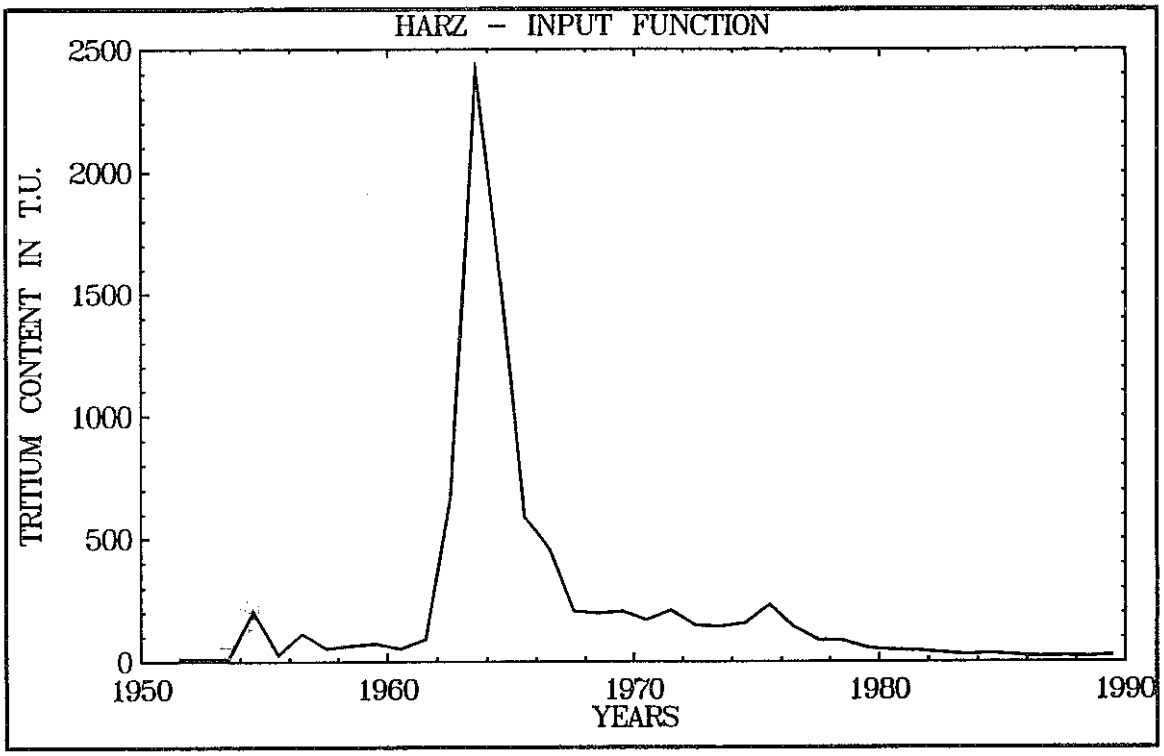

Fig. 45 **Input fuction of environmental tritium calculated for the Harz Mts, Germany, as yearly mean concentrations (1952-1988)**

Another problem is related to the examination of the applicability of the DM (eq. 39.1). As it was already shown in the previous chapter, the DM can be calibrated but it may happen that its parameters have no hydrological meaning. To solve this problem it is necessary to estimate the value of the p-parameter (eq. 11.3) and to compare the t_k value obtained from eq. (18.1) with the mean transit time of water obtained from the calibration of the DM. In general, for double-porosity media, it may be stated that eq. (41), if calibrated either directly in artificial tracer experiments or indirectly for the environmental tracer data in eq. (50), the parameter t_t is not necessarily related by eq. (85) to the real value of the mean transit time of water. One has first to examine if the value of t_t obtained can be regarded as that which is really sought. For a better documentation of the problems two examples taken from MALOSZEWSKI et al. (1990) are presented here.

In a small catchment basin, Lange Bramke, Upper Harz Mts, Germany, the environmental tracer investigations have been performed since 1978, whereas the hydrological investigations of the discharge and precipitation since 1954. The basin, which has the surface of $S_a=0.76$ km^2 consits of three types of aquifers: unsaturated soil on the slope of the valey ($S_{a1}=0.71$ km^2, mean thickness of about m=3.5 m), porous aquifer in bottom of the valey ($S_{a2}=0.05$ km^2, m=10 m) and dominant fissured rock aquifer ($S_a=0.76$ km^2, maximal m=66 m) of folded and fractured Lover Devonian sandstones, quarzites and slates (see HERRMANN et al. 1989). The mean discharge of the stream, which drains the valley, is 17.1 l/s (including 1.9 l/s estimated as a surface run-off flow component). The tritium input function shown in Fig. 45, was calculated as yearly mean values from the mean monthly precipitations and tritium contents in rain water from a simple model of infiltration (e.g., MALOSZEWSKI & ZUBER 1982). The calibration of the model was performed by making use of the DM (eq. 52) to the tritium concentrations measured in the stream water outflowing from the whole catchment. The best fit curve shown in Fig. 46 was obtained with $t_t=2.7$ yrs and $(P_D)^*=0.15$. Assuming that the parameter t_t is really equal to the mean transit time of tracer the whole volume of the water in the system can be estimated from eq. (54) as follows:

$$V = Qt_t = (17.1\text{-}1.9)\text{l/s} \cdot 2.7 \text{ yrs} = 1.29 \cdot 10^6 \text{ m}^3 .$$

HERRMANN et al. (1986) found that the volume of water in the unsaturated zone is about $V_{UA}=0.45 \cdot 10^6$ m^3 (for the mean moisture content of 18% vol.), which yields the volume of water in the saturated zone of $V_S=(1.29 - 0.45) \cdot 10^6$ m^3 $= 0.84 \cdot 10^6$ m^3. Taking into account that small porous aquifer in the bottom of the valey has porosity of about 30% one obtains that the maximal water volume in this aquifer (V_{PA}) is equal to $0.16 \cdot 10^6$ m^3. Then, the total volume of water if the fissured aquifer is about $V_{FA}=(0.84\text{-}0.16) \cdot 10^6=0.68 \cdot 10^6$ m^3. From the independent artificial tracer tests and laboratory measurements the following parameters were obtained: $n_p=0.02$, $n_f=0.0076$ and $2b=380\mu$m (see HERMANN et al. 1989). The retardation factor due to diffusion of tritium into porous matrix is then equal to $R_p=3.6$. Knowing R_p, the mobile part of the total water volume in fractured aquifer can easily be calculated from eq. (54) as follows:

$$V_f = V/R_p \tag{86}$$

what yields $0.19 \cdot 10^6$ m^3. Finally, from V_f, the fissure porosity of 0.0076, and surface of the fissured aquifer S=0.76 km^2, the mean saturated thickness of the aquifer can be calculated as

$$h = V_f/(Sn_f) \tag{87}$$

what gives h=33 m. It agrees reasonably with the maximal possible thickness of fissured aquifer of 66 m known from geological investigations.

If the transit time of tracer were interpreted as the mean transit time of water, the total volume of water would be considered as a mobile one, and, consequently, 3.6 times overestimated.

The whole above interpretation of tritium data is based on the assumption that the DM properly yielded the relation between the mean transit time of tracer and the mean transit time of water. To check the applicability of the DM one has to estimate first the value of the p-parameter. The p-parameter can be estimated if 2b, n_f and D_p are known or assumed, or if the parameters a, n_p and n_f are known. Taking $D_p=10^{-10}$ m^2/s and the other values as above one

obtains $p=0.2 \cdot 10^4$ $s^{1/2}$. The p-parameter yields the required transit time of water for the applicability of the DM to be greater than 5 months (eq. 39.1). The transit time of water through fissured aquifer can be estimated as

$$(t_o)_{FA} = V_f/Q = 0.19 \cdot 10^6 \text{ m}^3/(15.2 \text{ l/s}) = 4.8 \text{ months},$$

which shows the condition for the applicability of the DM to be well satisfied in the considered situation.

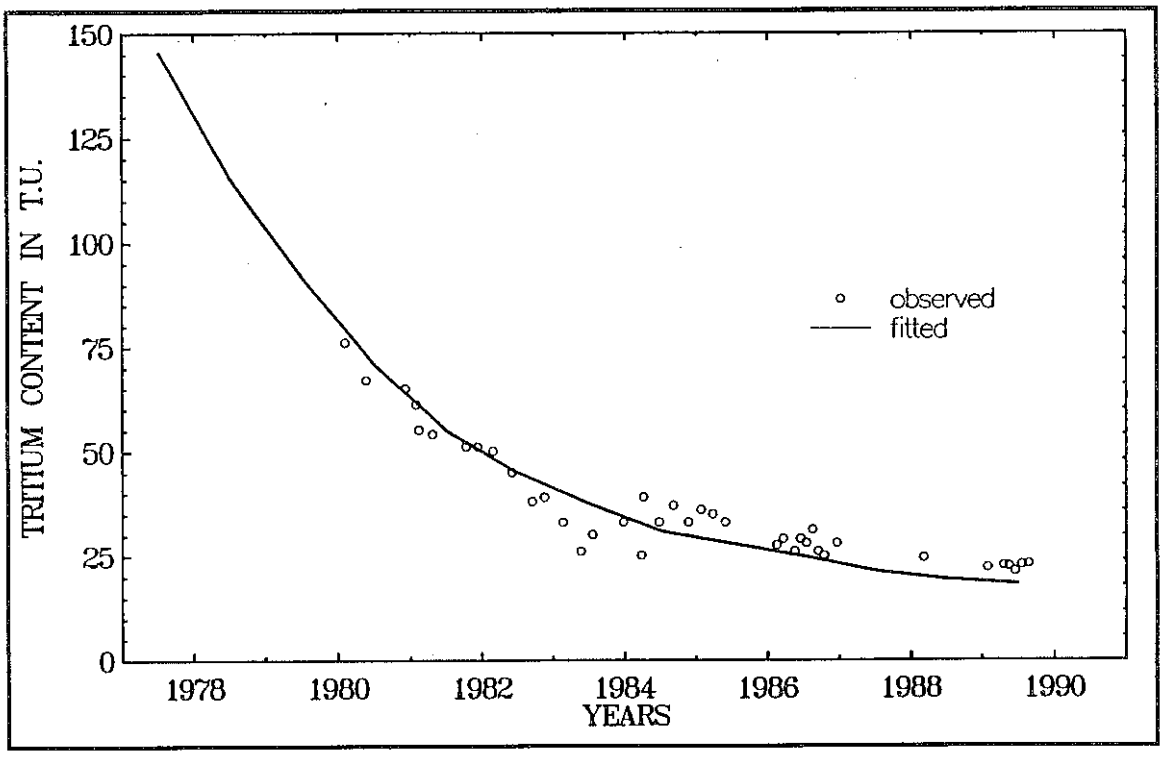

Fig. 46 **Observed and fitted (by applying the DM in black-box model approximation) tritium output concentration curves for the stream which drains the catchment basin of Lange Bramke, Harz Mts**

Another example is taken from the same area. A small spring, Saukappenquelle, has the mean discharge of about 2.1 l/s, the mean surface of the catchment area of 0.15 km^2 and the mean thickness of the aquifer of 75 m. This spring mainly drains fissured rocks. The best fit curve obtained with $t_t=4.2$ yrs and $(P_D)^*=0.4$ is shown in Fig. 47. Performing the same considerations and assuming the same fissure parameters as before, one obtains the total volume of water equal to $0.28 \cdot 10^6$ m^3 and the volume of mobile part equal to $0.08 \cdot 10^6$ m^3. This in turn yields for the fissure porosity of about 0.008, the saturated thickness of the aquifer equal to 66 m. In that case, if one did not take into account the delay of tracer movement due to diffusion into porous matrix, the resulting saturated thickness would be about 238 m, i.e. 4 times larger than the mean thickness known.

Concluding, in the interpretation of tritium data for fissured aquifers, one has also to take into account the retardation of tracer due to the matrix diffusion. It is proposed that for the estimation of the retardation factor needed for a full interpretation of environmental tritium data, an artificial tracer experiment, or experiments can be used as demonstrated in this Chapter.

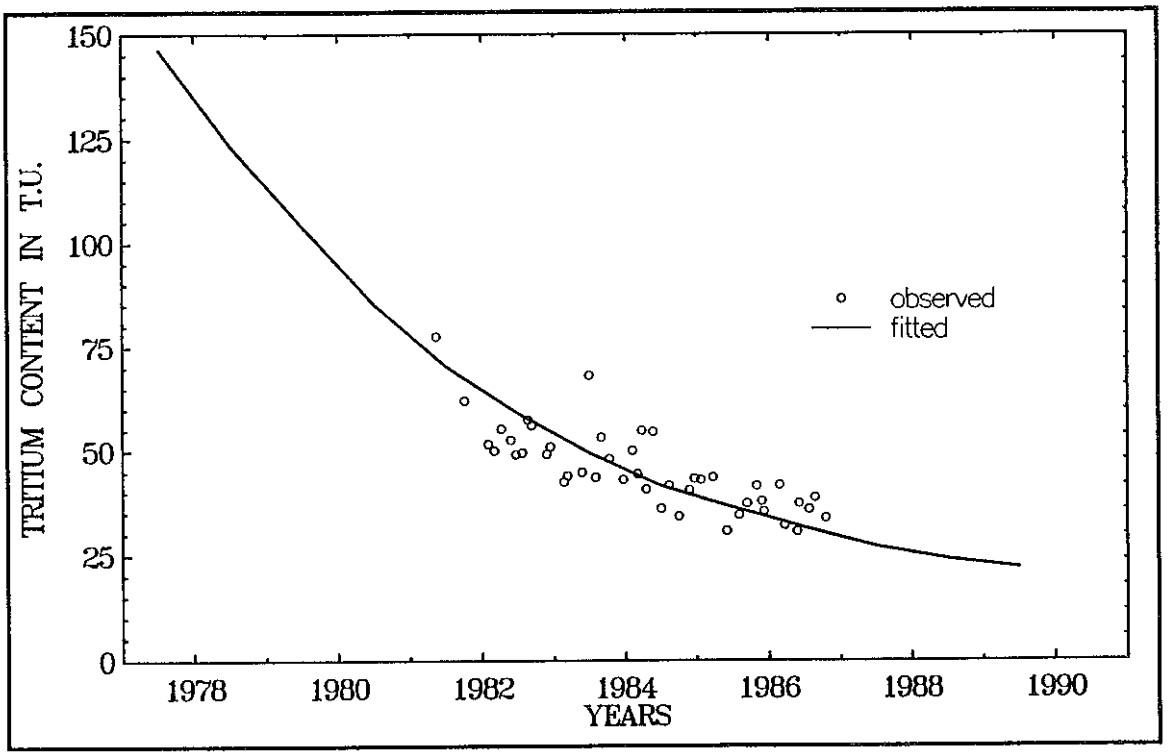

Fig. 47 **Observed and fitted (by applying the DM in black-box model approximation) tritium output concentration curves for a small spring, Saukappenquelle, Harz Mts**

4.2.3 Interpretation of environmental radioactive tracer ^{14}C (constant input concentration)

The radiocarbon dating of groundwater is mainly used to determine water velocities in confined aquifers, where the tracer transport from the reacharge area can be approximated by the piston flow model. The ^{14}C enters the groundwater system with a constant input concentration, C_o. Due to its long half-life time ($T_{1/2}$=5730 yrs), the radiocarbon method is often applied to determine very low water velocities (e.g., FONTES & GARNIER 1979; or BLAVOUX & OLIVE 1981). Usually, the water velocity is determined from the difference of radiocarbon ages (t_{a1} and t_{a2}, eq. 72 in Chapter 2.5.1) found in two observation wells beeing on the same flow line at a distance X. In the case of fissured aquifers, t_{a1} and t_{a2}, can only be used to estimate the tracer velocity

$$v_t = X/(t_{a2} - t_{a1}) \qquad (88)$$

whereas the real water velocity is (t_a/t_o) times greater

$$v = v_t(t_a/t_o) \tag{89}$$

and remains unknown.

To find the water velocity (v) the ratio (t_a/t_o) has to be known or estimated. Equation (73) in Chapter 2.4.1 describes this relation in the case of reactive tracer transported by piston flow through the fissured aquifer approximated by the system of parallel fissures. Equation (75) gives this ratio for a single fissure, which is equivalent to a confined porous aquifer of low thickness overlain and underlain by aquitards (see Chapter 2.4.2).

Generally, the radiocarbon dating of groundwater has strong limitations resulting from difficulties in determining the initial concentration of tracer at the entrance to the system (see e.g., WIGLEY et al. 1978; FONTES & GARNIER 1979; or MOOK 1980). Here it is assumed that the initial concentration, C_o, was already properly corrected, and then the problem is reduced to the estimation of the t_a/t_o factor. It is a common practice to take this factor as equal to one, i.e. no diffusion or reversible reaction is accounted for. The resulting velocity may then differ from the real water velocity by several orders of magnitudes. GARNIER & FONTES (1979) found in a carboniferous limestone the discrepancy between the radiocarbon velocity and water velocity of about 300. This discrepancy was explained later by MALOSZEWSKI & ZUBER (1985) as a result of matrix diffusion of the tracer which follows an instantaneous equilibrium reaction in the matrix. In a recent paper, MALOSZEWSKI & ZUBER (1991) concluded, that the exchange reaction model of radiocarbon in porous matrix is more complicated and introduced a combined reaction model of CAMERON & KLUTE (1978), described in Chapters 2.2.1 and 2.4.1. This approach shows that in addition to an instantaneous exchange of bicarbonate there is also a kinetic reaction which probably is a common phenomen in carbonate aquifers, and strongly contributes to the delay of carbon species. This model of reactions was already tested in artificial tracer experiment with $H^{13}CO_3^-$, as it was disscussed in Chapter 4.1.1.

It is self-evident that the radiocarbon data cannot be used directly to solve the inverse problem. After finding the tracer velocity, the water velocity can be found when t_a/t_o is known. This in turn can only be calculated, when the system parameters and the reaction parameters have already been estimated in an independent way. The exact formula given by eq. (73) or its simplified form, which can be deducted from equations given in Chapter 2.4.1, has then to be used. For the estimation of possible reaction parameters of ^{14}C, MALOSZEWSKI & ZUBER (1991) assumed that the interaction parameters of the $H^{13}CO_3^-$ tracer may represent the behaviour of the environmental radiocarbon in a given system. If such assumption is acceptable, artificial multitracer experiments in the groundwater systems may help in the prediction of the behaviour of the environmental radiocarbon as shown below.

Equation (73) results from the general solution (59) of the transport model. However, taking into account that fissure porosity is always much more smaller than unity and that the reaction rate constants are probably much greater than the decay constant of radiocarbon ($\lambda = 1.38 \cdot 10^{-8}$ hr^{-1}), the simplified solution (63) can be taken. For instance, for fissure porosity $n_p \geq 0.001$, fissure aperture $2b \leq 300$ μm and diffusion coefficient in the matrix $D_p \geq 10^{-10}$ m^2/s one obtains

$$R_{ap} + k_1/k_2 \leq 200,$$

which is probaly well satisfied in most cases. Then, eq. (63) can be further simplified to eq. (65.1), which finally yields relatively simple formula for the t_a/t_o factor in the case of the environmental ^{14}C

$$t_a/t_o = R_{af} + (R_{ap}+R_{ak})n_p/n_f \qquad (90)$$

where, as discussed earlier R_{af} and R_{ap} are the retardation factors due to instantaneous equilibriums in fissures and porous matrix, respectively, and R_{ak} is the ratio of kinetic reaction rate constants (eq. 66). The relation (90) given graphically in Fig. 48, shows that errors of several orders of magnitude in the estimation of water velocity can be committed if the exchange reactions are not taken into account. Particulary large errors may result from considering an instantaneous reaction only. It is also clear from Fig. 48, that even if there are no reactions ($R_{af}=1$, $R_{ap}=1$, $R_{ak}=0$), the radiocarbon age is larger than the mean transit time of water ($t_a/t_o > 1$). The t_a/t_o factor (eq. 90) simplifies then to:

$$t_a/t_o = n/n_f \qquad (91)$$

where n is the total porosity. From eq. (91) it is clear that $t_a/t_o=1$, i.e. the radiocarbon age is equal to mean transit time of water only if the matrix porosity is equal to zero. In the case of carbonate rocks, exchange reactions cannot be neglected. Consider the reaction parameters obtained in experiment described in Chapter 4.1.1: $R_{af}=1$, $R_{ap}=2.3$, $k_1=1.66$ hr^{-1}, and $k_2=0.1$ hr^{-1} ($R_{ak}=16.6$). For $n_f=0.0027$, $n_p=0.29$ one obtains $t_a/t_o=108$ by neglecting all the reactions, $t_a/t_o=247$ assuming the instantaneous reaction only, and $t_a/t_o=2023$ taking kinetic reactions into account. In other words the water and tracer velocities may differ in this formation by a factor of three orders of magnitude.

FONTES & GARNIER (1979) found the radiocarbon velocity (eq. 88) about 300 times lower than the water velocity obtained from the hydraulic data for an assumed fissure porosity of 0.01. It means that in that case the retardation factor was $t_a/t_o \approx 300$. Assuming, both the R_{af} factor to be equal to unity and a resonable value of the matrix porosity of 0.06, one obtains from eq. (90) that $R_{ap}+R_{ak} \approx 50$. The instantaneous equilibrium retardation factor (R_{ap}) was estimated by MALOSZEWSKI & ZUBER (1985), on the basis of data of THILO & MÜNNICH (1970), to be about 32, which yields $R_{ak}=18$. This value agrees quite well with the ratio of kinetic reaction rate constants (16.6) found in artificial tracer experiment with carbon-13 (Chapter 4.1.1). However, if a larger matrix porosity is assumed, as MALOSZEWSKI & ZUBER (1985) did, the total retardation factor can be explained without the concept of the R_{ak} factor. Therefore, it is evident once more that the matrix porosity should be independently controlled whenever possible.

It should be noted that eqs (90) and (91) are valid only for radiocarbon. Equation (90) cannot be so easily applied for another radioactive tracer because then the applicability of the simplifications given in Chapter 2.4.1 has to be examinated.

For instance, for the environmental tritium entering the groundwater systems with a nearly constant concentration (5 - 10 T.U.) before the year 1952, eq. (70) or eqs (71.1) and (71.2), have to be used. Then, if diffusion coefficient in the matrix is 10^{-10} m^2/s, and if

$$2b\ [m] \leq 0.06 n_f,$$

the t_a/t_o factor for tritium is equal to the ratio of total porosity to the fissure porosity. In other case the problem becomes more complex.

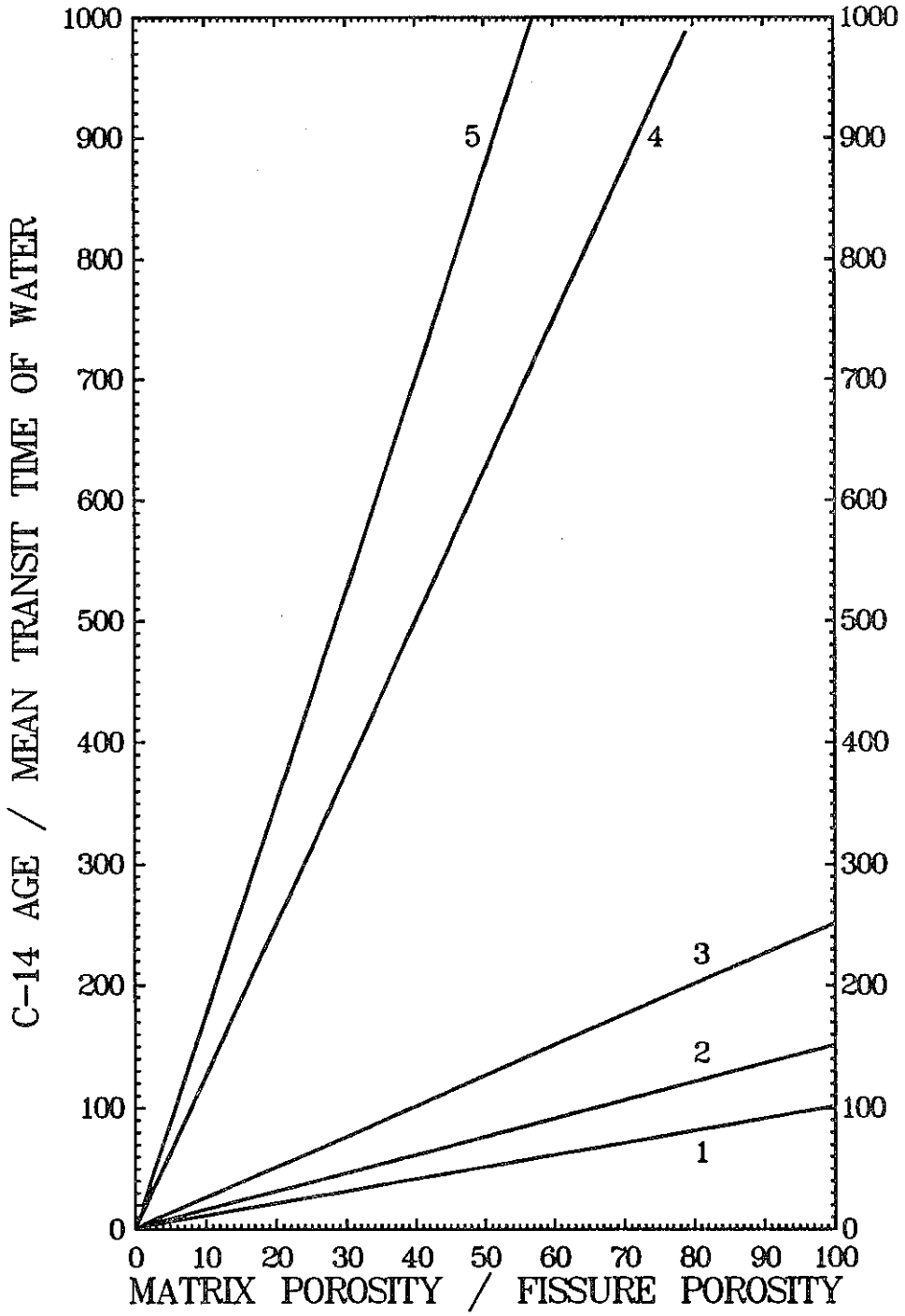

Fig. 48 **The ratio of radiocarbon age to real mean transit time of water (t_a/t_o) as a function of fissure to matrix porosity ratio, without reaction in fissures ($R_{af}=1$). In the case of ^{14}C as a nonreactive tracer (1); including instantaneous reactions in the matrix with $R_{ap}=1.5$ (2), and $R_{ap}=2.5$ (3); and including for $R_{ap}=2.5$ an additional kinetic reaction in the matrix with $R_{ak}=10$ (4), and $R_{ak}=15$ (5). Note that the lowest value of t_a/t_o is 1.**

5 Summary and conclusions

Analytical solutions (models) to the mass transport equation for fractured aquifers (double-porosity media) were developed and applied for solving direct and inverse problems. The groundwater system was approximated by parallel fissures equally distributed in the microporous matrix. The fissures contain the mobile water, whereas in the microporous matrix the water is stagnant or quasi stagnant. The tracer flows with water in the fissures and diffuses into the stagnant water in porous matrix. The general model, called the Parallel Fissure Dispersion Model consists of four nondisposable (model, fitting) parameters. It was shown that this model can be used for solving the direct problems, i.e. for modelling of tracer transport in known system, or for analyzing the influence of particular parameters. For solving the inverse problems (i.e. for finding the parameter values of the investigated system by fitting the model), the model cannot yield unique solutions because the number of nondisposable parameters is too large. To overcome that difficulty, two main simplifications of the PFDM and the conditions for their applicability were found. The first one is the Single Fissure Dispersion Model (SFDM), which is shown to be applicable for the interpretation of short-term tracer experiments performed at the short distances. The second one is the common dispersion model (DM), which is shown to be applicable in long-term tracer experiments, yielding tracer parameters, which are directly related to the PFDM-parameters. It was found that the applicability of one of the two approaches depends mainly on the value of a combined parameter, $p=2b/(2n_f\sqrt{D_p})$. Unfortunately, the value of this parameter is not known a priori, but it can be obtained under favorable conditions from the calibration of the SFDM. The applicability of the SFDM can be checked a posteriore by putting the physical parameters obtained into eq. (18.1). The scale of which the DM becomes applicable can also be estimated by putting the physical parameters found from the SFDM into eq. (39.1).

The single fissure approach is based on the assumption that the transit (flow) time of water between observation and detection wells is short enough to ensure that the tracer does not diffuse into porous matrix deep enough to be influenced by adjacent fissures. This condition was satisfied in all the artificial experiments discussed within this study.

For ideal (nonreactive) tracer, the SFDM has three model parameters which can be relatively easily found by fitting (calibration) of the model. It was shown that this model can be successfully applied for the interpretation of artificial tracer experiments performed under natural flow, radial convergent flow (monopol test) and in injection-withdrawal flow (dipole test) conditions. The application of the SFDM to experiments under natural flow conditions requires the normalization of the tracer concentration curve to its maximal concentration. Then, unfortunately, the conditions for the fitting procedure become worse and a unique solution is difficult to obtain (several fits with the same accuracy can often be obtained). To overcome that difficulty, a combined tracer experiment with pumping test is recommended in which the mass recovery of tracer is well controlled. An improved fitting procedure has been introduced in which the tracer concentration curve and the mass recovery curves are fitted in turn, till the minimum error is achieved. It is shown that the new procedure improves the accuracy of parameter determination and yields more reliable parameters than the fitting without the mass recovery curve. The SFDM was also extended for reactive tracers by adopting a combined model of exchange reactions in the matrix and an instantaneous equilibrium reaction on the fissure walls. In such a case the number of model parameters increases to five and a unique solution to the inverse problem is unobtainable. However, the problem can be solved with the

aid of a multitracer experiment combined with a pumping test. In such a case the flow parameters which are independent from the tracer properties are determined from the concentration and recovery curves of ideal tracer and used as known parameters in the fitting procedure for reactive ones. It was demonstrated that even in such a situation, the final determination of the reaction constnants is only possible when the information on the diffusion coeficients of tracers used is available.

It has been shown that the SFDM cannot be used for predicting the pollutant movement. The single fissure approach does not work at long distances because then the diffusion from adjacent fissures is not negligible. However, it is shown that the SFDM yields proper values of model and physical parameters which can in turn, be used for direct modelling (prediction of pollutant movement) with the aid either of the DM or the PFDM.

It has been shown theoretically that the common dispersion model (DM), with adequately chosen parameters, can successfully be used in long-term tracer experiments. This is especially important for the interpretation of environmental tracer data (e.g., tritium) obtained from a fractured aquifer. The tracer enters the groundwater system with the variable input concentration through the recharge area and its concentration is measured in the water outflowing from the system (springs, streams or pumping wells). In such a case the black-box model approach is used with the weighting function represented by the dispersion model (DM). It is shown how to check if the obtained mean transit time of tracer is related to the mean transit time of water by the R_p factor. The mean transit time of tracer is related directly to the tracer velocity or to the total volume of water in the groundwater system, i.e. mobile and stagnant reservoirs together. If the total porosity (fissure+porous) to the fissure porosity ratio is known (R_p factor) the mean transit time of water can be found. It shown that in some cases the retardation factor can be found from a properly performed and interpreted artificial tracer experiment. The interpretation of tritium data without taking into account the retardation in matrix leads to overestimation of volume of mobile water in the system or to underestimation of water velocity.

An example related to a relatively long-term artificial-tracer experiment in fractured granite shows that even properly calibrated DM may yield unacceptable parameters which in turn may lead to completely wrong predictions of pollutant movement. Such a case may happen when one assumes a priori that the model is valid, without performing its validation. The problem can be demonstrated by comparison of concentration curves calculated by making use of the PFDM and DM with parameters found based on the parameters of the SFDM.

Two approximations, based on the earlier works of the author, are discussed for the interpretation of environmental radioactive tracer with a constant input. They are of great importance for a proper interpretation of the radiocarbon and ^{36}Cl data. The tracers enter the groundwater system since thousands of years with a nearly constant concentration and their concentrations measured at present can be considered as being in a steady state (time elapsed since the beginning of the injection is infinitely long). In the first approximation parallel fissure model with piston flow in the fissures (PFPFM) coupled with the combined model of exchange reaction in the porous matrix is considered. This model has been shown to be especially useful for the explanation of anomalously low ^{14}C concentrations (great ages) in carbonate aquifers. The example of the radiocarbon dating discussed in the paper shows that improperly performed interpretation based directly on the radiocarbon age, can lead to an underestimation of the water velocity of some orders of magnitudes. The model developed can be used either to explain such a discrepancy or to estimate physical and/or reaction parameters when other parameters are known from independent determinations. The second approximation, is similar to the single fissure approximation (SFPFM), and is applicable in confined aquifers of limited thickness and extended

length, overlain and/or underlain by aquitard of low permeability. This approach is particularly useful for porous or fissured aquifers which can loose or gain some amounts of tracer due to the diffusional exchange between the aquifer and aquitard.

There is a common opinion that diffusion processes play a minor role in fissured aquifers of low matrix porosity. It has been shown that matrix porosity does not decide if the diffusion can be neglected or not. The decesive importance has the diffusion parameter, $a=n_p\sqrt{D_p}/(2b)$. In short-term tracer experiments its value has to be lower than 10^{-4} $s^{-1/2}$ to neglect the diffusion process into the porous matrix, whereas in long-term experiments this condition is much stronger (i.e. the a-value must be much lower). In all artificial tracer experiments performed in different formations discussed in this study and summarized in Table 13 it was necessary to take into account the diffusion process. Of course, it is possible that sometimes the matrix diffusion can be neglected.

In general, such parameters as matrix porosity and the coefficient of matrix diffusion (both measurable on core samples), as well as the hydraulic conductivity (known from pumping tests) are helpfull in the interpretation of tracer experiments. In the case of reactive tracers the dimensions of micropores or microfissures measurable by microscope observation of core samples and the distribution coefficient or reaction rate constants measurable in batch or column experiments of ground material should also be very helpful. In general, independend information, when available, gives a possibility to validate the model. Practically, in all the experiments performed with artificial tracers and dissccused within this study both calibration and validation (direct or indirect) of the SFDM was obtained. It has also been shown that even properly performed calibration does not necessarily mean that the model is validated.

The model developed in this study is probably the simplest one available for the solute transport in fissured systems. However, even this simple model, in the case of reactive tracers, is characterized by a large number of fitting parameters and even by a larger number of physical parameters. Further studies are probably needed to develope more realistic models which would take into account the diffusion processes into porous matrix and the distribution of fissure appertures and spacings. However, it is well known fact, that a more sophisticated model is always characterized by a large number of parameters. Unfortunately, an increased number of fitting parameters reduces the possibility to obtain a unique solution in inverse modelling. Therefore, it may be concluded, that the models developed within this study are applicable for practical purposes, in spite of their approximate character.

Acknowledgments

Sincere thanks are due to the authorities (Geschäftsführung) of the GSF-Forschungszentrum für Umwelt und Gesundheit, München-Neuherberg, and to Prof. Dr. Peter Fritz for the permission to perform the work in the GSF-Institut für Hydrologie.

Prof. Dr. Christian Leibundgut, Professur für Hydrologie der Universität Freiburg, is thanked for his interest and encouragement. Prof. Dr. Andrzej Zuber, Institute of Nuclear Physics in Cracow, Poland, is thanked for many years of fruitful cooperation as well as for valuable discussions and critical reading of the manuscript.

The work was performed within the GSF Research Programms FE-74311 and FE-74361 and in part under Research Agreement No. 6087/CF with the International Atomic Energy Agency (IAEA).

Notation

A	combination of physical constants [$\rho g/(12\mu)$; ρ - fluid density, g - gravitational acceleration, μ - dynamic viscosity] equal to $6.3 \cdot 10^5$ $m^{-1} s^{-1}$ for water at 10°C
C	tracer concentration measured at the outflow from a groundwater system, [M/L^3]
C_f	tracer concentration in water outflowing from fissures, [M/L^3]
C_n	normalized tracer concentration, eq. (26), [M/L^3]
C_{in}	variable input concentration, [M/L^3]
C_{max}	maximum observed concentration, [M/L^3]
C_p	tracer concentration in water in matrix, [M/L^3]
D	dispersion coefficient in fissures, [L^2/T]
D_p	molecular diffusion coefficient in water in matrix, i.e. $\delta D_m/\tau_p$, [L^2/T]
D_m	molecular diffusion coefficient in free water, [L^2/T]
D/v	intrinsic dispersivity in fissures, [L]
D/vx	intrinsic dispersion parameter, (P_D, or 1/Pe), [dimensionless]
I	number of stream tubes in dipole test, [dimensionless]
I_1	modified Bessel function of first kind and first order, [dimensionless]
K	permeability coefficient, [L^2]
L	fissure spacing, [L]
M	mass of tracer injected, [M]
M_i	mass of tracer transported in i-th stream tube, [M]
N	number of fissures in a given thickness, [dimensionless]
P_D	intrinsic dispersion parameter, (1/Pe, D/vx), [dimensionless]
$(P_D)^*$	apparent (artificial) fitting parameter, [dimensionless]
Pe	intrinsic Peclet number (vx/D or $1/P_D$), [dimensionless]
$(Pe)_i$	intrinsic Peclet number for i-th stream tube, (X_i/α_L), [dimensionless]
Pe_1	fitting parameter in dipole tests, [dimensionless]
Q	volumetric flow rate through the system, pumping rate, [L^3/T]

R	retardation factor caused by diffusion of tracer into porous matrix and exchange reactions, [dimensionless]
R_{af}	retardation factor caused by instantaneous equilibrium exchange reaction on the fissure walls, [dimensionless]
R_{ap}	retardation factor caused by instantaneous equilibrium exchange reaction in the porous matrix, [dimensionless]
R_p	retardation factor due to diffusion of tracer into porous matrix, [dimensionless]
RR	relative mass recovery of tracer, [dimensionless] or [%]
S	cross-section area perpendicular to flow direction, [L^2]
S_a	surface area of a catchment, [L^2]
T	transmisivity of water bearing layer, [L^2/T]
T_s	transmisivity of single fissure, [L^2/T]
$T_{1/2}$	half-life time of radioactive tracer, [T]
V	total volume of water in groundwater system, [L^3]
V_s	volume of water in porous matrix (stagnant), [L^3]
V_f	volume of water in fissures (mobile), [L^3]
X	distance between injection and observation well, [L]
X_i	flow distance in i-th stream tube, [L]
Z_f	surface of the fissure wall per unit volume of rock, [L^{-1}]
a	model (fitting) parameter, [$T^{-1/2}$]
b	half-fissure aperture, [L]
d_c	diameter of capillaries in the matrix, [L]
h	saturated thickness of aquifer, [L]
$g(t)$	weighting function in black box approach, normalized system response for instantaneous injection, [T^{-1}]
k	hydraulic conductivity, [L/T]
k_a	distribution coefficient for tracer concentration in solid phase expressed per unit rock surface, [L]
k_d	distribution coefficient, [L^3/M]
k_1	forward kinetic reaction rate constant, [T^{-1}]

k_1'	model (fitting) parameter, k_1/R_{ap}, $[T^{-1}]$
k_2	backward kinetic reaction rate constant, $[T^{-1}]$
k_3	distribution coefficient for instantaneous equilibrium with linear isotherm of exchange reaction in porous matrix, $[L^3/M]$
m	thickness of aquifer, [L]
n	total porosity, (n_f+n_p), [dimensionless]
n_e	macroscopic porosity of a porous aquifer, [dimensionless]
n_f	fissure porosity, [dimensionless]
n_p	matrix porosity, [dimensionless]
p	model (fitting) parameter, $[T^{1/2}]$
q_i	volumetric flow rate of water in i-th stream tube, $[L^3/T]$
q_1	tracer concentration in solid phase governed by instantaneous equilibrium, [M/M]
q_2	tracer concentration in solid phase governed by first order kinetic reaction, [M/M]
q_s	tracer concentration in solid phase expressed per unit rock surface, $[M/L^2]$
r_i	mean grain radius of i-th fraction of grain size curve, [L]
r_w	diameter of the pumping well, [L]
t	time variable, [T]
t_k	time defined by eq. (18.1), [T]
t_{max}	time of maximum concentration (C_{max}), [T]
t_{min}	flow time after which DM becomes applicable, [T]
t_o	mean transit time of water, [T]
t_o'	model (fitting) parameter, t_o/R_{af}, [T]
$(t_o)_i$	mean transit time of water in i-th stream tube, [T]
t_{o1}	model (fitting) parameter in dipole tests, [T]
t_t	mean transit time of tracer, [T]
v	mean water velocity, [L/T]
v_t	mean tracer velocity, [L/T]
x	space coordinate parallel to the fissure extension, [L]

y	space coordinate perpendicular to the fissure extension, [L]
α_L	longitudinal dispersivity, [L]
δ	constrictivity factor, [dimensionless]
λ	radioactive decay constant, [T^{-1}]
ν_i	weight fraction of i-th fraction of grain size curve, [dimensionless]
ρ	density of matrix material, [M/L^3]
$(\sigma_t)^2$	time variance of the tracer concentration curve, [dimensionless]
τ	transit time of tracer particle trough the system, [T]
τ_f	tortousity factor for fissures, [dimensionless]
τ_p	tortousity factor for micropores, [dimensionless]
ΔH	net imposed hydraulic head between injection and pumping well, [L]
Φ_1	mass transfer of tracer between liquid and solid phase in matrix, governed by linear exchange reaction isotherm with instantaneous equilibrium, [T^{-1}]
Φ_2	mass transfer of tracer between liquid and solid phase in matrix, governed by first order kinetic exchange reaction, [T^{-1}]

References

Abelin, H., Birgersson, L., Gidlund, J. & Neretnieks, I. (1991a): A large-scale flow and tracer experiment in granite, 1. Experimental design and flow distribution. Water Resour. Res., 22 (12): 3107-3117.

Abelin, H., Birgersson, L., Moreno, L., Widen, H., Agren, Th. & Neretnieks, I. (1991b): A large-scale flow and tracer experiment in granite, 2. Results and interpretation. Water Resour. Res., 22 (12): 3119-3135.

Barker, J.A. (1985): Block-geometry functions characterizing transport in densely fissured media. J. Hydrol., 77: 263-279.

Baudracco, J., Bel, M. & Perami, R. (1982): Effets de l'alteration sur quelques proprietes mecaniques du granite du Sidobre (France). Bull. of the Inter. Assoc. of Eng. Geology, 25: 33-38.

Behrens, H. (1985): Speciation of radioIodide in aquatic and terrestrial systems under the influence of biogeochemical processes. In: Speciation of Fission and Activation Products in the Environment, Elsevier, New York, 223-230.

Bibby, R. (1981): Mass transport of solutes in dual-porosity media. Water Resour. Res., 17 (4): 1075-1081.

Birgersson, L. & Neretnieks, I. (1990): Diffusion in the matrix of granitic rock: Field tests in the Stripa mine. Water Resour. Res., 26 (11): 2833-2842.

Blavoux, B. & Olive, Ph. (1981): Radiocarbon dating of groundwater of the aquifer confined in the Lower Triassic sandstones of Lorraine regione, France. J. Hydrol., 54: 167-183.

Cacas, M.C., Ledoux, E., de Marsily, G., Tillie, B., Barbreau, A., Durand, E., Feuga, B. & Peadecerf, P. (1990a): Modelling fracture flow with a stochastic discrete fracture network: Calibration and validation, 1. Flow model. Water Resour. Res., 26 (3): 479-489.

Cacas, M., Ledoux, E., de Marsily, G., Barbreau, A., Calmels, P., Gaillard, B., & Margrita, R. (1990b): Modelling fracture flow with a stochastic discrete fracture network: Calibration and validation, 2. The transport model. Water Resour. Res., 26 (3): 491-500.

Cameron, D.R. & Klute A. (1977): Convective-dispersive solute transport with a combined equilibrium and kinetic adsorption model. Water. Resour. Res., 13 (1): 183-188.

Chen, C.S. (1985): Analytical and approximative solutions to radial dispersion from an injection well to a geological unit with simultaneous diffusion into adjacent strata. Water Resour Res., 21 (8): 1069-1076.

Chen, C.S. (1986): Solution for radionuclide transport from an injection well into a single fracture in a porous formation. Water Resour Res., 22 (4): 508-518.

Fontes, J.Ch. & Garnier, J.M. (1979): Determination of initial ^{14}C activity of the total dissolved carbon: a review of the existing models and new approach. Water Resour. Res., 15 (3): 399-413.

Foster, S.S.D. (1975): The Chalk groundwater tritium anomaly - a possible explanation. J. Hydrol., 25: 159-165.

Freeze, J.A. & Cherry, J.F. (1979): Groundwater. Prentice-Hall, Englewood Cliffs, New York.

Garnier, J.M., Crampton, N., Preaux, C., Porel, G. & Vreulx, M. (1985): Tracage par ^{13}C, ^{2}H, I^- et Uranine dans la nappe de la craie senonienne en ecoulement radial convergent (Bethune, France). J. Hydrol., 73: 379-392.

Germain, D. & Frind, E. (1989): Modelling of contaminant migration in fracture networks: Effects of matrix diffusion. In: Contaminant Transport in Groundwater, A.A. Balkena, Rotterdam, 267-274.

Goltz, M.N. & Roberts, P. (1987): Using the method of moments to analyze three-dimensional diffusion-limited solute transport from temporal and spatial perspectives. Water Resour. Res., 23 (8): 1575-1585.

Grisak, G.E. & Pickens, J.F. (1980): Solute transport through fractured media, 1. The effect of matrix diffusion. Water Resour. Res., 16 (4): 719-730.

Grisak, G.E. & Pickens, J.F. (1981): An analytical solution for solute transport through fractured media with matrix diffusion. J. Hydrol., 52: 47-57.

Grisak, G.E., Pickens, J.F. & Cherry, J.A. (1980): Solute transport through fractured media, 2. Column study of fractured till. Water Resour. Res., 16 (4): 731-739.

Grove, D.B. & Beetem, W.A. (1971): Porosity and dispersion constant calculations for a fractured carbonate aquifer using two well tracer method. Water Resour. Res., 7 (1): 128-134.

Herrmann, A., Koll, J., Maloszewski, P., Rauert, W. & Stichler, W. (1986): Water balance studies in a small catchment area of paleozoic rock using environmental isotope tracer techniques. In: Conjuctive Water Use, IAHS Publ. No. 156, Wallingford, Oxfordshire, 111-124.

Herrmann, A., Koll, J., Leibundgut, Ch., Maloszewski, P., Rau, R., Rauert, W., Schöniger, M. & Stichler, W. (1989): Wasserumsatz in einem kleinen Einzugsgebiet im paläozoischen Mittelgebirge (Lange Bramke, Oberharz). Eine hydrologische Systemanalyse mittels Umweltisotopen als Tracer. Landschaftsökologie u. Umweltforschung, Braunschweig, Heft 17: 1-186.

Himmelsbach, Th. (1991): Dipoltests zur Untersuchung des Stofftransportes in Kluftgrundwasserleitern. Steir. Beitr. z. Hydrologie, Forschungsgesellschaft Joanneum, Graz, Band 42: 131-150.

Himmelsbach, Th. (1992): Tracer hydrological investigations in a high permeable fault and fracture zone. In: Tracer Hydrology, A.A. Balkena, Rotterdam, 15-20.

Himmelsbach, Th. & Maloszewski, P. (1992): Tracer tests and hydraulic investigations in the observation tunnel Lindau. Steir. Beitr. z. Hydrologie, Forschungsgesellschaft Joanneum, Graz, Band 43: 197-223.

Hodgkinson, D.P., Lever, D.A. & England, T.H. (1984): Mathematical modelling of radionuclide transport through fractured rock using numerical inversion of Laplace transforms: application to Intracoin Level 3. Ann. nucl. Energy, No. 3: 111-122.

Huyakorn, P.S., Lester B.H. & Mercer, J.W. (1983a): An efficient finite element technique for modeling transport in fractured porous media, 1. Single species transport. Water Resour. Res., 19 (3): 841-854.

Huyakorn, P.S., Lester B.H. & Mercer, J.W. (1983b): An efficient finite element technique for modeling transport in fractured porous media, 1. Nuclide decay chain transport. Water Resour. Res., 19 (5): 1286-1296.

Ivanovich, M. & Smith, D.B. (1978): Determination of aquifer parameters by a two-well pulsed method using radioactive tracers. J. Hydrol., 36: 35-45.

Johns, R.A. & Roberts, P.V. (1991): A solute transport model for channelized flow in a fracture. Water Resour. Res., 27 (8): 1797-1808.

Klotz, D., Lazik, D. & Maloszewski, P. (1992): Modelling of nonequilibrium pollutant behaviour in saturated porous media - interpretation of column experiments. In: Tracer Hydrology, A.A. Balkena, Rotterdam, 433-439.

Klotz, D., Maloszewski, P., & Moser, H. (1988): Mathematical modelling of radioactive tracer migration in water flowing through saturated porous media. Radiochimica Acta, 44/45: 373-379.

Kreft A. (1983): Problems of Mathematical Modelling the Hydrodynamic Dispersion. Mathematics-Physics-Chemistry, Sci. Bull. 61, Academy of Mining and Metallurgy, Cracow, 1-84.

Kreft, A., Lenda, A., Turek, B., Zuber, A. & Czauderna, K. (1974): Determination of effective porosities by the two-well pulse method. In: Isotope Techniques in Groundwater Hydrology 1974, Vol. II, I.A.E.A., Vienna, 295-312.

Kreft A., & Zuber A. (1978): On the physical meaning of the dispersion equation and its solution for different initial and boundary conditions. Chem. Eng. Sci., 33: 1471-1480.

Kreft A., & Zuber A. (1979): Determination of aquifer parameters by a two-well pulsed method using radioactive tracers - Comments. J. Hydrol., 41: 171-176.

Lenda, A. & Zuber, A. (1970): Tracer dispersion in groundwater experiments. In: Isotope Hydrology 1970, IAEA, Vienna, 619-641.

Lever, D.A., Bradbury, M.H. & Hemingway, S.J. (1985): The effect of dead-end pore porosity on rock-matrix diffusion. J. Hydrol., 80: 45-76.

Lowell, R.P. (1989): Contaminant transport in a single fracture: periodic boundary and flow conditions. Water Resour. Res., 25 (5): 774-780.

Maloszewski, P. (1992): Bemerkungen über die Interpretation von Markierungsversuchen im Grundwasser. In: Jahresbericht 1991, GSF-Institut für Hydrologie, Neuherberg, 2-19.

Maloszewski, P., Rauert, W., Stichler, W. & Herrmann, A. (1983): Application of flow models in an alpine catchment area using tritium and deuterium data. J. Hydrol., 66: 319-330.

Maloszewski, P., Rauert, W., Stichler, W. & Herrmann, A. (1990): Bestimmung hydrogeologischer Parameter in Einzugsgebieten mit Kluftaquiferen unter Verwendung von Umweltisotopen und mathematischen Fliessmodellen. Freiberger Forschungshefte, Geowissenschaften, C442: 11-21.

Maloszewski, P., Rauert, W., Trimborn, P., Herrmann, A. & Rau, R. (1992): Isotope hydrological study of mean transit times in an alpine basin (Wimbachtal, Germany). J. Hydrol., 140: 343-360.

Maloszewski, P., Witczak, S. & Zuber, A. (1980): Prediction of pollutant movement in groundwaters. In: Nuclear Techniques in Groundwater Pollution Research, I.A.E.A., Vienna, 61-81.

Maloszewski, P. & Zuber, A. (1982): Determining of turnover time of groundwater systems with the aid of environmental traces, 1. Models and their applicability. J. Hydrol., 57: 207-231.

Maloszewski, P. & Zuber, A. (1984): Interpretation of artificial and environmental tracers in fissured rocks with a porous matrix. In: Isotope Hydrology 1983, IAEA, Vienna, 635-651.

Maloszewski, P. & Zuber, A. (1985): On the theory of tracer experiments in fissured rocks with a porous matrix. J. Hydrol., 79: 333-358.

Maloszewski, P. & Zuber, A. (1989): Mathematical models for interpreting tracer experiments in fissured aquifers. In: The Application of Isotope Techniques in the Study of Hydrogeology of Fractured and Fissured Rocks, IAEA, Vienna, 287-301.

Maloszewski, P. & Zuber, A. (1990a): Mathematical modeling of tracer behavior in short-term experiments in fissured rocks. Water Resour. Res., 26 (7): 1517-1528.

Maloszewski, P. & Zuber, A. (1990b): On the parameter estimation from artificial tracer experiments. In: ModelCARE90: Calibration and Reliability in Groundwater Modelling, IAHS Publ. No. 195, Wallingford, Oxfordshire, 53-62.

Maloszewski, P. & Zuber, A. (1991): Influence of matrix diffusion and exchange reactions on radiocarbon ages in fissured carbonate aquifers. Water Resour. Res., 27 (8): 1937-1945.

Maloszewski, P. & Zuber, A. (1992): On the calibration and validation of mathematical models for the interpretation of tracer experiments in groundwater. Advances in Water Resources, 15 (1): 47-62.

Maloszewski, P. & Zuber, A. (1993a): Tracer experiments in fractued rocks: matrix diffusion and the validity of models. Water Resour. Res., 29 (8): 2723-2735.

Maloszewski, P. & Zuber, A. (1993b): Principles and practice of calibration and validation of mathematical models for the interpretation of environmental tracer data in aquifers. Advances in Water Resources, 16: 173-190.

Mook, W.G. (1980): Carbon-14 in hydrogeological studies. In: Handbook of Environmental Isotope Geochemistry, Vol. 1, Ed. Fritz P. & Fontes J.Ch., Elsevier, Amsterdam, 49-74.

Moreno, L., Neretnieks, I. & Eriksen, T. (1985): Analysis of some laboratory tracer runs in natural fissures. Water Resour. Res., 21 (7): 951-958.

Moreno, L. & Rasmuson, L. (1986): Contaminant transport through a fractured porous rock: impact of the inlet boundary condition on the concentration profile in the rock matrix. Water Resour. Res., 22 (12): 1728-1730.

Moreno, L., Tsang, Y.W., Tsang, C.F., Hale, F.V. & Neretnieks, I. (1988): Flow and tracer transport in a single fracture: a stochastic model and its relation to some field observations. Water Resour. Res., 24 (12): 2033-2048.

Neretnieks, I. (1980): Diffusion in the rock matrix. An important factor in radionuclide retardation ? J. Geophys. Res., 85 (B8): 4379-4397.

Neretnieks, I. (1981): Prediction of radionuclide migration in the geosphere: is the porous-flow model adequate ? IAEA Symposium, Knoxville, IAEA, Vienna, IAEA-SM-257/19, 635-657.

Neretnieks, I. (1983): A note on fracture flow dispersion mechanism in the ground. Water Resour. Res., 19 (2): 364-370.

Neretnieks, I. & Rasmuson, A. (1984): An approach to modelling radionuclide migration in a medium with strongly varying velocity and block sizes along the flow path. Water Resour. Res., 20 (12): 1823-1836.

Nolte, E., Krauthan P., Korschinek G., Maloszewski, P., Fritz, P. & Wolf, M. (1991): Measurements and interpretation of ^{36}Cl in groundwater, Milk River aquifer, Alberta, Canada. Applied Geochemistry, 6: 435-445.

Novakowski, K.S., Evans, G.V., Lever, D.A. & Raven, K.G. (1985): A field example of measuring hydrodynamic dispersion in a single fracture. Water Resour. Res., 21 (8): 1165-1174.

Pirson, S.J. (1963): Handbook of Well Log Analysis. Prentice-Hall, Englewood Cliffs, New York.

Price, M. (1987): Fluid flow in Chalk of England. In: Fluid Flow in Sedimentary Basins and Aquifers, Geological Society Special Publication No. 34, Wallingford, 141-156.

Rank, D., Völkl, G., Maloszewski, P. & Stichler, W. (1992): Flow dynamics in an alpine karst massif studied by means of environmental isotopes. In: Isotope Techniques in Water Resources Development 1991, I.A.E.A., Vienna, 327-343.

Rasmuson, A. (1984): Migration of radionuclides in fissured rock: analytical solution for the case of constant source strenght. Water Resour. Res., 20 (10): 1435-1442.

Rasmuson, A. (1985): Analysis of hydrodynamic dispersion in discrete fracture networks using method of moments. Water Resour. Res., 21 (11): 1677-1683.

Raven, K.G., Novakowski, K.S. & Lapcevic, P.A. (1988): Interpretation of field tracer tests of a single fracture using a transient solute storage model. Water Resour. Res., 24 (12): 2019-2032.

Saffman, P.G. (1959): Dispersion in flow through a network of capillaries, Chem. Eng. Sci., 11: 125-129.

Schwartz, F.W., Smith, L. & Crowe, A.S. (1983): A stochastic analysis of macroscopic dispersion in fractured media. Water Resour. Res., 19 (5): 1253-1265.

Seiler, K.P., Maloszewski, P. & Behrens, H. (1989): Hydrodynamic dispersion in karstified limenstones and dolomites in the Upper Jurassic of Franconian Alb, F.R.G. J. Hydrol., 108: 235-247.

Skagius, K. & Neretnieks, I. (1986): Porosities and diffusities of some nonsorbing species in crystalline rocks. Water Resour. Res., 22 (3): 389-398.

Snow, D.T. (1969): Anisotropic permeability of fractured media. Water Resour. Res., 5 (6): 1273-1289.

Snow, D.T. (1970): The frequency and apertures of fractures in rock. Int. J. Rock Mech. Min. Sci., 7: 23-40.

Stichler, W., Maloszewski, P. & Moser, H. (1986): Modelling of river water infiltration using oxygen-18 data. J. Hydrol., 83: 355-365.

Sudicky, E.A. & Frind, E.O. (1981): Carbon 14 dating of groundwater in confined aquifers: implications of aquitard diffusion. Water Resour. Res., 17 (4): 1060-1064.

Sudicky, E.A. & Frind, E.O. (1982): Contaminant transport in fractured porous media: analytical solutions for a system of parallel fractures. Water Resour. Res., 18 (6): 1634-1642.

Sudicky, E.A. & Frind, E.O. (1984): Contaminant transport in fractured porous media: analytical solution for a two-member decay chain in a single fissure. Water Resour. Res., 20 (7): 1021-1029.

Tang, D.H., Frind, E.O. & Sudicky, E.A. (1981): Contaminant transport in fractured porous media: analytical solutions for a single fracture. Water Resour. Res., 17 (3): 555-564.

Thilo, L. & Münnich, K.O. (1970): Reliability of ^{14}C dating of groundwater in view of carbonate exchange. In: Isotope Hydrology 1970, I.A.E.A., Vienna, 259-270.

Tsang, Y.W. & Tsang, C.F. (1987): Channel model of flow through fractured media. Water Resour. Res., 23 (3): 467-479.

Tsang, Y.W., Tsang, C.F., Neretnieks, I. & Moreno, L. (1988): Flow and tracer transport in fractured media: a variable aperture channel model and its properties. Water Resour. Res., 24 (12): 2049-2060.

Wigley, T.M., Plummer, L.N., Pearson, F.J. (1978): Carbon isotope evolution of groundwater. Geochim. Cosmochim. Acta, 42: 1117-1139.

Zuber, A. (1974): Theoretical possibilities of the two-well pulse method. In: Isotope Techniques in Groundwater Hydrology 1974, Vol. II, IAEA, Vienna, 277-294.

Zuber, A. (1986): Mathematical models for the interpretation of environmental radioisotopes in groundwater systems. In: Handbook of Environmental Isotope Geochemistry, Vol. 2, Edited by P. Fritz and J.C. Fontes, Elsevier, Amsterdam, 1-59.